IDENTIFICATION OF SMALL MOLECULE INHIBITORS OF POLYOMAVIRUS REPLICATION

by

Sandlin Preecs Seguin

B.S. Biochemistry, Western Washington University, 2006

Submitted to the Graduate Faculty of

Arts and Sciences in partial fulfillment

of the requirements for the degree of

Doctor of Philosophy

University of Pittsburgh

2011

UNIVERSITY OF PITTSBURGH

SCHOOL OF ARTS AND SCIENCES

This dissertation was presented

by

Sandlin Preecs Seguin

It was defended on

June 29, 2011

and approved by

Karen M. Arndt, Ph.D., Professor, Biological Sciences

Ole Gjoerup, Ph.D., Assistant Professor, Microbiology and Molecular Genetics, University of Pittsburgh School of Medicine

James M. Pipas, Ph.D., Professor, Biological Sciences

Anthony M. Schwacha, Ph.D., Associate Professor, Biological Sciences

Dissertation Advisor: Jeffery L. Brodsky, Ph.D., Professor, Biological Sciences

IDENTIFICATION OF SMALL MOLECULE INHIBITORS OF POLYOMAVIRUS REPLICATION

Sandlin P. Seguin, Ph.D.

University of Pittsburgh, 2011

Polyomaviruses (PyVs) are ubiquitous DNA viruses that are not generally associated with pathogenicity. However, in immunosuppressed populations, PyVs can cause diseases, including BK Virus associated nephropathy, hemorrhagic cystitis and progressive multifocal leukoencephalopathy. There is currently no PyV specific inhibitor for these diseases. Because all PyVs express a conserved large T antigen (TAg) that is essential for viral replication, I hypothesized that inhibitors of the model TAg from Simian Virus 40 (SV40) would inhibit the replication of PyVs in general. TAg has multiple essential activities, but my work focused on the ATPase activity of TAg, which provides the helicase activity during viral replication. Two high throughput screens were performed on purified TAg to identify inhibitors of TAg ATPase activity. In the first screen, a quinaldine red screen of the MS2000 library of commercially available compounds identified the FDA approved compounds bithionol and hexachlorophene as inhibitors of the ATPase activity of TAg. The structure activity relationship of these bisphenols was refined, and the results suggested that inhibition of TAg was unique to these compounds, and is not a general feature of bisphenols. The compounds also inhibited SV40 DNA replication and infection, and are the most potent SV40 inhibitors reported. Surprisingly, bithionol and hexachlorophene inhibit replication of the clinically relevant PyV BK Virus (BKV), but not to the same extent.

In the second screen, which employed the ADP Hunter assay and the NIH Molecular Libraries Probe Centers Network (MLPCN) compound library, three scaffolds of interest were identified. However, all three had limited potency when characterized in other *in vitro* assays. Chemical refinement of these scaffolds identified another bisphenol that inhibits TAg activity and TAg dependent DNA replication *in vitro*. Unfortunately, the known cytotoxicity of this compound limits its use as a therapeutic. Although I have not yet identified a PyV specific inhibitor that would be a suitable therapeutic, this work supports my overall hypothesis: small molecules that inhibit the ATPase activity of TAg reduce viral DNA replication, and viral infection. My work has also provided valuable insights to design future screens to identify inhibitors of PyV replication.

TABLE OF CONTENTS

LIST OF TABLES

LIST OF FIGURES

PREFACE

This dissertation could not have come together without the enormous support and encouragement of my colleagues, friends and family. I would need another 200 pages to quantify their many and splendid contributions to this process, and without listing you each by name, please accept my gratitude.

I would like to first acknowledge the contributions of my boss and mentor Dr. Jeff Brodsky. His role in my research and training has shaped both my experience and development as a graduate student and scientist. His critical insights have strengthened this dissertation and helped me become a more competent writer. I cannot thank him enough for the flexibility to develop many different aspects both of this project, but also my career at Pitt, including the unparalleled opportunity to design and teach my own course. My experience in the Brodsky lab has given me the training I need for lifelong success for which I cannot express enough gratitude.

Jeff designed a project that took advantage of the collaborative nature of our department, and as a result, I benefitted from the knowledge and experience of Dr. Jim Pipas and his lab. Jim's influence on my research and education has given me both the passion and expertise to succeed in this endeavor. He has also granted me the essential opportunity to share in his lab meeting, which proved to be an essential venue for training and developing the important relationships that helped me through innumerable challenges. Without the expertise and

institutional memory of both Paul Cantalupo and Mayte Saenz Robles, this work would no doubt have languished. Abhilasha Rathi and Nicole Seneca helped me to design formative experiments and provided essential feedback on this dissertation. I am so grateful to the past and present members of the lab for their reagents, protocols or feedback over the years.

Another unparalleled benefit of working in the Brodsky lab was the chance to work with his crew of fantastic scientists. Alex Ireland, an undergraduate, has worked with me since 2007 and provided some essential experiments discussed below. Thank goodness I had him to share my TAg woes with and that he was so forgiving of my laissez faire attitude towards organization. Thanks to World's Greatest Lab Manager, Jen Goeckeler, I never fully understood the designs that keep the lab up and running. The post-docs in the lab, Annette Chiang, Chris Guerriero, Patrick Needham, and especially Teresa Buck and Cristy Gelling, have provided insights, cookies and cocktails as needed. Karen Hecht kept me in school and taught me to love gin, for which I am forever indebted. My fellow graduate students, Sarah Grubb, Alex Kolb, Joe Tran, Stacy Hrizo and Shruthi Vembar have been encouraging and helped to celebrate both the milestones and setbacks. I must particularly acknowledge the mentorship of Christine Wright who provided the groundwork for this dissertation, pounds of protocols and troubleshooting by phone or email. Many thanks to the past and present members of the lab for their technical and emotional contributions.

My family has always had every confidence in my success, which has proven an essential source of strength. Many thanks to my parents and grandparents for never questioning that this is where I belong, and for encouraging me to excel. I can't begin to acknowledge the unending support from my husband, Matt, who has juggled every aspect of these last 5 years with patience and compassion, kept me fed and from getting evicted. I must also express my deepest gratitude

and affection my modern family, Shaoshu Jiang, Jessi Board and Wade Znosko for their joyous distractions and being such important people in my life.

I'd like to express my gratitude for the supportive community that developed as a result of the Women in Science Careers (WISC) meetings for encouraging my professional development. I also want to thank the co-op members of the Union Project for providing an encouraging learning environment that gave me the patience to return to the bench after comps. My sincere thanks to Dr. Space for encouraging me to use my own definition of success. I would also like to acknowledge the Silversun Pickups, Ratatat, and RjD2, without whom, this dissertation could not have been written. Finally, I must express my gratitude for the wonderful Pitt Libraries for providing many of the resources used in this document.

1.0 INTRODUCTION

When the work described in this dissertation was initiated in 2007, there was sufficient evidence that the diseases caused by the polyomaviruses BK Virus (BKV) and JC Virus (JCV) were in need of anti-virals. Fortunately, more than half a century of work studying Simian Virus 40 (SV40), the model polyomavirus, presented us with the necessary molecular and cellular tools to approach this need aggressively using high throughput techniques. During this time, an additional 7 human polyomaviruses have been described, some of which have been shown to cause disease. Therefore, what we know about polyomavirus biology has become increasingly relevant, and future investigations of these viruses may give us new insight into the basic biology that drives the replication of disease-associated polyomaviruses.

1.1 THE BIOLOGY OF POLYOMAVIRUSES

Polyomaviruses (PyVs) are small, double-stranded DNA viruses (Cole, 1996; Fanning et al., 2009; Pipas, 2009). On average, the circular genome is just over 5kB (Dulbecco and Vogt, 1963), physically constraining the genetic material carried by the virus. The genome is generally divided into an early and late region, with a regulatory region in between. The early region is responsible for preparing the cellular environment for viral replication and for initation of replication. Given the small size of the virus, viral replication relies heavily on host proteins,

which are redirected for this purpose by the early proteins. PyVs are also ecologically diverse. They infect many different host species, and cause a variety of pathologies depending on the host. Given the recent characterization of several new PyVs, what is known about this family is based on the study of a few model viruses, and may not prove to be true of all PyVs.

1.1.1 Life cycle

PyVs target non-dividing host cells, primarily epithelial or fibroblastic cells (Cole, 1996). Host cell specificity of PyVs starts with the viral receptor; each virus is thought to recognize a specific ganglioside structure, although some PyVs have been shown to bind specifically to sialic acid (Gilbert and Benjamin, 2004; Low et al., 2006; Neu et al., 2009; Tsai et al., 2003). Once attached at the plasma membrane, the virus enters the cell either by caveolae mediated entry (Eash et al., 2004; Jiang et al., 2009b; Pelkmans et al., 2001), or in the case of JCV, clathrin dependent transport (Pho et al., 2000). The virus is next trafficked from a caveosome directly to the endoplasmic reticulum (ER). The mechanisms that drive this sorting event are unclear and it is surprising that the virus never colocalizes with the Golgi (Jiang et al., 2009b; Norkin and Kuksin, 2005; Pelkmans et al., 2001). Once in the ER, protein disulfide isomerases and other factors required for the ER Associated Degradation (ERAD) pathway partially unfold the heavily disulfide-bonded capsid proteins and the virus is transported to the cytoplasm (Jiang et al., 2009b; Magnuson et al., 2005; Schelhaas et al., 2007; Walczak and Tsai, 2011). Through an unknown mechanism, the partially unfolded virion enters the nucleus where expression of the early proteins begins.

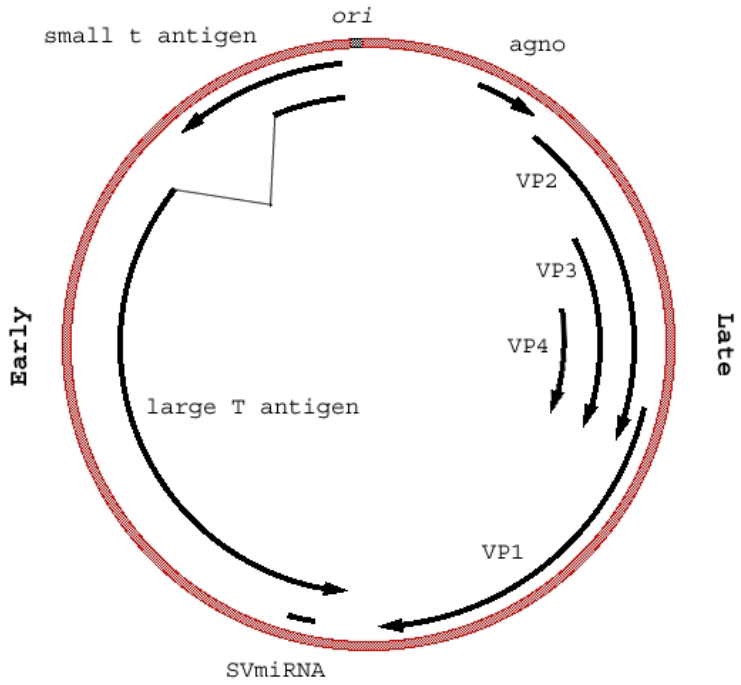

Figure 1. Genome map of SV40.

This map is based on genome NC_001669, and prepared in The Gene Construction Kit (West Lebanon, NH). The genomic organization of SV40 is common among PyVs. The SV40 genome is 5243 bases. The early and late regions are transcribed in opposite directions from the ori (denoted in black, at nucleotides 5211-31). The early message is alternatively spliced to form the small t (5163-4639) or large T antigen (5163-4918 spliced to 4571-2691). The late message is polycistronic; the first ORF is the agnogene (335-523). Downstream on this same RNA are the genes encoding VP2, VP3 and VP4 as in-frame messages with alternative starts (527-1620, 562-1620 and 1243-1620), and VP1 and an ORF from a separate reading frame (1499-2593). At the end of the late message, the SVmiRNAs are encoded (2861-2782). See text for additional details.

As shown in Figure 1, PyVs have a deceptively simple genome yet a highly complex regulatory gene network. These events are described in detail below (section 1.1.2), but in brief, the early proteins are responsible for making the non-dividing host competent for viral replication while initating and then blocking DNA damage and other immune responses (see Table 1). In turn, expression of the late genes, including the capsid proteins, decreases expression of early proteins, and may be responsible for virion exit by lysis (Daniels et al., 2007; Sullivan et al., 2005). Assembly of the virion around the viral minichromosome occurs in the nucleus just before cell lysis. Overall, the complete life cycle of polyomaviruses can range from a few days to weeks.

Table 1. Viral proteins encoded by SV40 and their functions.

Adapted from Fields Virology (Shah, 1996). The known functions of these SV40 proteins are known and assumed to be the same for other PyVs. However, especially in avian PyVs, the names VP4 or Agnoprotein B indicate a different ORF that is also thought to be a virulence factor.

Protein	**Molecular Weight (kDa)**	**Function**
Early		
Large T Antigen	80	Modifies cellular environment to favor conditions for viral replication through interactions with host proteins, including hsp, Rb and p53. Initates viral replication. Acts as the viral helicase during replication, and promotes transactivation of many other factors.
Small t Antigen	20	Modifies cellular environment via interactions with PP2A. Important for efficient viral replication.
Late		
Agnoprotein	8	unknown
VP1	40	Major capsid protein
VP2	37	Minor capsid protein
VP3	26	Minor capsid protein
VP4		Supports efficient capsid formation and lysis (Daniels et al., 2007)

1.1.2 Early region

The early region of polyomaviruses encodes the tumor, or t, antigen proteins. All polyomaviruses express a large tumor ("T") Antigen (TAg), and a small tumor antigen (tAg), which are splice variants of the same transcript (Figure 1). Some PyVs also express a middle tumor antigen (mTAg), or in the case of JCV, the very small tumor (t') antigens (Simmons et al., 1979; Trowbridge and Frisque, 1995). The N-terminal J domain-containing exon (see section 1.2.3) is shared in common between all T/t antigens (Cole, 1996; Shah, 1996). In some cell types, the virus can enter and express these early genes, but is unable to express late proteins or assemble virions. These non-permissive infections can lead to cellular transformation, which will be further described in section 1.2.1.

The activity of TAg is both conserved and essential for viral replication (see section 1.3). TAg drives replication of the viral genome, and manipulates the host cell environment by altering the activity of many cellular proteins (refer to Table 3 in section 1.3), including the tumor suppressors Rb and p53 (see sections 1.3.2 and 1.3.5, respectively). In SV40, tAg binds protein phosphatase 2A (PP2A) (Pallas et al., 1990; Yu et al., 2001), whose targets include components in the MAPK pathway. Specifically, tAg disrupts formation of the PP2A heterotrimer, altering the substrate specificity of PP2A with many downstream consequences, including stabilization of c-myc and transition to S phase (Sablina and Hahn, 2008; Sontag et al., 1993; Yeh et al., 2004). These activities are essential for transformation of some human cell lines (Hahn et al., 2002). Studies of tAg or mTAg from MPyV have greatly informed our understanding of these signaling pathways, as well as the role of PP2A as a tumor suppressor (Schaffhausen and Roberts, 2009).

1.1.3 Late region

The major products of the late region of the polyomavirus are the capsid proteins, VP1, VP2 and VP3 (Table 1 and Figure 1). The late region of polyomaviridae is more divergent than the early region (Gaynor et al., 2007; van der Meijden et al., 2010), which is predicted to prevent detection by the host immune system and determine cell type specificity. This is supported by the fact that multiple PyVs can infect a single host, suggesting that infection with one PyV does not provide seroprotection against other PyVs (Kantola et al., 2010; Kean et al., 2009). A polycistronic message expresses VP2 and VP3 (Fiers et al., 1978; Reddy et al., 1978), which share a common C Terminus (Figure 1), and some PyVs express a VP4 that aids in efficient cell lysis and viral release (Daniels et al., 2007).

The X-ray crystal structure of the whole virion has been solved for several polyomaviruses (Liddington et al., 1991; Stehle et al., 1996; Stehle et al., 1994). The major capsid protein, VP1, forms pentamers and hexamers that are coordinated by a combination of inter- and intramolecular interactions to form the stable icosahedral virion. Specifically, disulfide bonds form between the pentamers, which must be disrupted during viral entry for productive infection (as noted in section 1.1.1) (Walczak and Tsai, 2011). Although each pentamer associates with one copy of either VP2 or VP3, which may aid in viral entry (Chen et al., 1998), characterization of neutralizing monoclonal antibodies first suggested that VP1 is responsible for receptor recognition (Anders and Consigli, 1983). There is also evidence that the capsid proteins elicit host responses during entry, such as PARP and Akt activation, which are manipulated later during expression of the early genes (Butin-Israeli et al., 2010; Gordon-Shaag et al., 2003). The virion is more than just a coat for DNA; it has been shown that VP

proteins 1-3 bind to DNA, facilitating capsid packing and viral maturation (Clever et al., 1993; Mukherjee et al., 2010; Soussi, 1986; Tsukamoto et al., 2007).

The late region of some PyVs produces two additional transcripts, an agnoprotein and microRNAs (SVmiRNA). The agnogene was first predicted from a preliminary sequence analysis (Dhar et al., 1977), and the agnoprotein was confirmed to bind both single and double stranded DNA (Jay et al., 1981). The agnoprotein is associated with viral nucleoproteins, but not the mature virion (Jackson and Chalkley, 1981). The agnoprotein also promotes viral assembly and maturation, and although its role is poorly understood, it is conserved among the PyVs in which it is expressed (Khalili et al., 2005).

In 2005, viral microRNAs in SV40 were discovered to degrade early gene transcripts late in infection (Sullivan et al., 2005). Carefully regulating expression of early genes removes viral antigens from detection by cytotoxic T cells (Sullivan et al., 2005). Analogous microRNAs have been confirmed in other members of the polyomaviridae (Grundhoff and Sullivan, 2011).

1.1.4 The family of Polyomaviruses

Since the first PyV was discovered in mice (MPyV) (Gross, 1953), PyVs have been detected in a number of hosts, including many mammals and birds. In addition to its small size, all PyVs contain a similar genomic organization and express the hallmark TAg (Figure 1). Before the discovery of human PyVs, the MPyV, Murine Pneumotropic Virus, Rabbit Polyomavirus and Hamster Polyomavirus were all shown to infect rodents (Graffi et al., 1968; Hartley and Rowe, 1964; Kilham, 1952). Recently, the International Committee on the Taxonomy of Viruses

(ICTV) has proposed dividing the growing genera of polyomaviridae into three genera, *Avipolyomaviridae*, *Wukipolyomaviridae* and the *Orthopolyomaviridae* (Johne et al., 2011).

The best known non-human primate PyV, SV40, was originally described as a non-filterable agent from African Green Monkey cell culture which, when injected in hamsters, caused tumors (Eddy et al., 1961; Sweet and Hilleman, 1960). Because these cell cultures had been used in the production of the Salk Polio vaccine, and this virus was not inactivated by the formalin treatment that inactivated other viruses in the culture (Provost and Hilleman, 1979), significant effort focused on characterizing this virus and its role in transformation (See section 1.1.2). At this time, the virus was actually called Simian Vaculoating virus for causing this distinctive cytopathic effect (Sweet and Hilleman, 1960), and was classified as part of the Papovaviridae, a designation that included Papillomavirus, MPyV (then called simply Polyomavirus) and the Simian Vaculoating virus (Cole, 1996). Although known to transform a variety of cell lines, infection with SV40 has not been shown to cause human disease (section 1.4.1.1). However, SV40 replicated relatively quickly and so was adapted to develop molecular tools. It has also become the type species and model virus of this family. The early history of SV40 was recounted recently (Levine, 2009).

Several additional non-human primate polyomaviruses have been characterized, including the Lymphotropic Virus (LPV), which is known to infect only B-lymphoblasts of the African Green Monkey (zur Hausen and Gissmann, 1979). Approximately 30% of the human population express antibodies against this virus (Brade et al., 1981; Kean et al., 2009; Takemoto and Segawa, 1983). The ICTV also recognizes two orangutan viruses (Bornean Orangutan Virus and Sumatran Orangutan Virus), Sea Lion Virus, Bat Virus and Bovine Polyomaviruses among the members of the diverse family polyomaviruses (Johne et al., 2011).

The discovery of Avian Polyomavirus (APyV), originally called Budgerigar Fledgling Disease Virus, has increased interest in finding and treating PyVs in birds (Muller and Nitschke, 1986). Outbreaks of APyV can cause acute death in Psittacine birds, which is a concern for breeders (Katoh et al., 2010). Birds can be vaccinated against APyV after the fledgling stage, but this leaves the youngest birds at risk (Ritchie et al., 1998a; Ritchie et al., 1998b). Similarly, Goose Hemorrhagic Polyomavirus (GHPyV) is highly pathogenic in birds, and preliminary evidence suggests that both the Crow Polyomavirus and Canary Polyomavirus are pathogenic as well (Johne et al., 2006). These avian viruses tend to cause acute inflammatory disease in immunocompetent hosts (Halami et al., 2010; Johne and Muller, 2007). Unlike most polyomaviruses, there is no evidence that these avian viruses can transform cell lines (Halami et al., 2010).

In 1971, the first two human polyomaviruses, BKV and JCV, were discovered separately as disease causing agents in two immunosuppressed patients. BKV was isolated from a kidney transplant patient who was demonstrating features of what is now called Polyomavirus Associated Nephropathy (PVAN), including viruria, detection of viral inclusion by biopsy and poor renal function (Gardner et al., 1971). JCV was isolated post-mortem from an AIDS patient with progressive multifocal leukoencephalopathy (PML), which is characterized by palsy, neurodegeneration and acute demyelination of the white matter (Padgett et al., 1971). Since their initial discovery, both viruses have been shown to be quite common in the population and maintain a lifelong infection; 70-80% of the all people carry them (Kean and Garcea, 2009; Kean et al., 2009). However, BKV and JCV are not generally associated with disease in immunocompetent patients (Kean and Garcea, 2009; Kean et al., 2009).

In contrast, Merkel Cell Polyomavirus (MCPyV) was isolated from sequences found integrated into Merkel Cell carcinomas, which is a rare but fatal form of skin cancer associated with immunosuppression (Feng et al., 2008; Shuda et al., 2008). Although closely related to each other, WU Virus (WUV) and KI Virus (KIV) were discovered independently from acute respiratory tract infection patient samples (Allander et al., 2007; Gaynor et al., 2007). Evidence does not support either virus causing respiratory illness (Wattier et al., 2008). Rather, both viruses show a wide distribution, both geographically and demographically, and estimates of seropositivity range from 1%-65% of the population (Bialasiewicz et al., 2010; Bialasiewicz et al., 2007; Dang et al., 2011; Furuse et al., 2010; Kean et al., 2009; Zhao et al., 2010). In an effort to characterize the distributions of MCPyV, the Buck lab recently identified two new polyomaviruses, most closely related by sequence to WUV and KIV, Human Polyomavirus 6 and Human Polyomavirus 7, by sequencing viral genomes on healthy human foreheads (Schowalter et al., 2010). The authors proposed that the ancestral PyV may have been a skin virus, which took advantage of the frequent turnover of skin cells to replicate. While this hypothesis does not fully explain how polyomaviruses became so adept at replicating in non-dividing host cells, it is consistent with the virus's ability to maintain a lifelong association with its host.

In further support for a skin tropism, polyomavirus-like particles were also identified in the rare skin condition trichodysplasia spinulosa, a type of dysplasia unique among some transplant patients (Haycox et al., 1999; Wyatt et al., 2005). This virus was recently identified by sequencing and characterized as Trichodysplasia Spinulosa Polyomavirus (TSV) (van der Meijden et al., 2010). The very recent discovery of a Human Polyomavirus (HPyV9) with greater homology to the primate LPV may explain the previously detected high levels of human

seropositivity to LPV (Scuda et al., 2011). The detection of HPyV9 sequences in patients who were immunosuppressed for a variety of reasons does not preclude future disease association.

Together, as virus discovery techniques improve, the family of PyVs will likely continue to grow. Because many of the recently characterized viruses cannot yet be replicated in cell culture, the majority of what is known about these viruses is based on studies of the model virus, SV40.

1.2 POLYOMAVIRUSES AS TOOLS IN MOLECULAR BIOLOGY

PyVs have long provided a model to study viral biology and to some extent have driven the last half-century of molecular biology. The first virus identified in this family, MPyV, was isolated from a murine leukemia model, and gave the family the name "polyoma" for the many small tumors that were induced in rodents (Gross, 1953). As described above, SV40 was isolated from the monkey cell cultures used to culture the Salk Polio vaccine (Sweet and Hilleman, 1960). SV40 was also shown to induce tumors in rodents, and has proven to be an excellent model for tumorigenesis (see section 1.2.1). Because SV40 was discovered under such conspicuous conditions, it has catalyzed the development of new techniques and served as a means to ask a variety of biological questions. The utility of the PyV for developing tools and testing hypotheses is evidenced by the seven Nobel Laureates who credit a PyV in their development as scientists or award winning work (Berg, 2004; Dulbecco, 1975; Hartwell, 2001; Montagnier, 2008; Nathans, 1978; Tonegawa, 1987; zur Hausen, 2008). Here, I will highlight some of the major contributions to molecular biology from research on SV40, several of which have proved important for my dissertation work.

1.2.1 Characterization of cellular transformation and tumorigenesis

SV40 was first observed as a non-filterable agent that induced tumors in infected rodents (Sweet and Hilleman, 1960), and this observation laid the ground work to use SV40 as a model system for tumorigenesis. Following the description of SV40 causing tumors in hamsters, SV40 was quickly shown to cause a variety of tumors in other rodents, including hamsters (Ashkenazi and Melnick, 1963; Black and Rowe, 1963, 1964; Eddy et al., 1961; Gerber and Kirschstein, 1962; Kirschstein and Gerber, 1962; Rabson and Kirschstein, 1962; Vogt and Dulbecco, 1960). Both SV40 and MPyV were also shown to transform a variety of human and rodent cells and tissues in culture (Black and Rowe, 1963; Jensen et al., 1963; Koprowski et al., 1963; Ponten et al., 1963; Shein and Enders, 1962; Shein et al., 1962; Shein et al., 1963; Todaro and Green, 1966; Todaro et al., 1966). Assays were developed to further refine this transforming activity, and were used to show that PyV transformed cells lines are immortal, grow in low serum or independent of anchorage, and lose contact inhibition, which allows for formation of foci; they also induce tumors in mice, all of which are hallmarks of transformation (Aaronson and Todaro, 1968; Chiang et al., 1985; Damania and Pipas, 2009; Macpherson and Montagnier, 1964; Pipas, 2009; Smith et al., 1971; Todaro and Green, 1964).

Characterization of the transformed phenotype showed that a variety of host cell functions were altered in a carefully regulated manner (Oda and Dulbecco, 1968b). Enzymes such as DNA and RNA polymerases and kinases become activated (Frearson et al., 1966; Kit et al., 1967). Consequently, both cellular and viral DNAs, as well as mRNAs are synthesized (Dulbecco et al., 1965; Gershon et al., 1965; Hartwell et al., 1965; Oda and Dulbecco, 1968a, b). The demonstration that viral DNA carried the transforming ability of the virus focused the search for the cellular transforming factor (Crawford et al., 1964). Later work showed that

DNA fragments of the early region were required for transformation, and that temperature sensitive mutants of the A gene could confer a temperature sensitive transformation phenotype to various rodent cell lines (Abrahams et al., 1975; Brockman, 1978; Brugge and Butel, 1975; Kimura and Dulbecco, 1973; Kimura and Itagaki, 1975; Martin and Chou, 1975; Osborn and Weber, 1975; Tegtmeyer, 1972).

At this time, the focus of the field moved toward teasing out the role of the early region in transformation. Transformation by PyV is a relatively rare event, and is not an essential part of PyV replication or biology. Todaro and Green showed that one in 10^3 infections leads to transformation and that this rate increased in cells from Fanconi anemia patients, who have defective DNA damage repair (Todaro and Green, 1966; Todaro et al., 1966). In addition, the Koprowski group showed that while initially transformed human cells still produced some level of viral progeny, cells that survive crisis and are immortalized no longer produce infectious virus. These data suggest that there is no evolutionary advantage to viral transformation (Girardi et al., 1965). Interestingly, these immortalized cells did continue to produce what was known as the Complement Fixing Antigen, eponymous for the assay that was used to detect low levels of the virus, but later called the Tumor Antigen (TAg) (Girardi et al., 1965; Habel et al., 1965; Westphal and Dulbecco, 1968). Attempts to purify this antigen from tumors took advantage of its localization to nuclei and the complement fixing activity (Gilden et al., 1965; Lazarus et al., 1967; Sever, 1962). It was not until 1977 that mutagenesis (using techniques described in section 1.2.2) and immunoprecipitation experiments showed that the TAg was not an induced product of the host cell but was virally encoded by the early region (Rundell et al., 1977). Interestingly, in MPyV, transformation requires the activity of mTAg (Carmichael et al., 1984; Schaffhausen and Roberts, 2009; Templeton and Eckhart, 1984).

Studies of SV40 TAg then helped identify and characterize the major cellular tumor supressors, as well as elucidate the pathways necessary for immortalization and transformation. This is in part because the small genome of the PyV does not provide the functions required for viral replication. Rather, TAg manipulates the host cell environment to induce S phase and DNA replication while activating and blocking a DNA damage response (see section 1.3). As detailed below, TAg interacts with the tumor supressors Rb and p53, and the N-terminal J domain is further required for TAg mediated transformation (sections 1.3.2, 1.3.5 and 1.3.1, respectively). Additional host proteins have been shown to play a role in transformation, including the target of tAg and the MAPK pathway, PP2A (Hahn et al., 1999; Hahn et al., 2002). It is important to note, though, that virus-induced transformation is thought to occur as a result of a non-permissive infection, indicating that the activities that are essential for viral replication may lead to transformation when misregulated. This perspective has driven the use of the tumor virus model for understanding more general aspects of cancer.

1.2.2 Insights in viral and eukaryotic DNA replication

Viral replication requires replication of the viral genome, which in many virus systems is an extraordinarily complex event. Fortunately, the small genome of SV40 has made it a facile model to define how DNA architecture is established and to understand the molecular requirements for DNA replication. With the identification of restriction enzymes from *H. influenzae* (HindII/III), SV40 was the first complete genome mapped (Danna and Nathans, 1971; Danna et al., 1973). This allowed early investigators to assign functions to specific regions of the genome, including defining the coding sequences and regions essential for viral replication (Khoury et al., 1973; Scott et al., 1976). With a crude map available, the race to

sequence the genome of SV40 resulted in one of the earliest whole genome sequences (Fiers et al., 1978; Reddy et al., 1978). This detailed knowledge also provided the tools for the first example of site-specific mutagenesis, which involved nicking the DNA, excising one template strand, and treating the gap with a mutagen. The gap was then repaired by polymerase, thus introducing the mutation (Shortle and Nathans, 1978). Mutagenesis of this genome directed the initial description of the required sequence of the viral origin of replication, *ori* (Shortle and Nathans, 1979).

The small size of the viral minichromosome also made SV40 an ideal model for early characterization of the structural features of chromatin. Although not the first to recognize that histones bind DNA, the Chambon lab championed the use of SV40 to characterize the relationship between histones and DNA. Confirming their earlier results with DNA from other organisms (Oudet et al., 1975), they showed that SV40 DNA was associated with histones, and obtained electron microscopy (EM) images that supported the "Beads and Bridge" model of nucleosome structure (Germond et al., 1975). By proteinase treating the purified chromatin, these researchers also showed that the interaction between histones and DNA is responsible for DNA supercoiling. Refining these observations with a combination of EM and electrophoresis, the Chambon and Griffith labs then suggested that ~200bp are protected by the nucleosome, while the "bridging" DNA is of varying lengths (Bellard et al., 1976; Griffith, 1975). EM was also used to test the stability of the protein-DNA complexes, confirming that the ionic histone-DNA interactions are not sequence specific (Bellard et al., 1976).

SV40 also provided an early *in vitro* system to characterize eukaryotic DNA replication (Li and Kelly, 1984), which has been important for the work discussed in this dissertation. Because TAg manipulates host cell factors to replicate viral DNA, the proteins that are

necessary for viral DNA replication *in vitro* are also essential for eukaryotic DNA replication. In the original DNA replication system, monkey kidney cell lysate, an ATP regenerating system, and a plasmid with a viral *ori* were mixed, and the incorporation of a radiolabeled nucleotide into the synthesized DNA was measured. Later, more refined systems replaced lysate with purified components until the 10 essential proteins required for replication were identified (Waga and Stillman, 1994); only four of these proteins are required for initiation of replication. TAg binds to the pol α-primase (Murakami et al., 1986), either topoisomerase I or II (Yang et al., 1987), and RPA (Fairman and Stillman, 1988; Wobbe et al., 1987; Wold and Kelly, 1988). The activity of TAg and these three proteins is sufficient to initiate DNA replication as indicated by template unwinding and production of short DNA fragments, but full length copies of the DNA template were not produced. With the addition of PCNA (Prelich et al., 1987), activator I (or RF-C) (Lee et al., 1989; Tsurimoto et al., 1989), and pol δ (Lee et al., 1989; So and Downey, 1988; Tsurimoto et al., 1990; Weinberg and Kelly, 1989) the holoenzyme of pol δ is assembled, and a more processive polymerase activity was evident (Lee and Hurwitz, 1990; Tsurimoto and Stillman, 1989). This system also provided evidence for polymerase switching: pol α acted as a primase and pol δ functioned as the elongation polymerase, for the first time explaining the distinct biological functions of the multiple polymerases. However, many nicked circular DNA products were produced, due to a failure to remove RNA primers or ligate the generated Okazaki fragments. Subsequent isolation and addition of the final three components, the 5'-3' exonuclease MF-1 (or FEN-1), RNase H and DNA ligase I, together function to remove the primers and ligate the DNA fragments (Waga et al., 1994; Waga and Stillman, 1994). This purified *in vitro* system is fully competent to

replicate unnicked circular DNA products (Fanning and Zhao, 2009; Waga et al., 1994; Waga and Stillman, 1994).

1.2.3 Other activities essential for functional TAg expression: Splicing and Nuclear Localization

Two other activities of the early region are also essential for viral replication, namely the splicing of the early transcript and the localization of TAg to the nucleus. Evidence from the first sequence of the early region of SV40 suggested that large and small t antigens were splice variants (Fiers et al., 1978; Reddy et al., 1978), which prompted the use of the early transcript as a model of alternative splicing (Berk and Sharp, 1978). The Alternative Splicing Factor (ASF) was one of the early *trans*-acting factors shown to regulate the exon inclusion of the SV40 early transcript (Ge and Manley, 1990).

TAg must localize to the nucleus to recruit the host factors necessary for viral replication; mutations in the nuclear localization sequence (NLS) are defective for viral replication (Peden and Pipas, 1985). Analysis of the SV40 early sequences also helped identify one of the first minimal NLS motifs. While previous work had begun to show that some regions of proteins facilitated their nuclear localization, some TAg mutants that failed to localize to the nucleus were also described (Kalderon et al., 1984a; Lanford and Butel, 1984). Specifically, the Smith lab defined the NLS of TAg by characterizing a panel of TAg internal deletion mutants which failed to localize to the nucleus (Kalderon et al., 1984b). By appending β-gal to distinct TAg sequences, these investigators could artificially localize the majority of β-gal to the nucleus. The NLS sequence is a string of mostly basic amino acids, starting at residue 126 (PPKKKRKV). Mutations in any one of these residues shifts the population of TAg from

predominantly nuclear to being predominantly cytoplasmic (Smith et al., 1985). While similar basic regions are found on other nuclear proteins, the TAg NLS is shorter and shows a more potent localization effect compared to other NLS sequences identified. As such, it can easily be added to other proteins to modulate their localization (Smith et al., 1985; Yoneda et al., 1987).

1.3 LARGE T ANTIGEN

As the major early protein expressed by PyVs (Table 1), TAg encodes several activities and is responsible for changes to the cellular environment as well as for recruitment of essential host factors during viral replication. Indeed, the common features of TAg represent a shared solution to the challenge of replicating DNA in a non-dividing host without eliciting a defensive host cell response. To this end, TAg has several essential and independently folded domains: an N terminal J domain (1.3.1), an *ori* binding domain (OBD) (1.3.3) and a AAA+ ATPase domain (AAA+) (1.3.4). In addition to these domains, other essential and conserved TAg activities, binding Rb and p53, are described below (1.3.2 and 1.3.5). This 708 amino acid protein of SV40 is the best characterized TAg of the polyomaviridae. The high degree of sequence homology (see Table 2 and Figure 1) and the essential nature of these activities leads to a hypothesis that much of what we know about SV40 TAg will be true for other T antigens, although these activities have not yet been confirmed for all PyVs. Consistent with this view, the sequence conservation between TAgs is greater in the folded, functional domains in contrast to the less conserved linker regions (Table 2).

Table 2. Percent identity by pairwise alignment of full length TAgs and specific domains.

Pairwise alignments were done in Jalview and are reported as percent amino acid identity (Waterhouse et al., 2009). The alignments for each domain were based on the predicted SV40 domain boundaries, which are indicated. The alignments were performed with the following accession numbers P03070 (SV40), P03072 (JCV), P03071 (BKV), B6DVW7 (MCPyV) and E2ESL8 (TSV).

Comparison	**Full Length Protein**	**J domain (aa1-82)**	**OBD (131-246)**	**AAA+ (259-627)**
SV40 to JCV	72.6	81.7	81.0	74.8
SV40 to BKV	74.0	81.7	84.3	77.5
SV40 to MCPyV	39.6	40.2	53.7	47.4
SV40 to TSV	43.4	45.1	47.9	48.2
TSV to MCPyV	43.9	42.2	55.7	54.4

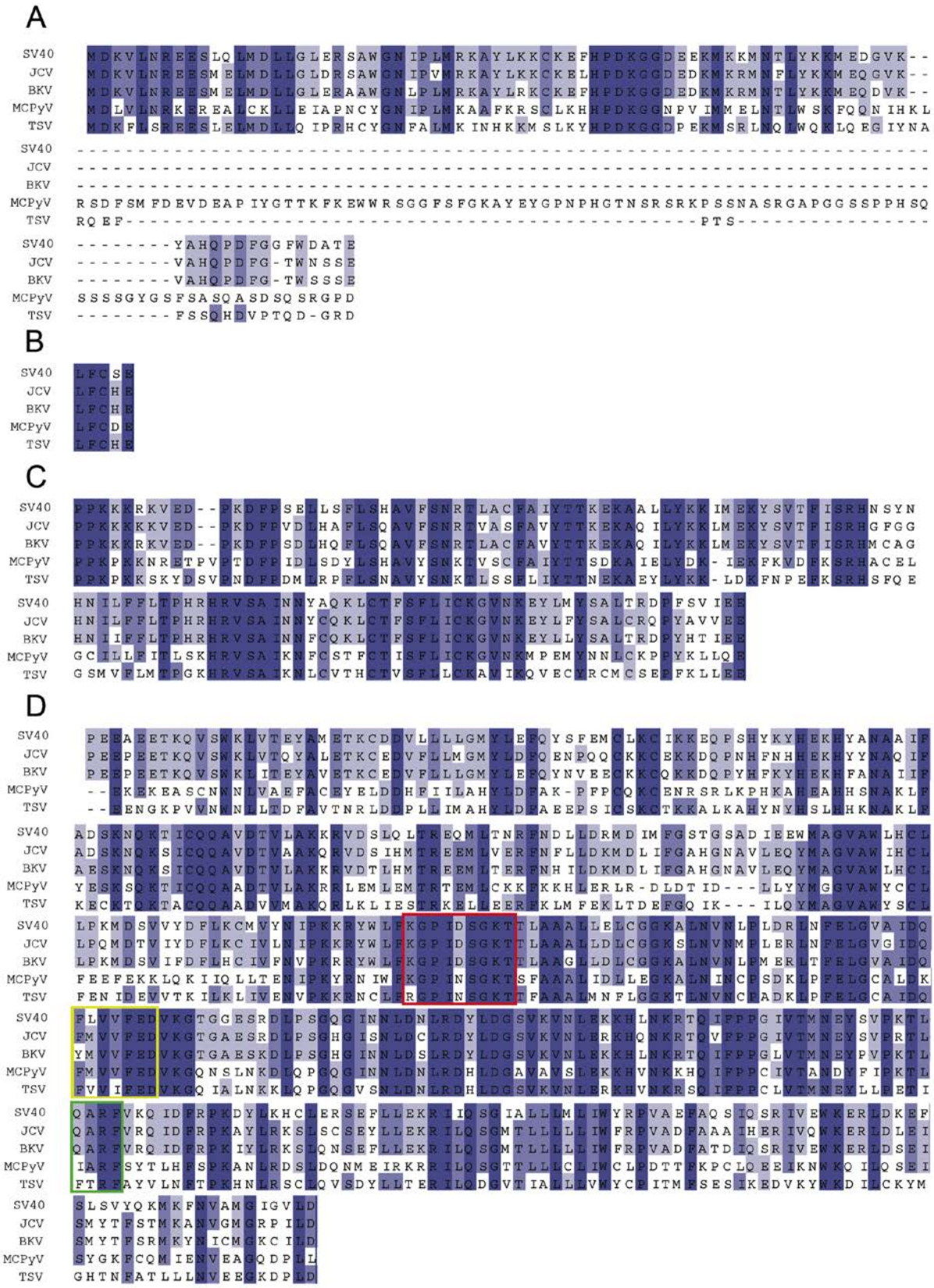
A
SV40
JCV
BKV
MCPyV
TSV
B
SV40
JCV
BKV
MCPyV
TSV
C
SV40
JCV
BKV
MCPyV
TSV
D
SV40
JCV
BKV
MCPyV
TSV

Figure 2. Alignment of the clinically relevant TAgs, displayed by domain.

Alignments were done in Jalview (Waterhouse et al., 2009). The alignments were performed with the following accession numbers P03070 (SV40), P03072 (JCV), P03071 (BKV), B6DVW7 (MCPyV) and E2ESL8 (TSV). Relative shades of blue indicate percentage shared identity: the darkest shade of blue indicates identity shared by all 5 viruses at that position, the lightest shade indicates that the identity is shared by only 3 of the viruses. A) Alignment of the J domain, based on the first 82 aa of SV40 TAg. This alignment highlights the insertion in the MCPyV J domain. B) Alignment of the Rb binding domain, showing conservation of the LXCXE motif. C) Alignment of the DNA binding domain, based on aa 130-251 of SV40 TAg. D) Alignment of the AAA+ ATPase domain. In this alignment, the Walker A motif (red box, SV40 TAg aa425-433) is highly conserved within the family, but both the Walker B (yellow box, SV40 TAg aa 467-474) and arganine finger motifs (green box, SV40 TAg aa 537-541) are less conserved between the TAgs and canonical AAA+ proteins (Koonin, 1993).

SV40 TAg interacts with a wide variety of host proteins to exert major and more nuanced effects on the host cell environment. A summary of the known TAg-protein interactions and the predicted function of the interaction is described in Table 2, highlighting the diversity and breadth of these interactions. Although my goal is to consider the importance of these interactions in normal virus replication, it is clear that many of these host-virus interactions have unintended consequences in the absence of a lytic infection. For example, TAg is capable of inhibiting the DNA damage response while encouraging DNA replication and endoreduplication. In addition, many of the proteins listed are known to be misregulated in cancer, including Fbw7 (Tan et al., 2008), AP-2 (Pellikainen and Kosma, 2007) and Bub1 (Williams et al., 2007). Such interactions have been used both to understand the role of the targeted protein in cancer, as well as to understand the roles of tumor suppressors in viral replication. It is of note that Table 2 does not include genetic interactions that influence protein expression patterns (Abend et al., 2010; Rathi et al., 2010; Rathi et al., 2009), DNA interactions (Bharucha et al., 1994; Montenarh and Henning, 1982; Tegtmeyer et al., 1983) or membrane affinity (Butel et al., 1989; Klockmann and Deppert, 1983; Lange-Mutschler and Henning, 1984), although many of each have been described. The remainder of this section will be dedicated to describing the specific roles of the major folding domains and activities of TAg both during infection and transformation.

Table 3. Summary of reported SV40 TAg interacting proteins and their predicted functions.

Interactors are organized by the general roles during viral replication, including DNA replication, cell cycle regulation, transactivation, modification of the DNA damage response, localization or unknown functions. Accession numbers from the NCBI Protein Database are included to minimize confusion regarding nomeclature, and were determined based on the species and details of the interaction noted in the reference column.

Binding Partner: Accession Number	**Protein Function**	**Binding Site (aa)**	**Viral Function**	**Evidence**	**References**
DNA replication					
Pol-prim: 2KEB_A	RNA primase for DNA replication	425 and AAA+ domain (259-627)	Initiates lagging strand DNA replication	Interaction mapped to p68 subunit of pol-prim, NMR structure	(Huang et al., 2010; Murakami et al., 1986)
PCNA: P12004	Processivity factor for pol δ/ε		Replication of viral genome	Co-purified in replicating fractions of human cell lysates	(Prelich et al., 1987)
RF-C: NP_001191676	Loads PCNA onto DNA		Replication of viral genome	Purified RF-C required for reconstituted DNA replication assay	(Lee et al., 1989; Tsurimoto and Stillman, 1989)
Pol δ	DNA polymerase		Replication of viral genome	Cofractionation experiments indicate this is a PCNA dependent interaction	(Lee et al., 1989; So and Downey, 1988; Tsurimoto et al., 1990; Weinberg and Kelly, 1989)

Topo I or II: AAI36298, P11388	Topoisomerase, involved in DNA supercoiling	83-106 and 612, 616, 617, and 621	Facilitates initiation of DNA replication by relaxing DNA	Mutational analysis of TAg disrupts Topo I binding and activity, purified Topo II required for reconstituted DNA replication assay	(Ishimi et al., 1992; Khopde and Simmons, 2008; Roy et al., 2003; Wold et al., 1989; Yang et al., 1987)
MF-1 Fen-1: CAG38799	5'-3' exonuclease		Replication of viral genome, required for Okazaki fragment processing	Purified MF1 required for reconstituted DNA replication assay	(Waga et al., 1994; Waga and Stillman, 1994)
RNase H			Replication of viral genome, required for Okazaki fragment processing	Purified RNase H required for reconstituted DNA replication assay	(Waga et al., 1994; Waga and Stillman, 1994)
DNA ligase I: AAA59518	Ligates Okazaki fragments		Replication of viral genome, required for Okazaki fragment processing	Purified DNA ligase required for reconstituted DNA replication assay	(Waga et al., 1994; Waga and Stillman, 1994)
RPA: AAA58350	Stabilizes ssDNA during replication	64-249	As part of the viral replisome, stabilizes viral ssDNA during unwinding	TAg specific monoclonal antibodies prevent interaction	(Melendy and Stillman, 1993; Weisshart et al., 1998)
Cell cycle regulation					
Hsc70 AAK17898	Molecular chaperone	1-82, specifically HPD motif at 42-44	Assembles virion and releases E2F from Rb	Mapped by mutational analysis and reporter assays, loss of J domain interaction results in decreased viral replication and transformation	(Chromy et al., 2006; Chromy et al., 2003; Sawai et al., 1994; Srinivasan et al., 1997; Sullivan et al., 2000)

pRb, p107, p130: AAA69808 P28749 Q08999	Inhibits E2F until initiation of S phase	LXCXE Motif, 102-107	By disrupting the Rb-E2F interaction, TAg activates transition to S phase	pRb-TAg co-crystal structure	(Amin et al., 1994; DeCaprio et al., 1988; Kim et al., 2001)
cdc2: AAI07751	Cell cycle regulator and kinase	Phosphorylates Thr124	Enhances ori binding	Mutant lacking Thr124 is not phosphorylated	(McVey et al., 1989)
Fbw7: NP_361014 NP_060785 NP_001013433	Substrate recognition for the SCF^{Fbw7} ubiquitination complex	Interaction occurs via phosphorylation at Thr701	TAg acts as a competitive inhibitor for the Ub-ligase, preventing ubiquitination and degradation of substrates such as cyclin E and other cdks	TAg co-immunoprecipitates with all three Fbw7 isoforms	(Welcker and Clurman, 2005)
Transactivation					
TFIIB: NP_001505	Transcription factor, member of the RNA pol II pre-initiation complex	133-249	Transactivation of the late promoter	Truncation mutants of TAg used to map recombinant TFIIB interaction by pull-down	(Johnston et al., 1996)
Sp1	Transcriptional activator protein	133-249	Transactivation of the late promoter. May promote TAg binding to ori	Truncation mutants of TAg used to map recombinant Sp1 interaction by pull-down, Sp1 isoform is unclear	(Johnston et al., 1996)
RNA pol II	RNA polymerase essential for transcription	133-249	Transactivation of the late promoter	Truncation mutants of TAg used to map RNA pol II interaction by pull-down, specific subunits interacting are unclear	(Johnston et al., 1996)
IRS1:	Insulin receptor,	107 (k1 mutant)	Mediates activation of	IRS1 is required for TAg	(DeAngelis et al., 2006;

NP_005535	tyrosine kinase transducer, which signals increased Glut4 expression		Akt, required for transformation	dependent transformation	Yu and Alwine, 2008)
TBP: P20226	TATA Binding protein, subunit of SL-1, TFIID and TFIIIB	181-205	In combination with other transcription factors, essential for activation of polymerase, may inhibit DNA replication	Truncation mutants of TAg used to map recombinant TBP interaction by pull-down	(Herbig et al., 1999; Johnston et al., 1996; Zhai et al., 1997)
SL1 complex-TAF_1110, $TAF_1$48: Q15573 Q15572	Transcription factor involved in target selectivity, subunit of SL-1	1-538	Co-activates transcription of ribosomal RNA, recruits RNA pol II	Radiolabeled co-immunoprecipitations with truncated TAg mutants map the interaction domain of TAg with $TAF_1$110, $TAF_1$48 but not $TAF_1$63 complex	(Mazzarelli et al., 1995; Zhai et al., 1997)
TEFI NP_068780	Transcription factor	133-249	May be involved in early-to-late transcription transition	Truncation mutants of both interacting partners used to map TAg interaction domain to TEF1 TEA domain by pull-down	(Berger et al., 1996)
c-Jun and c-Jun-related protein	Part of the AP-1 transcription factor, which targets genes required for cell cycle control		Repression of the P_o promoter, and P_o expression (a glycoprotein in the myelinated plasma membrane), possibly contributing to demyelination	TAg, c-Jun and c-Jun-related protein (identity unclear) co-immunoprecipitated and both bind P_o promoter *in vitro*	(Bharucha et al., 1994)
AP2: P05549	Transcription factor, targets		Inhibits AP2 mediated transcription	TAg changes the AP2 sedimentation	(Mitchell et al., 1987)

	genes required for cell cycle control				
Modification of the DNA damage response					
Bub1 O08901	Mitotic checkpoint kinase	89-97	Misregulates DNA damage response to promote viral replication	Identified by yeast two hybrid interaction, confirmed by co-immunoprecipitation from 3T3 cells. TAg mutant Δ89-97 fails to interact	(Cotsiki et al., 2004; Hein et al., 2009)
ATM: Q13315	DNA damage response and kinase	Phosphorylates Ser120	Phosphorylates Ser-120, which is thought to inhibit TAg. However ATM is required for efficient viral replication	Truncation mutants of TAg used to map the specific phosphorylation site in an *in vitro* ATM kinase assay	(Shi et al., 2005)
Nbs1: BAA28616	Required for dsDNA break repair via MRN complex	147-259	Promotes endoreduplication	TAg co-immunoprecipitates the entire MRN complex, truncation mutants used to identify both the region of Nbs1 and TAg responsible	(Wu et al., 2004)
TACC2: O95359	May organize microtubules at the centrosome	250-708	Inhibition of TACC2 inhibits microtubule assembly	Interaction identified by yeast two hybrid, confirmed by co-immunoprecipitation, results in mitotic defects that can be rescued by TACC2 overexpression	(Tei et al., 2009)
p53: P04637	Monitors DNA damage, provides a G1-S checkpoint	351-450 and 533-627	Prevents DNA damage response, promotes transition to S phase	Interaction confirmed by crystal structure	(Lilyestrom et al., 2006)
Localization					

Importin 58/97: NP_942021 NP_058759	Regulating protein entry into the nucleus	NLS-126-135	Imports TAg into the nucleus	Interaction showed by ligand-Western blot, and confirmed by phenotype using TAg mutants in NLS, and CKII and DNA-PK phosphorylation sites	(Hubner et al., 1997; Xiao et al., 1997)
casein kinase II (CKII): P19139	Serine/threonine kinase with a variety of targets, including Wnt signaling and DNA damage	Phosphorylates Ser112	Leads to phosphorylation which enhances interaction with importin, supports cell transformation	*In vitro* assays with TAg peptides indicate that CKII (presumed both subunits) specifically phosphorylates the TAg sequence, and that this increases affinity for importin.	(Gotz et al., 1995; Hubner et al., 1997; Xiao et al., 1997)
Tubulin: NP_001074440	Structural polymer	Requires p53	Possibly regulates intracellular trafficking	Co-immunoprecipitates with TAg and p53 in a complex that is dependent on the presence of both.	(Maxwell et al., 1991)
double-stranded DNA dependent protein kinase (DNA-PK) P78527	Involved in DNA damage repair	Phosphorylates Ser120, 665, and 667	Phosphorylates Ser120, enhancing nuclear import via CKII phosphorylation and importin interaction	*In vitro* reactions show DNA-PK phosphorylates TAg at the same sites, which are phosphorylated *in vivo*. Phosphorylation at Ser120 mediates the rate of nuclear import.	(Chen et al., 1991; Xiao et al., 1997)
Chromatin	Nucleoprotein complex comprised of histone and non-histone proteins bound to DNA		May be involved in several processes during infection and viral replication	Filter binding assays used to show affinity for both DNA and chromatin, localization experiments confirm a protein-protein interaction.	(Hinzpeter and Deppert, 1987; Persico-DiLauro et al., 1977)
Unknown function					

SCF –like ubiquitination complex including Cul7, Fbw6/Fbx29/Fbxw8 and Rbx1/Roc1 NP_079887 NP_796163 XP_358324, NP_766309, NP_062686	E3 ubiquitin ligase	98-102	Required for transforming MEFs, role unclear	Co-immunoprecipitates with TAg. TAg mutants that do not co-immunoprecipitate the Cul7 Fbw6 Rbx1/Roc1 complex are transformation defective.	(Ali et al., 2004)
CBP/ p300/ p400: NP_001020603 NP_808489 Q8CHI8	Histone acetyl transferases	Proposed via p53	Role during infection unclear	Co-immunoprecipitates with TAg. CBP acetylates K697, which stabilizes TAg.	(Avantaggiati et al., 1996; Eckner et al., 1996; Lill et al., 1997; Shimazu et al., 2006; Srinivasan et al., 1997)

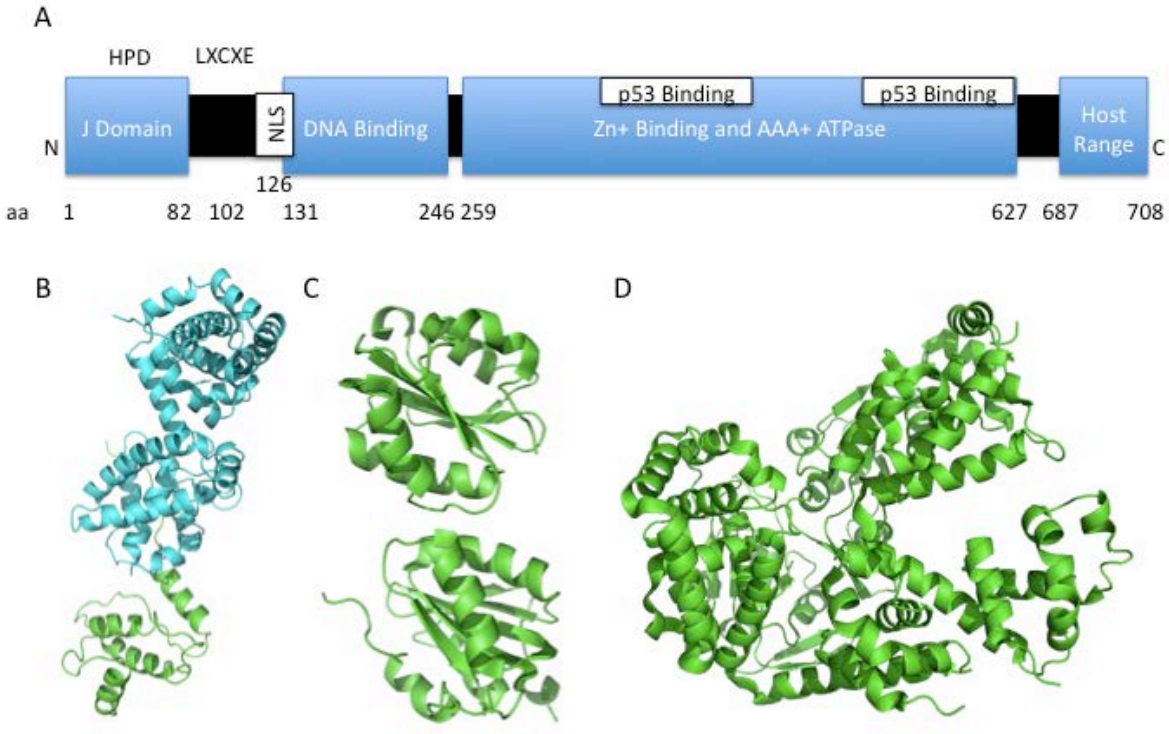

Figure 3. Domain map of TAg and crystal structures of three domains.

A) The domain map highlights the major features conserved between polyomaviruses based on SV40 TAg, including the folded domains depicted in green in B-D, the Rb binding sequence (LXCXE), a nuclear localization sequence (NLS) and p53 binding sites (aa 351-450 and 533-627). Not all TAgs have a host range domain, and the length of linker sequences between domains is different in many of the human polyomaviruses. Structures have been solved for the independently folding domains, which are displayed in green. B) The J domain (green) bound to the pocket domain of Rb (which is denoted in blue) (PDB: 1GH6) (Kim et al., 2001). C) The DNA Binding domain displayed as a dimer (PDB: 2IPR) (Bochkareva et al., 2006). D) The AAA+ domain, displayed as a monomer (PDB: 1N25) (Li et al., 2003). Structures are not to scale.

1.3.1 J domain and molecular chaperone activity

J domains stimulate the ATPase activity of the Heat Shock Protein of 70kDa (hsp70) molecular chaperones and are generally involved in processes such as protein folding or unfolding (Craig et al., 2006; Walsh et al., 2004). The J domain derives its name from the classical co-chaperone activity described by the *E.coli* protein DNAJ, which binds to and stimulates a bacterial hsp70, DNAK (Liberek et al., 1991; Mayer and Bukau, 2005). Although the family of hsp70s is known to respond to heat shock, the hsc70 is constitutively expressed in unstressed cells (Gething and Sambrook, 1992). Early reports had shown that TAg interacts with hsc70 (Sawai and Butel, 1989); however, because this protein functions as a general peptide binding protein, it was not clear whether the hsc70 interaction was biologically relevant.

The N terminal J domain of TAg (aa 1-82) (Figure 2) was first described in 1997 in three concurrent studies (Campbell et al., 1997; Kelley and Georgopoulos, 1997; Srinivasan et al., 1997). First, it was shown that chimeric proteins including the J domain of TAg could complement DNAJ mutants in a bacteriophage plaque assay (Kelley and Georgopoulos, 1997). Second, it was demonstrated that point mutants in the J domain abolished the interaction with hsp70, and that this interaction was necessary for efficient DNA replication in culture (Campbell et al., 1997; Peden and Pipas, 1992). Interestingly, the J domain is not required for *in vitro* DNA replication assay described in section 1.2.2 (Weisshart et al., 1996), suggesting some fundamental distinctions between the *in vitro* and *in vivo* assays (see section 4.3). Third, the Pipas lab found that deletions or point mutations in the J domain compromise cellular transformation. Moreover, a truncation mutant of TAg lacking the endogenous ATPase activity stimulated the ATPase activity of hsc70 and stimulated the ability of hsc70 to release an unfolded peptide, both of which are hallmarks of DNAJ-like activity. This study further

established that transformation deficient mutants incapable of binding the tumor suppressor Rb (section 1.3.2) cannot be rescued by J domain mutants. These data both established that hsc70 activity was essential for transformation and suggested that the J domain must act in *cis* with Rb-binding activity (Srinivasan et al., 1997). Based on the collective data, it was proposed that TAg uses hsc70 to disrupt the Rb-E2F complex, which is essential for moving the cell into S phase (Ahuja et al., 2005; Brodsky and Pipas, 1998). This hypothesis is further supported by the cocrystal structure of the J domain and Rb pocket domain (Figure 3), which confirmed that the Rb-E2F complex is positioned in proximity to hsc70 (Kim et al., 2001). The structure also confirmed that the first 82aa of TAg would form a 4 helical bundle, which all J domains possess, although the fourth helix is longer than typical J domain.

Other work has since shown that the activity of the J domain is essential for additional activities during viral infection. For example, the Garcea lab demonstrated that the J domain promotes both assembly and disassembly of the capsid *in vitro*, suggesting an important role for host chaperones in viral entry and exit (Chromy et al., 2006; Chromy et al., 2003). More recently, work in our lab confirmed that small molecules that target J domain stimulation of hsc70 activity inhibit viral replication in a cell culture system (Wright et al., 2009). Because molecular chaperones play dynamic roles in a variety of cellular processes, the J domain may represent a viable drug target for a variety of diseases (see section 1.4).

1.3.2 Binding and inactivating the Rb family

TAgs share a highly conserved Rb binding motif (LxCxE) (Figure 2), which is essential for transformation (DeCaprio, 2009; Kalderon and Smith, 1984; White and Khalili, 2006). The retinoblastoma susceptibility gene, Rb, was first identified following a genetic study suggesting

that childhood retinoblastoma has a hereditary component (Knudson, 1971). This gene was later shown to be mutated in retinoblastoma tumors, suggesting that loss of Rb function promotes cancer (Friend et al., 1986; Fung et al., 1987; Horowitz et al., 1989; Lee et al., 1987). The Livingston lab then demonstrated that TAg binds to the retinoblastoma susceptibility gene product (pRB) (Figure 3), and perhaps more interestingly, TAg mutants that are incapable of binding pRb also failed to transform cells (DeCaprio et al., 1988). TAgs from a variety of PyVs have been confirmed to bind Rb, indicating that this function is conserved (Dyson et al., 1990). Studies of Rb in TAg transformed cells also helped develop the "multiple hit" hypothesis of carcinogenesis, as well as enlightening our understanding of normal cell cycling (reviewed in (DeCaprio, 2009). By binding and inactivating Rb family members in a J domain dependent manner, TAg derepresses E2F and activates E2F mediated transcription (Ahuja et al., 2005; Srinivasan et al., 1997; Sullivan et al., 2004; Sullivan et al., 2000). This misregulation of E2F leads to initiation of S phase, which promotes viral replication by upregulating the host factors required for DNA replication (Chong et al., 2009; Rathi et al., 2007; Saenz-Robles et al., 2007).

1.3.3 DNA binding domain

The DNA binding domain, or *ori* binding domain (OBD) of TAg (Figure 3), is essential for recognizing and melting the viral origin of replication. Structures of this domain have been solved, and the essential activity maps to aa 131-250 (Bochkareva et al., 2006; Luo et al., 1996; Meinke et al., 2006). The DNA binding activity of TAg has been well described (reviewed in (Bullock, 1997; Fanning and Zhao, 2009). Using a series of *ori* mutants and by measuring effects on DNA replication, the Tegtmeyer lab defined the core *ori* and TAg binding site as the 60 nucleotide sequence between 5211 and 31 (Deb et al., 1986). Sedimentation of this complex

implied that the DNA binding activity of TAg required oligomers (Bradley et al., 1982; Gidoni et al., 1982). Detailed mutational analysis of the binding site indicated that TAg makes specific contacts within the GAGGC pentanucleotide palindrome sequence of the *ori* (Deb et al., 1987), which suggested that multiple TAgs may orient to and bind at this site if each TAg recognizes two of the four pentanucleotide palindrome sites. Moreover, based on the known structures of TAg at the *ori*, it is known that TAg monomers bind first, then recruit an asymmetric TAg tetramer, and finally a dodecamer capable of bidirectionally unwinding DNA assembles (Bochkareva et al., 2006; Mastrangelo et al., 1989). It is clear from these structures that some conformational rearrangements are required to adapt the bound structure to the unwinding activity, and the nature of this change remains an active area of investigation. Using competition experiments, the Simmons lab was able to demonstrate that TAg can bind to non-specific DNA sequences (although with less affinity than to the *ori*), and that this non-specific binding requires cooperativity in trans between the ATPase domains (described below; (Lin et al., 1992; Wun-Kim and Simmons, 1990). A variety of host transcription factors interact also via this domain (Table 3, TFIIB, Sp1, RNA-pol II, TBP and TEF-I), indicating that this domain is not only essential for viral DNA replication but also transactivation.

1.3.4 AAA+ ATPase and associated activities

The AAA+ ATPase domain of TAg is conserved and essential for viral replication. This domain is involved in many activities during viral replication, including binding p53 (refer to section 1.3.5 and Figure 3) and other host proteins (Table 3, Topo I and II, TACC2). The most central of these activities is the helicase activity, even though it was initially unclear whether TAg could unwind DNA (Giacherio and Hager, 1980; Myers et al., 1981). Although TAg bound

to chromatin (Stahl and Knippers, 1983) and TAg-specific monoclonal antibodies prevented viral DNA replication (Mercer et al., 1983; Stahl et al., 1985), the biological function of the TAg ATPase activity was mysterious until helicase activity was demonstrated *in vitro* (Stahl et al., 1986). Subsequent sequence analysis indicated homology between TAg and the MCMs, which are the eukaryotic replicative helicases (Koonin, 1993). As a result, this homologous region of TAg has been described as a AAA+ ATPase domain, which acts as a hexamer with the ATPase active site at the interface of two monomers (Neuwald et al., 1999). In this active site, the Walker A motif from one monomer binds ATP and coordinates a Mg ion, while the Walker B motif of the same monomer provides the catalytic glutamate that hydrolyzes the ATP held by the Walker A motif. The conserved arginine finger (some times called box IV) also interacts with the nucleotide and iscontributed by a second monomer (Figure 2). The hydrolysis of ATP induces a conformational change that provides the mechanical action necessary for helicase activity (Snider et al., 2008).

The solved structure of the AAA+ ATPase domain revealed a central channel, which is hypothesized to channel DNA during unwinding (Li et al., 2003). The solved structure of aa 251-627 also contains the Zn binding domain, which was shown to be important for hexamerization, although it is not clear if the Zn ion itself plays any role beyond supporting the folding of this domain. Finally, helicase activity, which was previously mapped to aa 131-627, can also be demonstrated with a shorter fragment (aa 251-627), suggesting that the DNA binding activity of TAg is not essential for helicase activity (Li et al., 2003). This helicase activity has since been used as a model for the study of other helicases, including the MCMs, papillomavirus E1 and adeno-associated virus Rep68 (Bochman and Schwacha, 2010; Mansilla-Soto et al., 2009).

1.3.5 Binding and misregulation of p53

p53 was identified as a host protein that was upregulated in TAg expressing cells, was recognized by sera from rodents with SV40-induced tumors and bound directly to TAg (DeLeo et al., 1979; Kress et al., 1979; Lane and Crawford, 1979; Linzer and Levine, 1979). It was hypothesized that this 54kDa protein may be an important oncogene, but the connection was not proven until efforts by several labs showed that transfection with p53 cDNA in addition to Ras could transform rat embryo fibroblast cells (Eliyahu et al., 1984; Jenkins et al., 1984; Parada et al., 1984). Surprisingly, later work cloned the p53 cDNA from these transformed fibroblasts and determined that the cells expressed a mutant form of p53, and that this mutant form lost the tumor suppressing function of the wild-type gene (Finlay et al., 1989; Hinds et al., 1989; Pennica et al., 1984). We now know that wild-type p53 is a transcription factor that mediates cell cycle arrest or apoptosis in response to cellular stress as a result of DNA damage; this can prevent progression to S phase as a result of the TAg-mediated DNA damage response (Talos and Moll, 2010; Wu and Levine, 1994). TAg binds to and inactivates p53 function during an infection (Bargonetti et al., 1992; Harris et al., 1998; Lilyestrom et al., 2006). The p53 binding site was originally mapped to two distinct regions in the ATPase domain of TAg (Table 3; (Kierstead and Tevethia, 1993). The cocrystal structure of the TAg ATPase domain bound to p53 has been solved, which indicated that TAg inhibits p53 by binding a region overlapping the p53 DNA binding site, and requiring a single region on TAg (Figure 3; (Lilyestrom et al., 2006)).

The consequences of TAg dependent inactivation of p53 during viral infection are more complex than simply preventing a DNA damage response, although this is one important result of this interaction. Given the diversity of downstream targets that are modified by p53 (Zhao et al., 2000), it is becoming clear that TAg binding to p53 may fine tune a response, the outcomes

of which are incompletely understood. Microarray data have suggested that some targets of p53 are up regulated, while the DNA damage response itself is prevented (Rathi et al., 2009). A careful characterization of the transformation effeciencies and growth properties of TAg in the presence of p53 and p53 mutants suggests that TAg may induce a p53 gain of function (Hermannstadter et al., 2009). Data from the Dornreiter lab have shown that one consequence of TAg binding p53 is stabilization of cyclin A-Cdk kinase activity, suggesting that TAg expressing cells are trapped in S phase (Rohaly et al., 2010). While initially it seemed surprising that the TAg oncogene would manipulate the activity of another tumor supressor, it has since become clear that targeting oncogenic pathways is the *modus operandi* during the replication of PyVs.

1.3.6 Host range domain

Although the C terminal host range domain is poorly conserved and largely mysterious, there is an eponymous phenotype associated with this region. Specifically, truncations of TAg that contain only the first 627 amino acids retain the ability to transform cells lines, but lose the ability to replicate in some types of African green monkey cells (mutants grow on BSC, but not CV1 cells; (Pipas, 1985; Tornow and Cole, 1983a, b). This region is also essential for the "adenovirus helper function," which is the enhancement of adenovirus type 2 (Ad2) infection in an SV40 dependent manner (Cole et al., 1979; Cole and Stacy, 1987). The host range region is post-translationaly modified with multiple phosphorylation and acetylation marks by several targets, which would suggest complex regulation, but the biological functions of these modifications are not yet understood (Kress et al., 1982; Poulin et al., 2004; Scheidtmann et al., 1991; Scheidtmann et al., 1982; van Roy et al., 1983). While there is evidence that host range mutants fail to assemble mature virions, the molecular basis for this effect also remains unknown

(Spence and Pipas, 1994). In fact, discovering the function of this domain has proved challenging. There is little evidence that the C terminus of SV40 TAg is structured. It has been suggested that the diverse activities associated with the host range domain may require host cell interactors, but the identities of these proteins remain elusive. In one case, Fbw7 was shown to bind to this region, but the predicted role for this interaction is stabilization of cyclin E kinase (Welcker and Clurman, 2005), which cannot explain the diverse activities associated with this region. Perhaps more confounding is the lack of conservation of this domain: a host range is only predicted in SV40, BKV and JCV (Pipas, 1992). If this domain truly supports virion assembly, how do the TAgs that lack this domain assemble virions?

1.3.7 Differences between TAgs

Although there are many important structural and functional similarities between TAgs from different viruses, the distinctions between them may help to highlight the differences in life history and other activities. While most PyV share the ability to transform cells, few are efficient at transformation or as quick to replicate as SV40, which is why SV40 has been favored as the model for this virus family. One key difference between the other PyVs and their TAgs is tropism. Tropism is partially determined by receptor recognition, but infection efficiency can be affected by changes to the sequences of the viral promoter-enhancer regions and in the early coding regions of PyVs (Bollag et al., 1989; de Villiers et al., 1982; Fujimura et al., 1981; Katinka et al., 1980). Given that manipulation of native host protein function is the dominant theme of PyV infection, it seems likely that changes in either promoter or protein sequences may affect their recognition by host factors. For example, there is evidence that not all TAgs bind host partners like Rb and p53 with similar affinity (Bollag et al., 1989; Dyson et al., 1990; Harris

et al., 1996). Because this conclusion is based on co-immunoprecipitations, it is possible these data may instead reflect relative antibody affinities. Notably, binding affinities for these partners have not been determined for all TAgs (especially from the seven PyVs discovered after 1996), but differences in binding affinities for these host factors would be predicted to alter infection efficiency.

In contrast to SV40 TAg, most of the TAgs in this family are not yet well characterized, but there are some predictions that can be made based on sequence analysis. While all TAgs share the major domains described above (see sections 1.3.1, 1.3.3, 1.3.4), as well as sequences that bind Rb, the intervening sequences are less conserved. Specifically, the length of the linker region between the J domain and OBD is quite divergent and only the TAgs of SV40, BKV and JCV are predicted to express a host range. It is expected that these features may alter interactions with host proteins, and in fact MCPyV TAg binds the host protein VAM6P via the long linker region between the J domain and OBD (Liu et al., 2011a). Even among the large number of cellular partners for TAg (Table 3), VAM6P has not been shown to interact with SV40 TAg. These differences might explain some of the disparate efficiencies in transformation and infection.

1.4 POLYOMAVIRUSES AND HUMAN DISEASE

Since the initial characterization of SV40 induced neoplasms in mice (Stewart et al., 1958), there have been questions about the role of PyVs in disease. Although these viruses are widely distributed, there is generally little disease burden from PyV infection. The polyomavirus-related diseases that have been described predominantly affect the immunosuppressed, and as

such the majority of these diseases are not studied in great detail. Given the long history and detailed understanding that we have of PyV biology, it seems ironic that these orphan diseases are inadequately treated.

1.4.1 Disease in immunocompetent patients

1.4.1.1 SV40

Although known as a DNA tumor virus, there is little convincing evidence to link SV40 infection to human cancers or cancer in the natural host, which is the Rhesus Macaque (Eddy et al., 1961; Sweet and Hilleman, 1960). Much of the evidence for SV40-induced transformation (section 1.2.1) derives from studies in non-permissive cell lines, specifically in rodent lines. Nevertheless, researchers have looked for a link between SV40 and cancer. The official stance of the US government is that the data are insufficient to determine if there is a causal relationship between SV40 and cancer (Stratton et al., 2003). However, this is in large part due to the difficulty of determining which individuals were exposed to SV40 and at what dose (Stratton et al., 2003). It is generally accepted among most researchers that there is not a credible direct link between SV40 infection and increased cancer risk (Levine, 2009).

Current evidence does not discount the possibility that SV40 may be a synergistic risk factor for mesothelioma when combined with asbestos exposure. SV40 sequences can be identified in some but not all mesothelioma samples (Klein et al., 2002; Shivapurkar et al., 2000; Shivapurkar et al., 1999; Testa and Giordano, 2001). The Carbone lab showed that neither exposure to asbestos nor SV40 infection could transform cells, but when combined cells were transformed (Bocchetta et al., 2000). In these experiments, asbestos exposure activated p53, preventing cell lysis and maintaining TAg expression from the episomal viral vector (Bocchetta

et al., 2000). The episome may explain the failure of some groups to detect SV40 sequences in mesotheliomas, while others have suggested that SV40 sequences are detected as a result of lab contamination (Klein et al., 2002). Together, one view is that SV40 may be one risk factor for the complex disease of mesothelioma, which may also arise from a number other factors besides asbestos exposure (Klein et al., 2002; Pershouse et al., 2006).

1.4.1.2 Other PyVs

Current evidence based on seropositivity and PCR detection suggests that the majority of the human PyVs are acquired early in childhood and remain persistent (Bolen and Consigli, 1980; Kantola et al., 2010; Kunitake et al., 1995; Zheng et al., 2004). Based on detection in fecal matter or urine, it is thought PyVs are acquired through a fecal-oral or possibly respiratory route (Bofill-Mas et al., 2001; Monaco et al., 1998). The initial infection is presumably benign in healthy patients. Although sometimes identified in acutely ill patients, there has not yet been any specific set of symptoms linked to initial PyV infection (Dalianis et al., 2009; Neske et al., 2009; Wattier et al., 2008). Interestingly, even in healthy patients, periodic levels of increased viral shedding throughout life are thought to maintain seropositivity, although it is not clear what prompts this apparent increased viral replication (Kean et al., 2009; Schowalter et al., 2010). However, the persistence of infection leaves these viruses free to replicate should the host become immunocompromised.

1.4.2 Known disease in immunosuppressed patients

Both BKV and JCV were discovered in 1971, and represent the first native human PyVs (Gardner et al., 1971; Padgett et al., 1971). As both were discovered in acutely sick patients,

efforts focused on characterizing the role of these viruses in disease. It has been reported that between 20-80% of the population has antibodies against most PyVs, depending on geography, and that there is little if any seroprotective effect (Kean et al., 2009; Pastrana et al., 2009). Given the wide distribution of PyVs and their lifetime prevalence, immunosuppressed patients have an increased susceptibility to developing PyV related diseases.

It is important to note that immunosuppressed populations are growing worldwide. Advances in transplant technology have improved outcomes for many patients who suffer organ failure, and those patients are surviving longer after transplant (OPTN, 2009). Further, the World Health Organization estimated that 33 million people globally are living with AIDS, and that number continues to grow as anti-retroviral drugs prolong AIDS survival rates (WHO, 2008). As these populations continue to grow, so will the apparent impact of PyVs.

1.4.2.1 BKV

A role for BKV is well established in BKV Associated Nephropathy (BKVAN) after kidney transplant (Binet et al., 1999; Nickeleit et al., 1999). BKVAN is marked by increased viral shedding in urine and blood, and more than doubles the probability of organ rejection (Dharnidharka et al., 2009). This condition is also sometimes called Polyomavirus Associated Nephropathy (PVAN), in part, because it was previously difficult to distinguish between the different PyVs by histological methods, and it is not yet clear if other PyVs can cause similar symptoms. Estimates are that BKVAN occurs in between 3-30% of kidney transplant patients (Basse et al., 2007; Giraldi et al., 2007; Hirsch et al., 2002). Previously, diagnosis required an invasive biopsy, but fortunately rapid detection is now possible with qPCR techniques, which has lead to better standards for monitoring disease progression (Bechert et al., 2010; Elfaitouri et al., 2006; Vats et al., 2006).

BKV also causes hemorrhagic cystitis after hematopoietic stem cell transplant in an estimated 10% of patients (Bedi et al., 1995; Kondo et al., 1998; Peinemann et al., 2000; Seber et al., 1999). Hemorrhagic cystitis is a painful inflammation and causes bleeding in the bladder and urethra that puts the patient at risk for further complications (Sencer et al., 1993). Interestingly, only half of patients shedding BKV after transplant will develop hemorrhagic cystitis (Bedi et al., 1995; Hirsch and Steiger, 2003), and preliminary evidence suggests that rearrangements in the noncoding regulatory region of BKV correlate to the development of clinical symptoms (Broekema et al., 2010; Chen et al., 2001; Stoner et al., 2002). With improved monitoring and treatment options, the total risk of disease has decreased, but there are risks associated with treatment (discussed in section 1.4.2.5). In both cases, these diseases suggest tropisms for the kidney or urinary tract.

1.4.2.2 JCV

JCV was first detected in the brain of a patient who died of progressive multifocal leukoencephalopathy (PML) (Padgett et al., 1971). In contrast to BKV and SV40, JCV has a tropism for glial cells, and under immunosuppression can cause rapid demyelination, leading to neurodegeneration and eventually death (Padgett et al., 1977; Tan and Koralnik, 2010). As the majority of patients with this disease have AIDS, highly active antiretroviral therapy (HAART) has decreased some of this burden, perhaps by strengthening the immune system. However, while HAART allows relatively long-term survival with PML, the neurological effects persist (Gasnault et al., 1999; Gray et al., 2003). The progression of this fatal disease in an immunosuppressed person may take less than one year without intervention, although with HAART therapy median survival is lengthened to 1.8 years (Engsig et al., 2009; Khanna et al., 2009). Unfortunately, HAART therapy is unavailable for some 90% of AIDS patients (Gray et

al., 2003). Additionally, patients undergoing some types of antibody treatment for multiple sclerosis (including the monoclonal antibody natalizumab) or some types of chemotherapy are at risk for PML (Tan and Koralnik, 2010). The best treatment option to prevent progression of PML is to remove immunosuppression or improve immune function (Marzocchetti et al., 2009), but this is clearly not an option for the entire affected population.

1.4.2.3 MCPyV

The populations most affected by Merkel Cell Carcinoma (MCC), a rare but aggressive skin cancer, are the elderly and immunosuppressed (Engels et al., 2002). This observation suggested that there may be an infectious agent involved in the development of this cancer. The Moore and Chang lab first showed that an estimated 80% of these carcinomas include sequences incorporated from a novel polyomavirus, which they named Merkel Cell Polyomavirus (MCPyV) (Feng et al., 2008; Gjoerup and Chang, 2010; Shuda et al., 2008). Expression of the MCPyV TAg is required for proliferation in the MCC cell lines (Houben et al., 2010). This discovery was the first clear and direct connection between a polyomavirus and human cancer, and it was quickly confirmed that MCPyV TAg had many shared characteristics with SV40 TAg, including a requirement for Rb binding (Houben et al., 2011), and nuclear localization (Liu et al., 2011b). Most interestingly, the integrated MCPyV encodes a truncated TAg, lacking an ATPase domain and p53 binding site (Shuda et al., 2008). These data suggest that transformation by MCPyV takes advantage of some novel features of this virus. The majority of Merkel Cell Carcinomas are reported to require these monoclonally integrated TAg sequences, this strengthens the case for an etiological role of MCPyV in disease (Becker et al., 2009; Garneski et al., 2009). However, the broad distribution of MCPyV in the general population makes this

relationship difficult to define and may suggest there are other contributing factors for development of MCC.

1.4.2.4 TSV

Although a rare condition, trichodysplasia spinulosa had been described as an affliction in select transplant patients, characterized by alopecia, follicular spines, and erythematous papules predominantly on the face (Haycox et al., 1999; Wyatt et al., 2005). The earliest reports of this condition suggested that there were viral structures within the papules, and that these might be papovaviridae (Haycox et al., 1999). However, the limited number of patients reported with this condition (Wyatt and colleagues reported the 3rd and 4th known case (Wyatt et al., 2005)) made it difficult to confirm this hypothesis. In 2010, rolling circle PCR was used to amplify and sequence the viral particles, confirming the identity of a novel polyomavirus termed Trichodysplasia Spinulosa Virus (TSV) (van der Meijden et al., 2010). The authors went on to show that while both the patient and his mother carried this virus, the young transplant patient carried much higher titers of the virus. After topical treatment with a 1% cidofovir, cytosine analog and general antiviral sometimes used to treat PyV infection (see section 1.4.2.5), the patient's viral titers decreased, as did the symptoms (van der Meijden et al., 2010). While these data suggest an etiological role for TSV, a direct test of the hypothesis will prove challenging given the rarity of condition.

1.4.2.5 Current treatment options for PyV-related diseases

Given that most patients who have a PyV-associated disease are already immunosuppressed, the consequences of not treating the disease symptoms are too severe to deprive patients of the available therapeutics, regardless of their inadequacy. A summary of the

current treatments for the common PyV-related diseases is summarized in Table 4. These treatments are commonly used in conjunction with reduction of immunosuppressive therapies, which has made the available data on these treatment options even more difficult to interpret.

Table 4. Commonly used therapeutics and the dosages for PyV-related diseases.

Drug	Disease	Dosage
cidofovir	BKVAN	40 mg/day (Wu and Harris, 2008)
leflunomide	BKVAN	20–40 mg/day (Wu and Harris, 2008)
ciprofloxacin	Hemorrhagic cystitis	oral (500 mg twice daily) or intravenous (200 mg twice daily) (Leung et al., 2005)
cidofovir	Trichodysplasia Spinulosa	Topical cidofovir 1% (van der Meijden et al., 2010)
none	PML	

Transplant patients receive a high standard of care. This is in contrast to the 90% of AIDS patients who do not receive standard care for their primary disease (WHO, 2008). As a result, the efficacy of specific therapeutics is best described for the BKV related diseases. For example, the commonly used drug cidofovir (brand name Vistide™) is a cytosine analog that targets cytomegalovirus and DNA polymerases in general, which has made it useful as an anti-viral (De Clercq, 2002; De Clercq et al., 1987). Unfortunately, cidofovir is nephrotoxic, and while this may be the mechanism of action for this compound (Bernhoff et al., 2008), cidofovir may be a poor choice to treat many kidney transplant patients (Izzedine et al., 2005). Similarly, characterization of cidofovir and leflunomide (brand name Arava™) in a culture system suggests that while leflunomide may be two fold more effective at inhibiting BKV replication, it is also more toxic than cidofovir, as indicated by the selectivity index (the ratio of the effective dose to

the toxic dose; (Bernhoff et al., 2010; Farasati et al., 2005). Clinical use of leflunomide has been associated with viral clearing and improved patient outcomes, although this has ranged from 100% of patients showing a decrease in viral load to 66% of patients with improved kidney function (Faguer et al., 2007; Josephson et al., 2006a; Wu and Harris, 2008). Ciprofloxacin (brand name Cipro™) is another compound that was shown to inhibit viral infection and viral DNA replication *in vitro*, but has yet to be fully tested clinically (Ali et al., 2007). Ciprofloxacin seems to be favored for hemorrhagic cystitis patients, in whom it has been shown to reduce the viral load (Johnston et al., 2010; Leung et al., 2005). Some physicians caution that ciprofloxacin may not be selective enough for treatment of transplant patients (Randhawa, 2005). Of these three commonly used treatments, cidofovir, leflunomide and ciprofloxacin, none have been tested in a large-scale clinical trial (Hilton and Tong, 2008; Wu and Harris, 2008), and retrospective studies have suggested the effect is indistinguishable from reduction of immunosuppression (Johnston et al., 2010).

There is not currently any specific treatment for PML (Tan and Koralnik, 2010). It should be noted that while an ideal therapeutic would need to cross the blood-brain barrier to be effective, administering drugs intrathecally is relatively common in the following treatments. Cidofovir has been used to treat PML based in part on *in vitro* data suggesting that other nucleoside analogs inhibit viral replication in a cell culture system (Hou and Major, 1998). While there may be an increase in survival rates, researchers suggest that this treatment simply prolongs life with moderate to severe disability (De Luca et al., 2008). Rarely, non-AIDS patients, including those with leukemia or lymphoma, develop PML; evidence from the treatment of non-AIDS PML patients suggested cytarabine, a chemotherapeutic and cytosine arabinoside, prevents PML (Aksamit, 2001), but trials of cytarabine in AIDS patients showed no

survival benefit (De Luca et al., 1999; Hall et al., 1998). This raises the possibility that there may be fundamental differences in the disease progression of PML in non-AIDS versus AIDS patients, which should be considered during treatment (Boren et al., 2008; Tan and Koralnik, 2010). After a demonstration that JCV may use the serotonin receptor $5HT_{2a}$ as the viral docking site (Elphick et al., 2004), efforts to treat PML with the serotonin receptor blocker mirtazapine (brand name Remeron™) are currently under investigation. While preliminary results suggesting improved clinical outcomes appear promising (Cettomai and McArthur, 2009), a small trial comparing patient survival did not demonstrate significant improvement over patients receiving no treatment (Marzocchetti et al., 2009).

1.4.3 Linking recently discovered PyVs to disease

The recent discovery of new members to the PyV family such as WUV (Gaynor et al., 2007), KIV (Allander et al., 2007), MCPyV (Feng et al., 2008; Shuda et al., 2008), HPyV6 and 7 (Schowalter et al., 2010), TSV (van der Meijden et al., 2010) and HPyV9 (Scuda et al., 2011) opens the possibility that these viruses may be associated with diseases. As molecular epidemiologists race to characterize the distributions of these poorly characterized viruses, the evidence required to support or disprove disease etiology will become readily available (Hill, 1965). It is now possible to quantitate the levels of virus associated with diseased tissues using molecular techniques such as ELISAs, qPCR and rolling circle PCR (Kean et al., 2009; Murata et al., 2009; Schowalter et al., 2010). However, suitable molecular methods may not be sufficient to describe causation of pathology. None of the PyVs discovered in the last decade replicate outside the host, in culture or otherwise; clearly development of replication systems for these viruses will greatly facilitate their characterization. Both JCV and MCPyV can be studied in

unique cell lines that express viral components, specifically, the JCV produces viral particles, but the MCPyV only expresses the truncated TAg that correlates with MCC. These cell culture systems represent adaptation from both the host cell and the integrated virus that may not reflect the natural biology of JCV or MCPyV (Elphick et al., 2004; Feng et al., 2008; Liu et al., 2011b). Even the replication systems used for BKV and JCV are slow and deliver low viral yield, it is not clear if this reflects the native biology of the virus, or is a limitation of the system. Another complicating factor in tying PyVs to disease is that PyVs establish a life-long infection and appear to be widely distributed, which may obscure the role of benign and malignant replication. More practically, the bulk of the world populations of immunosuppressed patients are not within reach of modern medicine, reemphasizing that finding novel ways to prevent or treat PyV-related diseases should remain a priority for the field.

1.5 PERSPECTIVES

Although studies of SV40 and other PyVs have driven important discoveries in many fields of biology, important and relevant questions remain. It is of interest whether PyVs have roles in disease, and how the molecular differences in TAg or other viral features affect the pathogenicity of viral replication. However there are less familiar although equally interesting questions remain unanswered. While the roles of most PyV in disease have yet to be established, it remains to be seen why healthy patients occasionally shed high levels of PyVs. What determines the periodic activation of PyV replication in humans, and how do PyVs continue to evade clearance by the immune system despite these bursts of activity? The trafficking of PyVs from the cell surface to the nucleus is a conspicuously slow process, and the mechanisms by which this

happens are not well described. How does a PyV transit from a caveosome to the ER, and how does the virus direct this trafficking?

More recent virus discovery efforts have increased the number of known human PyVs to nine. While molecular epidemiologists work to determine if there are further links between PyVs and disease, it is clear that treatment options are insufficient for the PyV-related diseases already identified, namely BKVAN, PML and MCC. The work described in this dissertation represents one effort to address this paucity.

1.6 DISSERTATION OVERVIEW

As described above, the family of PyVs is a growing public health concern, both as the members of this family increase and as the population of immunosuppressed patients increases. Since all PyVs express a large TAg, which carries a conserved and essential viral replication activity, I believe that TAg is a viable drug target to universally treat PyV-associated diseases. The goal of my project was to identify small molecular inhibitors of the ATPase activity of TAg and characterize these compounds in viral replication assays.

The first phase of this work was initiated by a collaboration with the Gestwicki lab at the University of Michigan. A library of small molecules was screened using quinaldine red (QR) to identify inhibitors of SV40 TAg endogenous ATPase activity. From a library of a 2500 compounds, two small molecules were identified which are more potent than any previously described SV40 inhibitor. A structure activity relationship (SAR) was described, and methods were established to test these compounds for the efficacy on BKV replication. This effort is detailed in Chapter 2.

Given the promising results of the QR screen, a search for SV40 TAg ATPase inhibitors was expanded. In a parallel effort, 330,000 compounds from the NIH Molecular Libraries Probe Centers Network (MLPCN) compound library were screened in collaboration with the Noah lab at the Southern Research Institute and the Golden lab at the University of Kansas. The screen was adapted to use a commercially available reagent, ADP Hunter, which facilitated assay miniaturization. Hits from this screen were chemically refined and more potent derivatives were obtained. Although the toxicity of the identified compounds makes them difficult to use in culture systems, the activity of these "tool" compounds is described in Chapter 3.

The parallel nature of my dissertation work presents an opportunity to comment on the prospect of finding PyV inhibitors using these and other approaches. Chapter 4 is a discussion of the impact and relevance of my work.

2.0 HIGH THROUGHPUT SCREENING IDENTIFIES BISPHENOL INHIBITORS OF POLYOMAVIRUS REPLICATION.

2.1 INTRODUCTION

Polyomaviruses are a family of double stranded DNA viruses that replicate in non-dividing cells, and in humans these viruses persist as a life-long infection (Imperiale and Major, 2007). The majority of the population appears to be infected with at least one if not more of the human polyomaviruses (Kean et al., 2009). In healthy patients, polyomavirus infection does not result in disease symptoms, but in immunosuppressed patients replication of these viruses can proceed unabatedly and results in several catastrophic diseases (Jiang et al., 2009a). For example, reactivation of BK virus in clinically immunosuppressed patients can lead to BK Virus Associated Nephropathy (BKVAN), or hemorrhagic cystitis (Hirsch and Randhawa, 2009). JC virus can cause progressive multifocal leukoencephalopathy in AIDS patients and in patients receiving specific treatments for Multiple Sclerosis (Safak and Khalili, 2003).

In the past few years, six new polyomaviruses have been identified, each with varying links to human disease (section 1.4): The KI and WU viruses were identified from patients with respiratory infections (Allander et al., 2007; Gaynor et al., 2007); Merkel Cell Polyomavirus was recognized as sequences incorporated into Merkel Cell Carcinomas (Feng et al., 2008; Shuda et al., 2008); Human Polyomaviruses 6 and 7 were identified as high copy sequences on the skin of

healthy individuals (Schowalter et al., 2010); Trichodysplasia spinulosa virus was found in high copy in dysplastic hair follicle cells (van der Meijden et al., 2010); and most recently a human virus that is highly similar to the monkey lymphotropic virus was sequenced from immunosuppressed patients and named Human Polyomavirus 9 (Scuda et al., 2011). Early evidence suggests that these viruses may be reactivated in immunosuppressed individuals (Sharp et al., 2009). Given the recent and rapid increase in the number of known polyomaviruses, it is likely that additional members of this virus family with connections to other diseases will emerge, particularly as the immunocompromised population expands (Kunisaki and Janoff, 2009) and because polyomaviruses are adept at replicating at low levels in non-dividing host cells (Fanning et al., 2009). Unfortunately, the current treatments for polyomavirus related diseases are not specific, inadequate and/or have undesirable side effects (Josephson et al., 2006b).

In addition to the message encoding capsid proteins, polyomaviruses express only one other essential transcript, which encodes the highly conserved, multidomain transforming factor, the large tumor antigen (TAg) (Cantalupo et al., 2005; Pipas, 1992). TAg activates the cellular DNA damage response while blocking the apoptic response, triggers cell cycle progression via binding to Rb and p53 family members, as well as a variety of other factors that regulate host cells (Pipas, 2009). To initiate viral DNA synthesis, TAg binds to the viral origin of replication and serves as the replicative helicase via its AAA+ ATPase domain (Li and Kelly, 1984). In addition, TAg harbors an essential "J domain" that stimulates the ATPase activity of the hsp family of molecular chaperones (Campbell et al., 1997; Fewell et al., 2002; Kelley and Georgopoulos, 1997; Srinivasan et al., 1997). The TAg-hsc70 complex is hypothesized to help release the transcription factor E2F from Rb (Sullivan et al., 2000), which is required for cell

cycle activation. These properties are essential for viral replication and are conserved amongst most of the TAgs (Cantalupo et al., 2005).

Of the eight known human polyomaviruses, *in vitro* replication systems only exist for BK and JC virus. In contrast to the very slow replication of these viruses in culture, the related Simian Virus 40 (SV40) replicates well in monkey kidney cell lines and expresses a highly conserved version of TAg. In fact, most of our current understanding of TAg function emerged from studies on SV40 (Pipas, 2009).

Because the TAgs are highly conserved, and because human cells lack a TAg homologue, I suggest that this protein may provide a therapeutic target to prevent polyomavirus replication and treat associated diseases. I further hypothesized that compounds that inhibit the ATPase activity of TAg, which is specifically required for viral replication, might be identified. As a first proof-of-principle for this concept, our lab recently determined that one compound, MAL2-11B, which modestly slows both the ATPase activity of TAg and the ability of the TAg J domain to stimulate hsp70 ATPase activity, can inhibit the replication of SV40 and BKV (Wright et al., 2009). However, MAL2-11B is not suitable as a therapeutic agent due to its low solubility, poor membrane permeability, and relatively low antiviral potency. Moreover, MAL2-11B was not identified in a systematic screen using TAg as a probe, but was a structural analogue of compounds already known to alter the ability of J domain-containing proteins to activate the ATPase activity of hsp70 (Fewell et al., 2004; Wright et al., 2008). Thus, the agent was neither identified nor optimized as a TAg-specific target.

To identify more potent and selective polyomavirus inhibitors, in collaboration with the Gestwicki lab at the University of Michigan, we developed a novel high throughput screen with purified SV40 TAg. The screen took advantage of a new platform to assess modulators of ATP-

hydrolyzing enzymes, and the library included MAL2-11B-like compounds, as well as compounds that have been developed and approved for other uses. As hoped, this approach led to the isolation of inhibitors of the TAg ATPase activity that were significantly more potent than MAL2-11B. A preliminary structure-activity relationship (SAR) was then performed to identify the key chemical features of the molecules that give rise to their effects. The two lead compounds from these subsequent efforts also inhibited the replication of both SV40 and BKV in cultured cells with an ED_{50} that was 10-fold higher than the dose at which modest toxicity was apparent, thus providing a satisfactory therapeutic index (TI). Because the lead compounds were approved by the FDA for other applications, our collaborative efforts set the stage for the continued development and testing of a new class of anti-polyomavirus agents.

2.2 MATERIALS AND METHODS

2.2.1 Materials

The MicroSource MS2000 library contains ~2200 bioactive compounds with a minimum of 95% purity. The collection includes drug components (50%), natural products (30%) and other bioactive compounds (20%) (Miyata et al., 2010).

Bithionol (CAS 97-18-7) and hexachlorophene (CAS 70-30-4) were purchased from Sigma-Aldrich, and the compounds ST024951 (**1**), ST029256 (**2**), ST033374 (**3**) ST033385 (**4**), ST057728 (**5**) and ST5308743 (**6**) were purchased from Timtec (Newark DE). The compound 5250892 (**7**) was obtained from ChemBridge (San Diego, CA), and resorcinol sulfoxide (**8**) and R128546 (**9**) were purchased from Sigma-Aldrich. The purities of these bisphenol-like

compounds were confirmed by HPLC/UV, and by mass spectrometry when ionization was possible. Cidofovir was kindly provided by Dr. Abhay Vats (University of Pittsburgh). Eight known dihydropyrimidines were synthesized as described (Wisen et al., 2008), and their structures were confirmed using high resolution mass spectrometry and ^{1}H NMR.

SV40 TAg was purified essentially as reported (Wright et al., 2009). In brief, Sf9 cells were infected with a baculovirus engineered for the expression of wild type TAg for 45 h. The cells were harvested and lysed, and the lysate was clarified by high-speed centrifugation. The resulting supernatant was loaded on to an immunoaffinity column containing the monoclonal TAg antibody pAB419 (Harlow et al., 1981) covalently linked to Protein G Sepharose Fast-Flow beads. The column was washed, and fractions highly enriched for TAg were eluted at pH 11. After the pH was adjusted to neutrality, the protein was dialyzed against 10mM Tris-Cl, pH 8.0, 1mM EDTA, 100mM NaCl, 10% glycerol, and 1mM DTT. TAg-containing fractions and the purity of the final preparation were verified by Coomassie Brilliant Blue staining of SDS-polyacrylamide gels and by western blot analysis. TAg was stored at -80°C until use.

2.2.2 A high throughput screen to identify inhibitors of TAg ATPase activity

A collection of ~150 dihydropyrimidines was screened in 96-well plates by our collaborators in the Gestwicki lab at the University of Michigan. Briefly, a stock solution of TAg was prepared in assay buffer (100 mM Tris-Cl, pH 7.4, 20 mM KCl, and 6 mM $MgCl_2$, 0.01% Triton X-100) to yield a final concentration of 2.5 nM (0.018 μg/μL). An aliquot of this solution (14 μL) was added to each well of a clear 96-well plate and 1 μL of either the assay compound (final concentration 200 μM) or DMSO was added. The reaction was initiated with the addition of 10 μL of 2.5 mM ATP. The plates were then incubated for 3 h at 37 °C. After incubation, each

well received 80 μL of the quinaldine red reagent (Miyata et al., 2010), which was quenched by the addition of 10 μL of a 32% sodium citrate solution. However, screening of the larger MS2000 collection necessitated development of a higher density format platform. Toward this goal, a high throughput screen to identify inhibitors of the ATPase activity of TAg was performed as described (Miyata et al., 2010), but with several modifications. First, 5uL of the a stock solution of TAg (final concentration 2.5 nM) was added to each well of opaque, white, low-volume, nonsterile, polystyrene 384-well plates (Thermo Fisher Scientific, Inc). It was critical to use these plates because assay sensitivity was strictly dependent on fluorescence quenching between the polystyrene plates and the quinaldine red agent (data not shown). To each well, 0.2 μL of either the compound (at ~5 mM in DMSO) or DMSO was added. The Gestwicki lab found that assay performance decreased above 5% DMSO. The reaction was then initiated with the addition of 2 μL of 3.2 mM ATP, and the plates were incubated for 3 h at 37 °C. After incubation, each well received 15 μL of the quinaldine red reagent, which was quenched by the addition of 2 μL of a 32% sodium citrate solution. The plates were incubated for an additional 15 min before fluorescence intensity (excitation 430 nm, emission 530 nm) was measured on a PHERAstar plate reader. The Z factor (Zhang et al., 1999) was calculated to be 0.70, which is indicative of a large and consistent difference between the signals of the positive and negative controls. The coefficient of variation ranged from 6 to 10% and the signal:noise was approximately 50.

2.2.3 Biochemical and kinetic assays to assess TAg activity

A steady state ATPase assay with purified SV40 TAg was performed as reported previously (Cyr et al., 1992; Wright et al., 2009). In short, TAg was preincubated with the indicated compound

for 15 min on ice, and upon addition of α^{32}P-ATP the reaction was moved to 30ºC. At the indicated times, aliquots were removed, the reaction was quenched, and the ATP and generated ADP species were resolved by thin layer chromatography. The resulting data were analyzed on a Fujifilm BAS-2500 phosphoimager and quantified using ImageGuage software (Fuji Film Science Lab). The data obtained represent the results from at least 3 independent replicates. IC_{50} values were determined by titrating compounds into this assay such that the volume of DMSO was constant, and data were standardized relative to a DMSO control. A sigmoid, 3-parameter line regression of the resulting data was performed using SigmaPlot (Systat Software, San Jose, CA).

A variation of this assay was used to obtain the desired kinetic constants via a Lineweaver-Burk plot. In these assays, ATP was titrated from a final concentration of 7.14 μM to 50 μM and in the presence or absence of the indicated compound, and the rates of the reactions were determined as described above. Each assay was performed at least three times. These data were plotted as a double reciprocal, and the K_m and V_{max} values were determined from a line fit. The differences in the obtained data sets were determined by ANCOVA, performed by SAS (SAS Institute, Cary, NC). Pairwise comparisons were performed for both the slope (used to determine the K_m) and intercept (used to determine the V_{max}) of the line determined by SAS, and the p values for these comparisons are reported.

Similarly, the steady state ATPase assay was performed with two other purified proteins, hsp70 and p97. The human hsp70 was supplied by Raj Chovatiya and is described elsewhere (Chiang et al., 2009); although purified hsp70 is not a potent ATPase alone, this protein is active in this assay due to a proteolytically cleaved and active ATPase domain fraction that co purifies with full length hsp70. Each reaction used 3 μg of protein. The bovine p97 was a generous gift

from the DeMartino Lab (University of Texas Southwestern) and 5 μg were used in each ATPase reaction. All other conditions for this assay are the same as described for TAg.

TAg dependent DNA replication was assayed *in vitro* using a revised Li and Kelly method (P. Cantalupo, personal communication; (Li and Kelly, 1984; Wright et al., 2009). Reactions were prepared in a buffer solution that includes a mix of nucleotides, creatine-phosphate, creatine kinase and a plasmid containing the SV40 *ori*, pUC.HSO (Wold et al., 1987). In the assay shown in Figure 11, 3 μg TAg and 90 ng HeLa cell lysate prepared by freeze-thaw were incubated with the compound for 15 min on ice prior to addition of the radiolabeled dCTP and DNA. Samples were collected after 30, 60 and 90 min at 37 °C and ethanol precipitated. The resulting samples were separated on a 1% agarose gel and visualized using a phosphoimager.

Expression of TAg was detected by Western blot as previously described (Wright et al., 2009). Briefly, cells were infected with SV40 at MOI=1. At 48 hpi, lysates were harvested using Branton's lysis buffer, and the concentration of lysates was normalized by Bradford assay. For each sample, 30 μg of lysate was loaded and separated by SDS-PAGE. The proteins were transferred to a nitrocellulose membrane, and decorated with pAB419 (to detect TAg) or anti-hsp70 or anti-actin antibody (Cell Signaling) as indicated. The primary antibody was decorated with an HRP conjugated anti-mouse (TAg) or anti-rabbit (hsp70 and actin) antibody, and visualized with Pierce Supersignal ECL reagents on a Kodak image station IS440.

Limited proteolysis was based on a previously described protocol with some modification (Weisshart et al., 2004). TAg was purified as above (section 2.2.1). Reactions were assembled with 3 μg TAg, 30 μM compound in DMSO and 4mM nucleotide (either ATP or AMP-PNP), then incubated for 20 min on ice prior to addition of protease. As denatured TAg control sample

included 3.5 μL of TCA sample buffer (80 mM Tris HCl pH 8, 8 mM EDTA, 120 mM DTT, 3.5% SDS, 0.29% glycerol, 0.08% Tris base and 0.01% bromophenol blue) in place of DMSO or nucleotide, then heated at 75 °C for 15 min and cooled before addition of protease. Reaction were incubated at 37 °C for 5 min with 1.8 ng of Proteinase K (Sigma) diluted in 10 mM Tris pH8.0, 1.0 mM EDTA, 100 mM NaCl and 10% glycerol; the final volume of 25 μL, and this. The reaction was stopped with 5 μL of 100% trichloroacetic acid (Fischer Scientific) and incubated for 10 min on ice. Reactions were centrifuged at 13,000x*g* at 4 °C for 10 min and the supernatants were removed. The pellets were resuspended in TCA sample buffer, and then separated by 12.5% SDS-PAGE. The proteins were visualized with Coomassie Brilliant Blue. As a control, the same procedure was performed using 3 μg Bovine Serum Albumin (Fermentas) in lieu of TAg, and these samples were separated by 10% SDS-PAGE and visualized by Coomassie Brilliant Blue.

2.2.4 Viral replication and cell culture assays

CV1 cells were grown in MEM with 10% FBS and pen/strep and Vero cells (kindly provided by Dr. Bruce McClane, University of Pittsburgh) were grown in DMEM containing 10% FBS and pen/strep at 37 ºC in a 5% CO_2 incubator.

BKV stocks were provided by Dr. Michael Imperiale, University of Michigan. Crude BKV stocks were prepared based on a protocol from the Imperiale lab. Vero cells were expanded to 50-60% confluence on 12 T150 flasks in DMEM containing 10% FBS, and pen/step. Vero cells were infected at MOI 0.1 IU/cell with crude stock of BKV (made on RPTE cells (Low et al., 2004)) in DMEM containing 2% FBS, pen/step and 0.5 μg/mL Amphotericin B (Invitrogen) at 37° C for 1 h in a total volume of 6mL. After infection, the media was replaced

with 20mL fresh DMEM containing 2% FBS, pen/strep and 0.5 μg/mL Amphotericin B. Some flasks were supplemented with 2 mL media 2dpi, and this seemed to improve the viral yield (Table 7). The infection continued for 3-4 weeks, until all cells appeared nonadherent. Cells were lysed by 3 freeze-thaw cycles, and the cell debris was further harvested from cultures by scraping up all cells into the media. The crude stock was stored at -20 °C. Given the cell debris, before further infection, the viral stock was agitated with a vortex mixer for 10-20 sec to release virus bound to cell membranes and then spun briefly to separate the membranes from virus containing supernatant immediately before infection.

Immunofluorescence microscopy was performed based on a protocol from the Weisz lab (University of Pittsburgh (Guerriero et al., 2006)). Vero cells were grown on poly-Lys treated glass coverslips and infected with BKV. At 48 hpi, cells were washed with PBS, then fixed with 4% paraformaldehyde for 20 min at room temp. Fixation was stopped with two washes of PBS with 1 mM glycine. The cells were permeabilized with 0.5% Triton X-100, after which they were washed twice again with PBS with 1mM glycine. In preparation for addition of antibody, the cells were "blocked" with PBS with 1mM glycine and 0.25% Bovine Serum Albumin for 5 min. Cells were incubated for 20 min with 50 μL of a 1:20 dilution of pAB416 hybridoma supernatant (unpurified). Preparation of this supernatant is discussed in section 3.2.2. Cells were washed twice briefly in PBS with 1mM Glycine. Next, cells were incubated with a 1:100 dilution of the secondary antibody, Alexa Fluor488 goat anti-mouse (Invitrogen), for 20 min in the dark. Coverslips were mounted on slides with AntiFade Gold with DAPI (Invitrogen) and were visualized on an Olympus BX60 epifluorescence microscope with 100x oil immersion objectives, unless specified. A Hamamatsu Argus-20 CCD camera was used to capture images.

Focus fluorescence units were calculated by determining the ratio of infected (TAg-expressing) cells to uninfected cells from multiple random fields from several slides.

To quantitate the effect of compound on viral replication, plaque assays were performed. SV40 stocks were prepared by plating CV1 cells into 24-well dishes and infecting the cells with SV40 at a MOI of 2 for 2 h. Next, the media was removed and replaced with media containing the desired compound or an equivalent volume of DMSO. Two biological replicates corresponding to each treatment were performed. The media was refreshed at 24 hpi, and again supplemented with either DMSO or the indicated compound. At 48 hpi, the cells were frozen and thawed 3 times to provide a viral stock. This stock was titered by plaque assay using at least 3 technical replicates, based on a previously reported protocol (Murata et al., 2008). In brief, CV1 cells were grown on 6 cm dishes to near confluence and dilutions of the viral stock were plated onto the monolayer for 2 h, and then replaced by a 4mL overlay of media in 0.9% Noble agar. On 3 and 6 dpi, an additional agar overlay was made. At 9 dpi, the agar was removed and the monolayer was stained with crystal violet. Plaques were counted by eye, and viral mediated cell clearing was confirmed by light microscope.

A quantitative DNA replication assay for SV40 was performed as previously described (Huryn et al., 2011; Murata et al., 2009; Randhawa et al., 2005b). CV1 cells were infected with SV40 at an MOI of 6, and after a 2 h infection the media was removed and replaced with media containing the desired compound or an appropriate volume of DMSO. The media containing the compound was refreshed at 24 hpi and at 48 hpi before the media was aspirated and DNA was harvested by a modified Qiagen mini-prep. Specifically, cells were washed in PBS and then 250 μL of buffer P1 was added to each well. Next, 250 μL of P2 was immediately added to lyse the cells. When cells were visibly lysed by examination by light microscope, the lysate was

removed and incubated with 500 μg Proteinase K at 55 ºC for 1 h. The lysate was neutralized with N3 Buffer, and mixed gently. Samples were centrifuged for 10 min at 15,000*g* at 4 ºC, and the resulting supernatant was loaded onto the supplied mini-column and centrifuged for 1 min at 15,000*g* at room temp. The column was washed in 700 μL PE, and briefly centrifuged to remove residual ethanol. Finally, 50 μL of TE pre-warmed to 50 ºC was added to the column and equilibrated for 5 min before a final 1 min elution at room temperature was performed. The resulting DNA stock was then quantified by quantitative PCR (qPCR; see below).

To quantify the replication of BKV, Vero cells were infected with BKV for 1 h at an estimated MOI of 0.01. The infectious media was removed and replaced with 1 mL media containing the indicated compound or DMSO. Media containing the compound or the DMSO control was refreshed daily for 5 d. The cultures were lysed 5 dpi by three freeze-thaw cycles at -20 ºC. This viral stock was further homogenized by pipetting before quantification by qPCR.

qPCR was performed to quantify the amount of SV40 or BKV DNA and to assess the extent of viral replication. These DNA stocks, obtained above, were serially diluted for qPCR assays as described (Huryn et al., 2011). Absolute quantification was performed using pSVB3 (Pipas et al., 1983) as a reference for SV40 and using pBKV (Dalrymple and Beemon, 1990) as a reference for BKV. Each of these plasmids contain the entire viral genome cloned in to a BamH1 site. A mix of primers and Taqman probe (IDT DNA) (for SV40 5' (FAM)/ATCAGGAACCCAGCACTCCACT/(IOWA BLACK) 3', primer 1- 5' GATGAACACTGACCACAAGG 3', primer 2- 5' GCACATTTTCCCCACCT 3') were used to detect SV40. The primers for BKV detection are reported elsewhere (Huryn et al., 2011).

To assess compound toxicity, an MTS (3-(4,5-dimethylthiazol-2-yl)-5-(3-carboxymethoxyphenyl)-2-(4-sulfophenyl)-2H-tetrazolium) assay was performed (Cory et al.,

1991; Minguez et al., 2003). CV1 cells were plated in 96 well dishes and grown to 90% confluency. The desired concentration of compounds was added to warm MEM and plated onto cells in at least three technical replicates. At 24 h, the media was aspirated and the indicated compound dissolved in media was added fresh. At 48 h, the media was again aspirated but was replaced with diluted MTS reagent (Promega) in MEM lacking phenol red. The plate was returned to the 37 °C incubator for 3 h. Data were collected on a BioRad iMark Microplate Reader (Hercules, CA) at 490 nm. The data were compared to both a DMSO (negative) and 1 μM staurosporine (positive) control. The LD_{50} was determined by sigmoid 3-parameter line regression of the data using SigmaPlot (Systat Software, San Jose, CA).

2.2.5 *In silico* chemical similarity searches

Similarity searches were conducted by our collaborators in the Gestwicki lab in an in-house database MScreen (http://mscreen.lsi.umich.edu/) using each scaffold against the external library set consisting of structures from Asinex, ChemBridge, ChemDiv, MayBridge, NCI, PubChem, Sigma, and TimTec. All structures within 70% similarity were retrieved for each chemical scaffold. The combined results were imported into the software program DVS and fingerprints using the 166 public MACCS keys were computed for the structures. Fingerprints were not successfully computed for all of the structures. Tanimoto distances were computed for each chemical scaffold against all of the retrieved structures. The results were then imported into Benchware DataMiner along with the structures and the original scaffolds. To aid in sorting, each original scaffold was given a Tanimoto distance of "-1" to itself.

2.3 RESULTS

2.3.1 Identification of bisphenols that inhibit TAg ATP hydrolysis

I hypothesized that inhibitors of the conserved and essential SV40 TAg ATPase activity would be general inhibitors of polyomaviruses, since each virus encodes a highly conserved TAg. Toward this goal, the Gestwicki lab adapted a procedure originally developed to identify inhibitors of the ATPase activity of hsp70 (Chang et al., 2008; Miyata et al., 2010). Briefly, this method involves measuring the enzymatic release of inorganic phosphate from ATP using the quinaldine red (QR) reagent. First, a library of approximately 150 dihydropyrimidines was screened to identify close structural derivatives of MAL2-11B that may be better TAg inhibitors (Wisen and Gestwicki, 2008; Wright et al., 2009). The compounds in this collection were screened at 200 μM in 96-well plates, as described in section 2.2.2. From this process, thirteen compounds were identified that inhibited > 35% of the ATPase activity of TAg. The activities of these compounds were then confirmed by re-screening them against TAg in duplicate. To complement these inhibitors and to identify alternative chemical scaffolds, the Gestwicki lab next screened the commercially available Spectrum Collection (MicroSource Discovery Inc., Groton, Conn), which contains 2,240 known bioactives and drugs approved by the FDA for a range of indications. However, because of the larger size of this library, a higher throughput (e.g. 384-well plates) version of the QR assay was required. Therefore, pilot experiments were conducted with TAg to understand whether a miniaturized version would still give robust screening performance. Briefly, it was found that the signal was linear for at least 3 h when the concentration of TAg was at least 2.5 nM (0.018 μg/μL), the levels of ATP were 1 mM, and the reaction was performed at 37 °C (see Figure 4). Moreover, the assay exhibited good screening

parameters under these conditions, with an average Z factor between 0.6 and 0.7. Encouraged by these findings, the MS2000 collection in low volume, 384-well microtiter plates was screened to identify potential inhibitors. These compounds were screened at approximately 100 μM and, from this process, 33 (1.4% of the collection) compounds were identified as potential inhibitors because they reduced ATPase activity by > 20% (Figure 4). Of these compounds, the twenty compounds with the best inhibitory activity were confirmed in duplicate. Together, these combined screening efforts resulted in the identification of 13 dihydropyrimidines and 20 other compounds that appeared to directly inhibit TAg ATPase activity.

(A) Rate of ATP hydrolysis by TAg

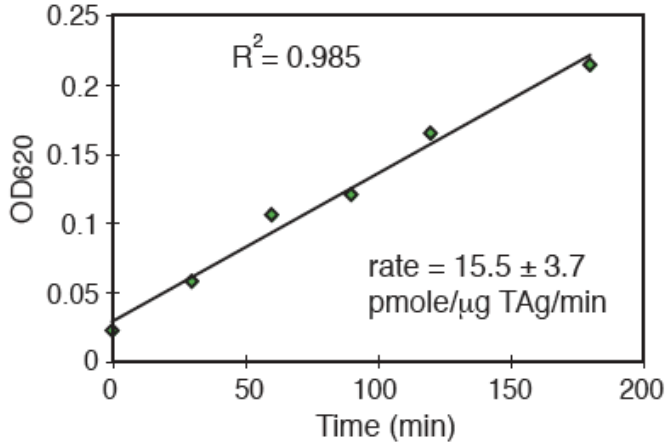

(B) Effects of TAg concentration on phosphate signal

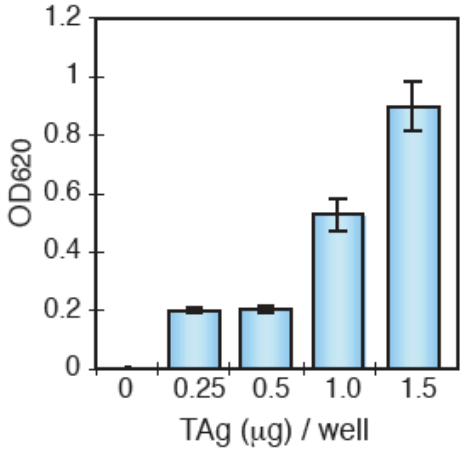

(C) Sample of the primary screening results (Spectrum MS2000)

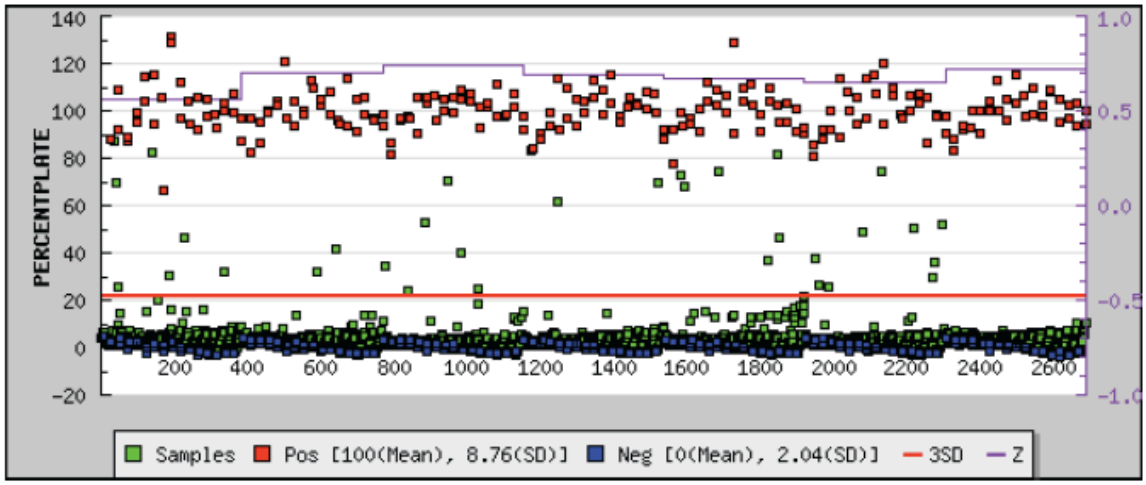

(D) Chemical structures of the active compounds from the two screens

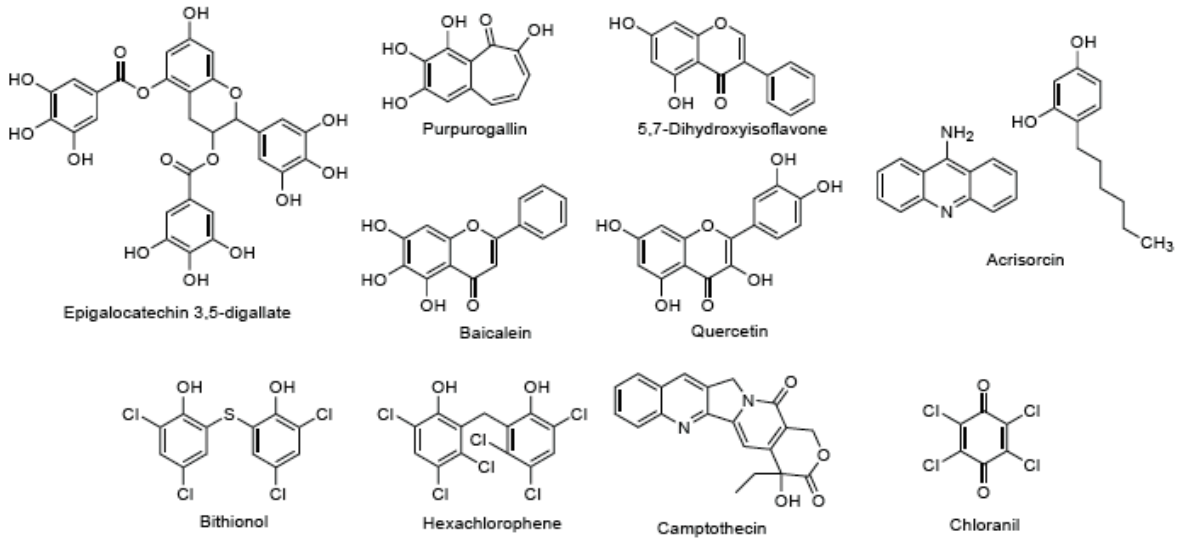

Figure 4. Development of a high throughput screen for TAg ATPase inhibitors.

(A) The phosphate signal is linear for at least 3 h at 0.25 µg/well (2.5 nM) of TAg, 1 mM ATP and 37 °C. Phosphate levels were measured using quinaldine red (QR) and converted to pmoles using a set of sodium phosphate standards. (B) Relationship between TAg concentration and raw phosphate signal (OD620). To conserve protein, 0.25 µg per well (2.5 nM) was chosen for screening. Results are the average of triplicate wells and the error bars represent the standard deviation. (C) The results from screening the MS2000 collection. TAg was screened in 384-well plates, as described in section 2.2.2. The red line is 3 standard deviations of the negative control. The purple line is the Z factor, calculated by plate. The controls (positive (red): no enzyme; negative (blue): DMSO) were present on each plate. (D) Chemical structures of the active compounds from the MS2000 collection that were confirmed in duplicate and then screened in the steady-state, radioactive ATPase assay (Figure 5A).

Next, to remove false positives, I wanted to test these compounds in an independent, steady state ATPase assay. This assay relies on ^{32}P radioactivity instead of the colorimetric QR reagent. From the list of active compounds, 8 of the most potent dihydroyrimidines were re-synthesized and 12 of the commercially available compounds from the MS2000 list were purchased. These compounds included a number of flavones, polyphenols and bisphenols, such as quercitin, baicalein, and chloranil (Figure 4). Using the radioactivity-based ATPase assay, Alex Ireland, an undergraduate with whom I worked, established that only three of these compounds, bithionol, chloranil and hexachlorophene, were significantly more potent inhibitors than MAL2-11B when used at a final concentration of 100 µM (Figure 5). The remainder of the compounds were either false positives or their activities were not significantly better than MAL2-11B. One possible application for these compounds is discussed in section 4.2. Because chloranil caused TAg to aggregate under the utilized assay conditions (Figure 6), I focused my efforts on bithionol and hexachlorophene (Figure 5B). Titrations of bithionol and hexachlorophene into the steady state ATPase assay revealed apparent IC_{50} values of 2 and 4 µM, respectively (Figure 5C). Thus, the potencies of bithionol and hexachlorophene were greater than those of any other reported TAg inhibitor, including MAL2-11B, ellagic acid, and spiperone (Goodwin et al., 2009; Wright et al., 2009).

A

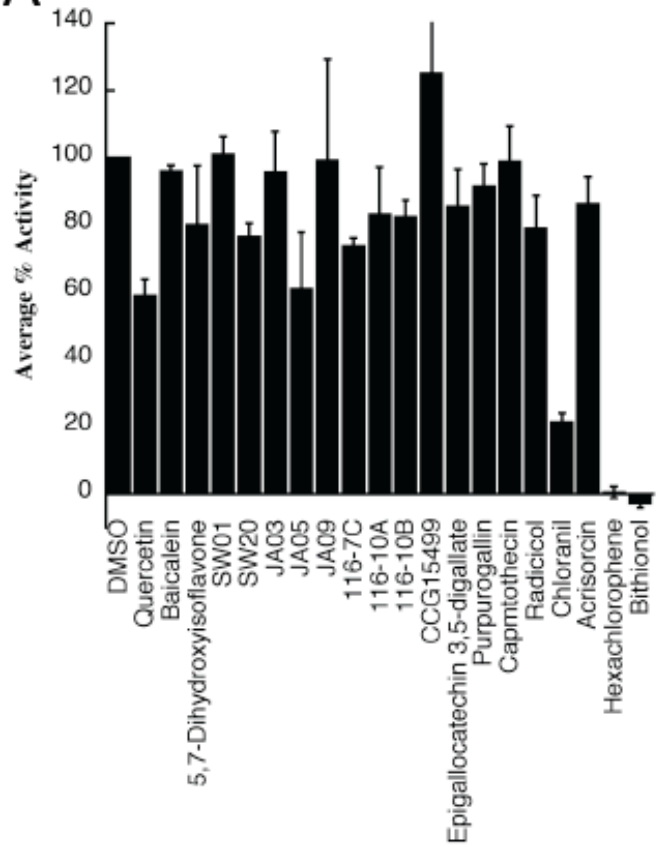
Average % Activity
140
120
100
80
60
40
20
0
DMSO
Quercetin
Baicalein
5,7-Dihydroxyisoflavone
SW01
SW20
JA03
JA05
JA09
116-7C
116-10A
116-10B
CCG15499
Epigallocatechin 3,5-digallate
Purpurogallin
Capmtothecin
Radicicol
Chloranil
Acrisorcin
Hexachlorophene
Bithionol

B

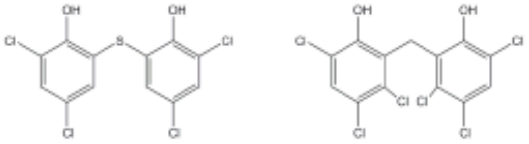

C

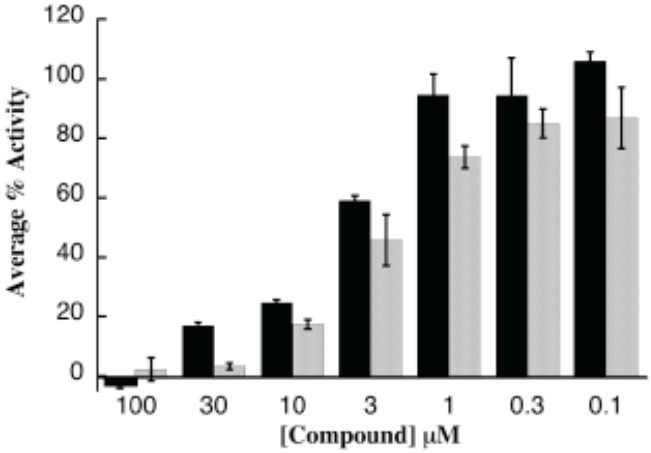
Average % Activity
120
100
80
60
40
20
0
100
30
10
3
1
0.3
0.1
[Compound] μM

Figure 5. A high throughput screen identifies inhibitors of TAg ATPase activity.

A. The indicated compounds were tested in triplicate at a final concentration of 100 µM in a steady state ATPase assay. B. The structures of bithionol, right, and hexachlorophene, left, are shown. C. Results from triplicate ATPase assays are shown, +/- SD, for bithionol, grey bars, and hexachlorophene, black bars, at the indicated concentrations. In parts A and C, results were standardized to a DMSO control.

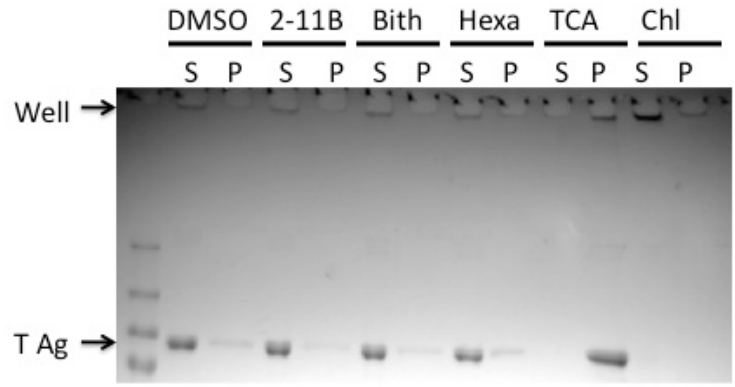

Figure 6. Chloranil cause TAg aggregation *in vitro*

Mock steady state ATPase assays were assembled in the presence of a final concentration of 100 µM of either MAL2-11B (2-11B), bithionol (Bith) hexachlorophene (Hexa), chloranil (Chl), or an equal volume of DMSO. 2% TCA was added a pellet control. After a 15 min pre-incubation on ice with the indicated compound, 50 µM ATP was added and the reaction was incubated for another h at 30°C. Reactions were centrifuged for 5 min at 15,000*g*. Next, the supernatant (S) and pellet (P) fractions were resolved by 10% SDS-PAGE, and proteins were visualized by Coomassie Brilliant Blue stain. TAg remained soluble in the presence of DMSO, MAL-211B, bithionol or hexachlorophene, but the majority of the detected protein in the presence of chloranil appear as a high molecular weight aggregate in the well (top arrow) and was absent at the predicted position for TAg (bottom arrow).

2.3.2 A structure-activity relationship for bisphenol-like TAg ATPase inhibitors

Because both bithionol and hexachlorophene are bisphenols, I hypothesized that the directed screening of related compounds would help to establish a structure-activity relationship (SAR) for the inhibition of TAg ATPase activity. To this end, an *in silico* search was performed and 60 compounds were identified that were either structurally similar to these compounds or could be employed to test specific hypotheses regarding the chemical groups that mediate the inhibitory activity on TAg. I selected a subset of these compounds based on commercial availability, using structures that would address specific hypothesises about this structure, such as substituents at different positions and flexibility between rings (Figure 7A), and these were screened in the steady state ATPase assay at a final concentration of 30 μM (Figure 7B). This concentration was chosen based on the fact that bithionol and hexachlorophene inhibited the ATPase activity of TAg by ~80% at this concentration (Figure 5C). Alex Ireland found that only two of the tested compounds inhibited the ATPase activity of TAg, and these agents, (compounds 7 and 9, 6,6'-thiobis(2-bromo-4-chlorophenol) and 6,6'-methylenebis(2-bromo-4-chlorophenol)), are most structurally similar to bithionol. Based on the data in Figure 7B, I also conclude that some essential features for TAg inhibition include a bisphenol moiety, flexibility at the biraryl linker group, and the presence of substituents at positions 2 and 4 on the phenols; however, bulky groups at these positions appeared to disrupt inhibitory activity.

A

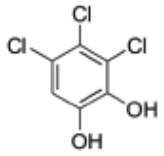

1

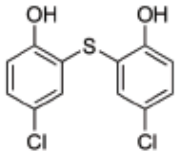

2

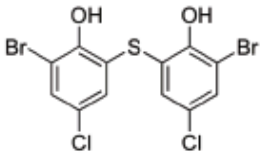

3

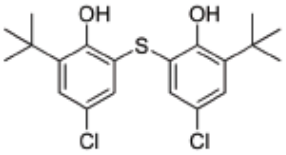

4

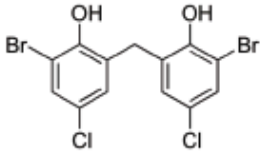

5

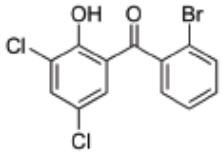

6

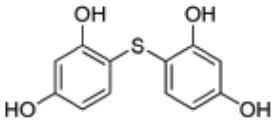

7

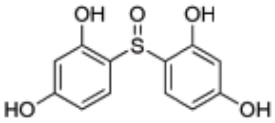

8

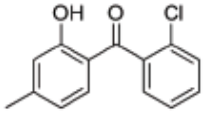

9

B

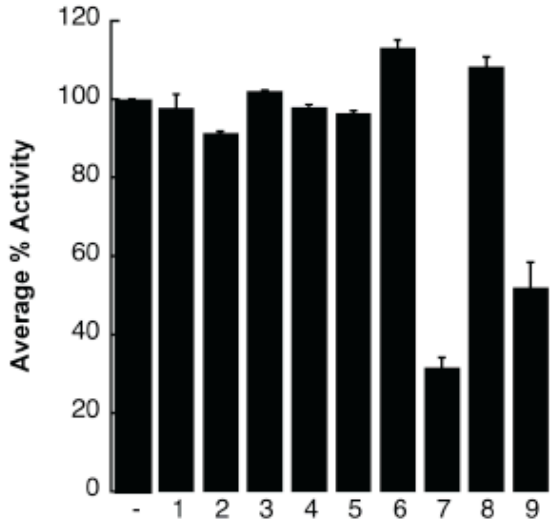

Figure 7. A structure activity relationship for the action of select bisphenols and bisphenol-like compounds for inhibition of TAg ATPase activity.

A. An *in silico* search for bisphenol-related structures based on Tanimoto distances was performed (see section 2.2.5), and from these results nine compounds were selected for further analysis (see section 2.2.1). B. The indicated compounds were tested in a steady-state ATPase assay at a final concentration of 30 µM. The results are shown relative to a DMSO control (-), in triplicate, +/- SD.

2.3.3 Bithionol and hexachlorophene have off target effects on hsp70 and p97

Convinced of the *in vitro* efficacy of both compounds on TAg, I wanted to determine whether these compounds would act as general ATPase inhibitors. Two other ATPases, a mammalian hsp70 and bovine p97, were tested. Previously, work in the lab demonstrated that the control compound MAL2-11B was an inhibitor of the TAg-stimulated hsp70 activity, but did not inhibit the stimulation of all J domain containing proteins (Wright et al., 2008; Wright et al., 2009). Before attempting such assays with the bisphenols, I wanted to test whether the bisphenols might directly inhibit the activity of hsp70. While hsp70 normally has very little ATPase activity without a co-chaperone, at this time, there was a preparation of hsp70 in the lab that contained a mix of full-hsp70 and the ATPase domain of hsp70 (R. Chovatija, data not shown). This preparation had a high level of endogenous activity, which is thought to be the activity of the uncoupled ATPase domain. I showed this activity could be inhibited by the bisphenols (Figure 8). For this reason, I determined it would be difficult to distinguish whether the bisphenols might have a bipartite inhibition of both the J domain and ATPase domain of TAg. Although this is not conclusive evidence that bithionol and hexachlorophene are hsp70 inhibitors, I chose not to pursue this activity further.

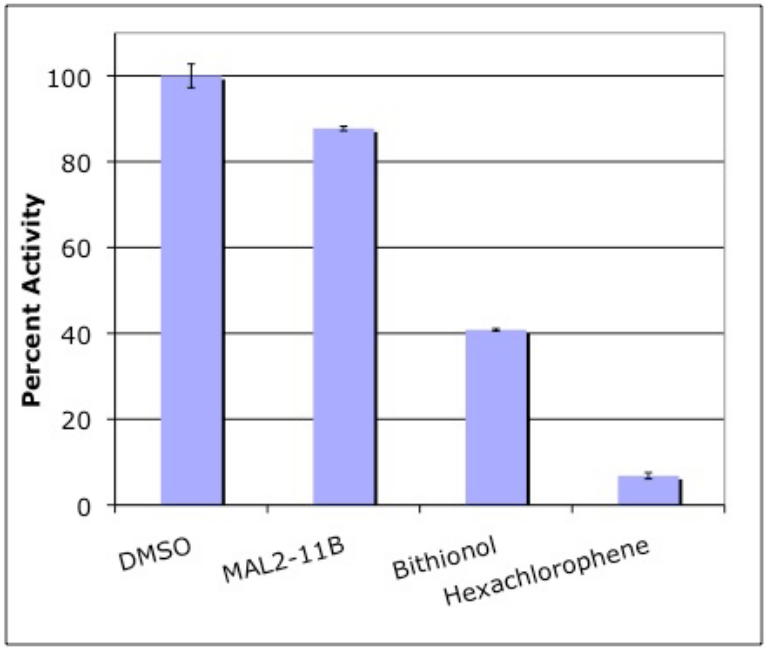

Figure 8. Bithionol and hexachlorophene are more potent inhibitors of hsp70 activity than MAL2-11B.

The effect of each compound at 100 µM was tested on hsp70 in a steady state ATPase assay. Percent activity was calculated relative to the activity of the hsp70 with DMSO control over the duration of the reaction. Each condition was performed in triplicate, and reported +/- SD.

I also wanted to test the effects of these compounds on p97, which is both a multifunctional essential chaperone-like protein and a mammalian AAA+ ATPase (Ju and Weihl, 2010; Kakizuka, 2008). I was surprised to find robust, but differential effects on p97 ATPase activity with these compounds at 30 μM. Alex Ireland further characterized this difference by performing steady state ATPase assays with additional time points (Figure 9). As shown in Figure 9, bithionol stimulates p97 activity, while hexachlorophene inhibits p97. The hexachlorophene inhibits p97 slightly less than TAg at the same concentration. Given that the activities of p97 are essential for a variety of protein folding and homeostasis functions in the cell (Ju and Weihl, 2010; Ye et al., 2005), I was concerned that this might lead to cytotoxic and off target effects. Fortunately, when cytotoxicity was assessed by MTS assay (Table 5) it appeared not to be a concern.

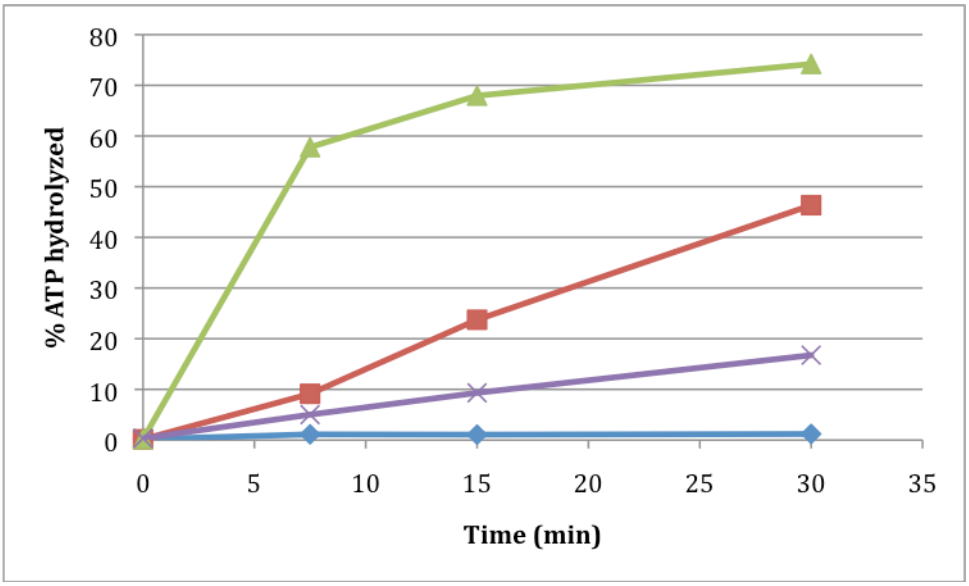

Figure 9. Bithionol stimulates p97 ATPase activity while hexachlorophene inhibits p97.

This ATPase assay was performed under the same conditions as demonstrated for TAg ATPase assays. This experiment is displayed as a time course to highlight the rapid stimulation of p97 activity by bithionol. Red squares indicate p97 with DMSO, blue diamonds indicate no p97, green triangles represent p97 with 30 µM Bithionol, purple Xs indicate p97 with 30 µM hexachlorophene. Both reactions including bisphenols are demonstrated n=3, and error bars indicate +/- SD.

2.3.4 Bithionol and hexachlorophene inhibit SV40 replication

Bithionol and hexachlorophene were derived from the Spectrum 2000 library as FDA-approved compounds for their bacteriostatic and antiparasitic properties. In fact, both compounds were widely used as topical antiseptics before more potent and less toxic alternatives became

available. In addition, bithionol has successfully been used to treat outbreaks of the parasite *Paragonimus westermani* in humans, and can be taken orally at a concentration of 40 mg/kg every other day (Kim, 1970; Price et al., 1993). To our knowledge, neither compound has been examined for its ability to treat a viral infection.

To examine whether the bisphenolic TAg inhibitors inhibit polyomavirus replication, the activities of bithionol and hexachlorophene were first tested in an SV40 plaque assay. CV1 monkey kidney cells were infected with SV40 and treated with bithionol and hexachlorophene at a final concentration of 30 µM. As a control, we also retested MAL2-11B at a final concentration of 100 µM. Next, a crude viral stock was obtained and titered by plaque assay. We first observed that MAL2-11B reduced the number of plaques by nearly 60% (Figure 10A), which is consistent with previously published results (Wright et al., 2009). We also discovered that bithionol and hexachlorophene inhibited viral replication nearly 100-fold relative to the DMSO control, indicating that both compounds are significantly more potent inhibitors of SV40 propagation than MAL2-11B.

To confirm these results and to provide a quantitative method to rapidly test TAg inhibitors, a qPCR assay was developed to measure SV40 DNA replication in our cell culture system. This assay is based on previous work to detect the human polyomavirus BKV in patient samples (Randhawa et al., 2005a). The assay takes advantage of the small size of the polyomavirus genome (~5 kb), which can be purified like plasmids. In short, cells were infected as described for the plaque assay and were then washed and lysed using commercial mini-prep buffers. The viral DNA was collected and titered by absolute quantification in a qPCR assay (see section 2.2.4). Finally, the data were compared to an untreated, infected control.

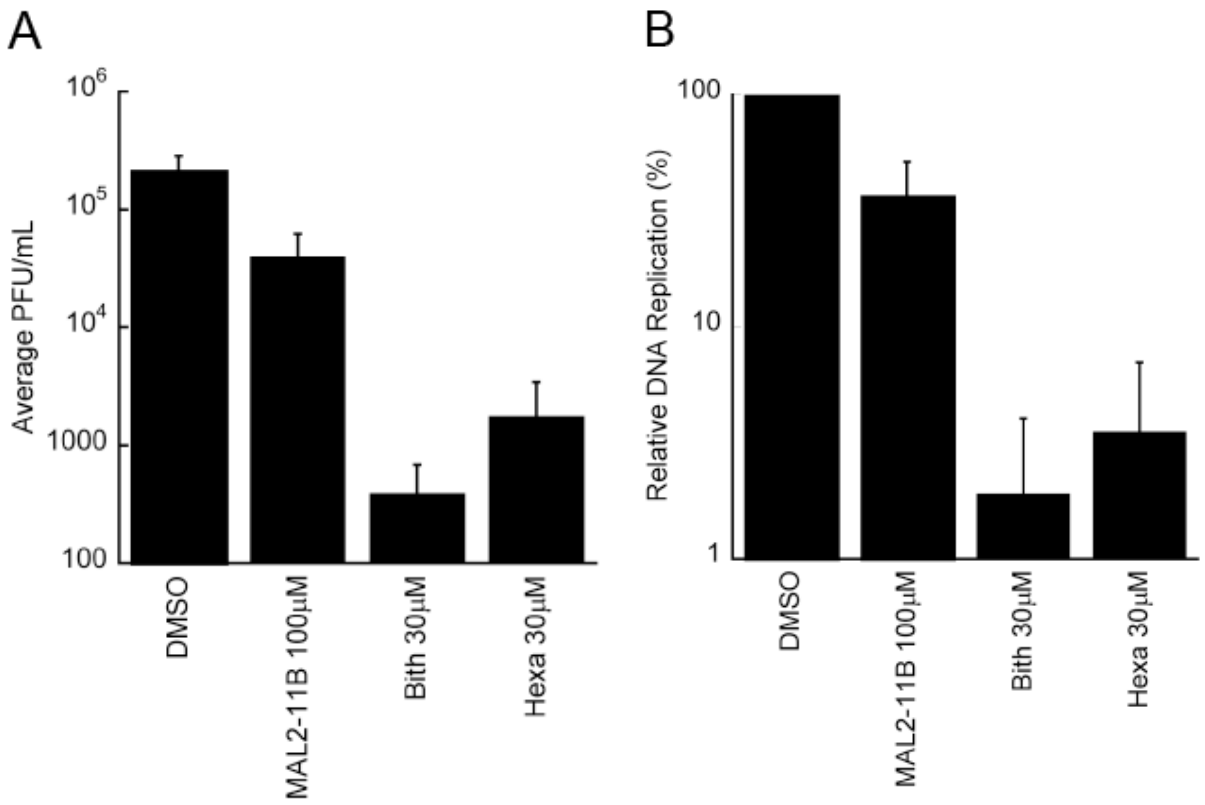

Figure 10. Bithionol and hexachlorophene inhibit SV40 replication.

A. SV40 replication in CV-1 monkey kidney cells was assessed in the presence of MAL2-11B, bithionol or hexachlorophene for 2 d, after which the replication-competent virus was titered by plaque assay. The data represent 3 separate infections, each measured in at least two technical replicates, +/- SD. B. Replication of viral DNA in a parallel experiment was quantified by qPCR under identical conditions to those used in part A. The data represent the means of 12 independent experiments, +/- SE.

As anticipated, I again found that MAL2-11B at a final concentration of 100 μM inhibited DNA replication in culture by ~60% (Figure 10B). Further, both bithionol and hexachlorophene inhibited DNA replication ~100-fold at 30 μM (Figure 10B). This result is completely consistent with the results of the plaque assay, thus validating this protocol. Although not all viral DNA replicated during infection leads to infectious viral particles (Rigby and Berg, 1978), I observed a clear correlation between the outcome of the plaque assay and the qPCR assay. More generally, the data support my hypothesis that a directed isolation of TAg ATPase inhibitors can be used to identify compounds that inhibit polyomavirus replication.

In an effort to refine the mechanism of these drugs, an *in vitro* DNA replication assay was performed. This assay was based on a classical assay, which takes advantage of the ability of TAg to recruit host cell machinery from HeLa cell lysate to replicate DNA (Li and Kelly, 1984). The readout for this assay is incorporation of a radiolabeled nucleotide into growing, replicated DNA. Although my experiments indicated that both bithionol and hexachlorophene inhibit viral DNA replication in the cell culture system, neither compound inhibits DNA replication in this assay (Figure 11). Many conditions were explored for this assay, including preincubation of TAg with the small molecules, modification of time and temperature, but under no conditions did bithionol and hexachlorophene inhibit DNA replication. Although this result was unexpected, noted differences between the *in vitro* and in culture systems may partially explain this outcome, which will be discussed in greater detail in sections 2.4 and 4.3.

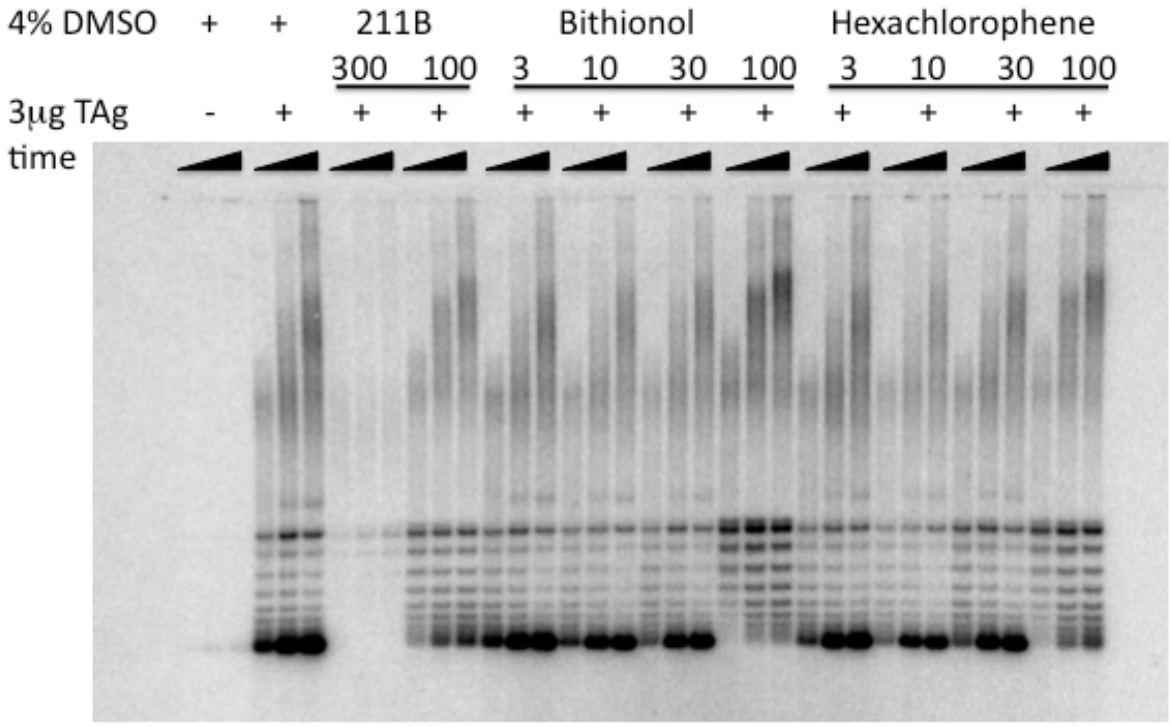

Figure 11. Bithionol and hexachlorophene do not inhibit DNA replication *in vitro*.

In this figure, 3 µg TAg and HeLa lysate at a final concentration of 9 ng/µL were incubated with the compound for 15 min on ice prior to addition of the radiolabel and DNA. In each reaction, DMSO alone (+) or the indicated compound (MAL2-11B denoted 211B) was added at multiple concentrations, denoted below the compound (values are µM). These samples were collected at t=30, 60 and 90 min (increasing time is indicated by black triangles), and ethanol precipitated. The products were separated on a 1% agarose gel, which was visualized by phosphoimager. Note: higher concentrations of the bisphenols were not examined since beyond 100 µM effects would most likely be non-specific.

One possible mechanism to explain the inhibition of viral replication is that the compounds compromise host cell viability. To exclude this scenario, a cell viability assay—the MTS assay (see section 2.2.4)—was performed with each compound in CV1 cells. The data were also compared to a DMSO negative control and to a positive control, the toxic agent staurosporine (Tanaka et al., 1995). Importantly, the compounds were added and the cells were treated under conditions that were identical to those used when the effects of the compounds on SV40 replication were assessed. In this assay, the MI_{50} (metabolic index-50) is defined as the concentration of compound that yields one-half the MTS signal compared to the negative (DMSO) control. The MI_{50} values obtained for bithionol and hexachlorophene were 50 μM (Table 5). We therefore conclude that the antiviral effects of these agents are independent of their modest toxicities.

Table 5. MI_{50} and Therapeutic index for bithionol and hexachlorophene.

Both the MI_{50} and Therapeutic Index were determined by an MTS assay in CV1 monkey kidney cells. MI_{50} is defined as the concentration of compound that yields one half the MTS signal of the control cells. Therapeutic Index is calculated as the MI_{50}/IC_{50}, and indicates compound specificity.

Compound	MI_{50}	Therapeutic Index
Bithionol	50 μM	12.5
Hexachlorophene	50 μM	25

One clue about the difference in the *in vitro* and cell culture replication assays came from looking at TAg expression during an infection. TAg expression was examined 48 hpi with or without drug treatment (Figure 12). Given the unstructured linkers that connect the folded domains of TAg, it is common to see aggregation of TAg in the well and at the interface of the stacker and separating gel (M. Saenz, personal communication; see also Figure 17). However, even with aggressive use of reductants, in cells treated with bithionol or hexachlorophene TAg appeared to be an insoluble aggregate when infected lysates were examined by Western blot. Expression levels of the chaperone hsp70, which would normally be upregulated by a global stress response, did not appear to respond to drug treatment (Figure 12)(Mayer and Bukau, 2005), suggesting the effect on TAg solubility is not due to global denaturing of cellular proteins.

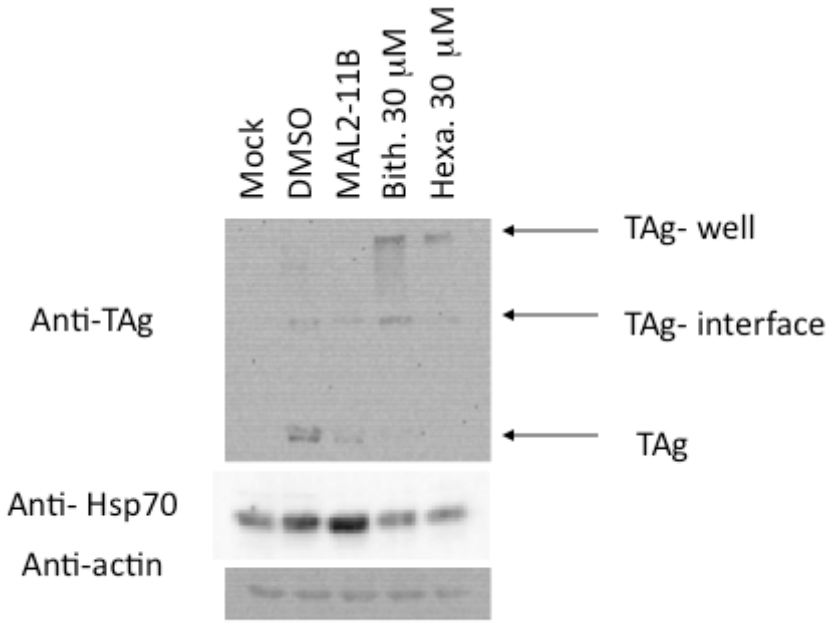

Figure 12. Expression of soluble TAg is decreased during treatment with bithionol and hexachlorophene.

CV1 cells were infected with SV40 (or a Mock infection, as indicated), and then incubated with media with the indicated concentration of compound or an equivalent volume of DMSO for 48 h. MAL2-11B was used at 100 µM. Cells were lysed and equal amounts of lysate were separated by SDS-PAGE and transferred to nitrocellulose. Western blot analysis of 30 µg of cell lysates was performed using antibodies specific for TAg, hsp70 and actin.

It may be possible that bithionol and hexachlorophene cause TAg-specific unfolding, or gross conformational changes. One way to detect such changes would be by limited proteolysis with a protease. The tryptic fragments of TAg have already been characterized (Weisshart et al., 2004). Based on this evidence, I tested whether these fragments would be changed by the presence of bithionol or hexachlorophene. As demonstrated in Figure 13A, neither bithionol nor hexachlorophene changed the conformation of TAg as detected by limited proteolysis with Proteinase K. Since this was consistent between experiments, I tested whether these compounds might affect the proteolysis of a control protein, in this case BSA. Figure 13B shows that while these compounds do not denature BSA, in contrast to the SDS control, there are some fragments that are not resolved in the presence of bithionol or hexachlorophene. This may suggest a modest change in BSA conformation, in contrast to the patterns shown in Figure 13A. Combined with the evidence in Figure 12, these data suggest that neither bithionol nor hexachlorophene cause global denaturing of proteins in general or TAg specifically. These data imply that the mechanism of action of these compounds stems from a particular interaction with TAg.

A

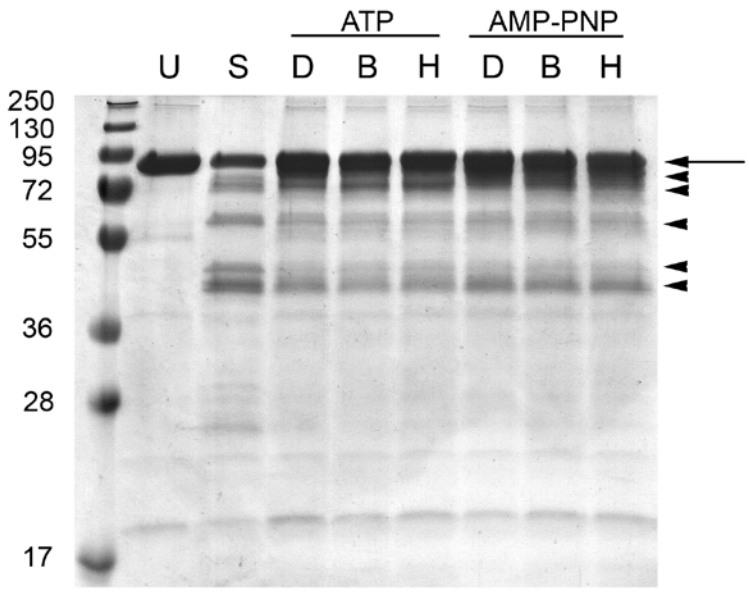
ATP
AMP-PNP
U
S
D
B
H
D
B
H
250
130
95
72
55
36
28
17

B

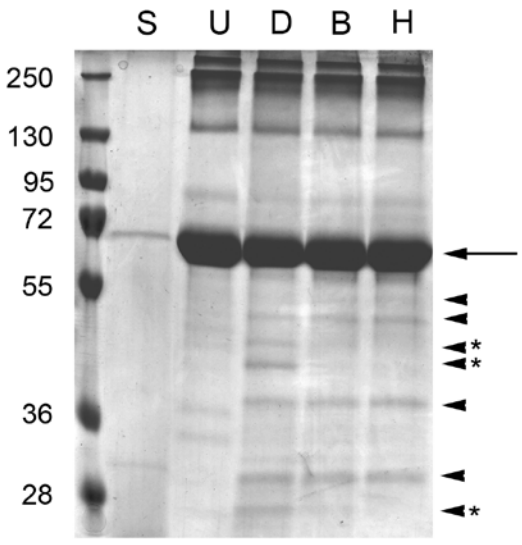
S
U
D
B
H
250
130
95
72
55
36
28
*
*
*

Figure 13. Limited proteolysis indicates bithionol and hexachlorophene do not cause TAg unfolding.

A. Reactions were assembled with 4mM of the indicated nucleotide, 3 µg TAg with DMSO (D), 30 µM bithionol (B) or 30 µM hexachlorophene (H) and incubated for 20 min on ice. As a control, a sample of TAg that was heated to 75 °C in the presence of SDS (S) before addition of Proteinase K. To start the digest, 1.8 ng of Proteinase K were added to each reaction for 5 min at 37 °C, before the reaction was quenched with trichloroacetic acid, and the protein fragments were precipitated. The resulting protein fragments were separated by SDS-PAGE and visualized with Coomassie Brilliant Blue stain. A sample of undigested TAg (U) was included for comparison. Arrow indicates full length TAg, triangles indicate fragments that result from proteolysis. B. BSA was Proteinase K digested under similar conditions, including addition of DMSO (D), 30 µM bithionol (B) or 30 µM hexachlorophene (H). No nucleotide was present in these reactions. The reactions were stopped with trichloroacetic acid, and the resulting protein fragments were separated by SDS-PAGE and visualized with Coomassie Brilliant Blue stain. A sample of undigested BSA (U) was included for comparison. Arrow indicates full length BSA, and the triangles indicate fragments that result from proteolysis. The * indicates fragments that are only present in the absence of bithionol or hexachlorophene.

In order to test this hypothesis and to characterize how bithionol and hexachlorophene inhibit the ATPase activity of TAg, ATP was titrated into the steady state ATPase assay while the concentration of inhibitor was held constant. These data were analyzed by double reciprocal (i.e., Lineweaver-Burk) plots. To verify that meaningful kinetic information could be obtained, I also assessed the ability of ADP to function as a *bona fide* competitive inhibitor for TAg's ATPase activity. Figure 14 presents an example of this analysis, and as expected ADP increases the K_m for ATP whereas the V_{max} stays relatively constant, which is typical of competitive inhibition (Segel, 1976). When bithionol and hexachlorophene were examined at a final concentration of 3 μM, which inhibits TAg ATPase activity by ~50%, there were statistically significant increases in the K_m values for ATP. Effects on the V_{max} values were also apparent but these were not significantly different from the DMSO control (Table 6). The simplest interpretation of these data is that bithionol and hexachlorophene act as competitive inhibitors for ATP. However, because of the significant differences in the structures of ATP and these two bisphenols, it is also possible that the compounds bind another site, which alters the conformation of TAg (see section 2.4).

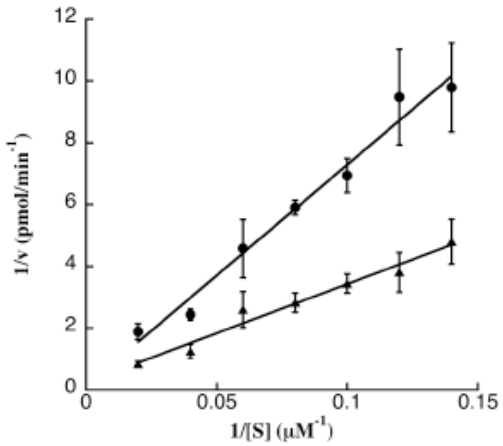

Figure 14. Example of Lineweaver Burk analysis of TAg with ATP and ADP.

A Lineweaver-Burk analysis of TAg was performed over a range of ATP concentrations and was used to determine the K_m and V_{max}. Data represent values obtained in the presence of either DMSO (triangles) or 150μM ADP (circles). Assays were performed at least in triplicate, and are shown as means of the data, +/- SD.

Table 6. Bithionol and hexachlorophene change the K_m of TAg ATP hydrolysis.

Kinetic parameters (K_m and V_{max}) were determined by Lineweaver-Burk analysis of TAg in the presence of 150 μM ADP or 3 μM bithionol or hexachlorophene over a range of ATP concentrations, as shown in FIGURE 4. ANCOVA was used to determine the p values for each pair-wise comparison.

	Km (μM)	Vmax (pmol/min)
TAg + DMSO	110	3.5
TAg + ADP	200 *	2.9
TAg + Bithionol	590 *	10
TAg + Hexachlorophene	290 **	6.6

*** p<0.01, TAg + DMSO versus TAg + ADP or bithionol;**

**** p<0.05, TAg + DMSO versus TAg + hexachlorophene;**

TAg + DMSO versus TAg + ADP, bithionol or hexachlorophene, p>0.5

2.3.5 Bithionol and hexachlorophene inhibit BKV replication

I next wanted to examine whether bithionol and hexachlorophene could inhibit the replication of a clinically relevant polyomavirus, BKV. Although I was able to establish conditions for examining BKV infection by immunofluorescence (IF, Figure 15), this method did not detect BKV infection with sufficient resolution to examine the effects of inhibitors. This is a predictable limitation of this slow growing virus. However, this assay did validate the BKV stock and infection conditions used in later assays. Based on a protocol from the Imperiale lab, Vero cells grown on cover slips were infected for 3 d with BKV, and then co-stained with DAPI and pAB416 (1:20), an antibody that recognizes both SV40 and BKV TAg (Harlow et al., 1981) (Figure 15). The Imperiale lab demonstrated that expression of BKV TAg begins within 12 h of infection (Jiang et al., 2009b); quantitation of focus fluorescence units (ffu) can be a faster way to assay the titer of viral stocks compared to quantitation of the plaque forming units (pfu), which requires multiple complete rounds of infection. However, not all PyV infections proceed from initiation to replication; Todaro and colleagues suggested that 1 in 100 viral particles of SV40 lead to a successful infection (Todaro and Green, 1966) As a result, this method can over-estimate the actual titer of virus.

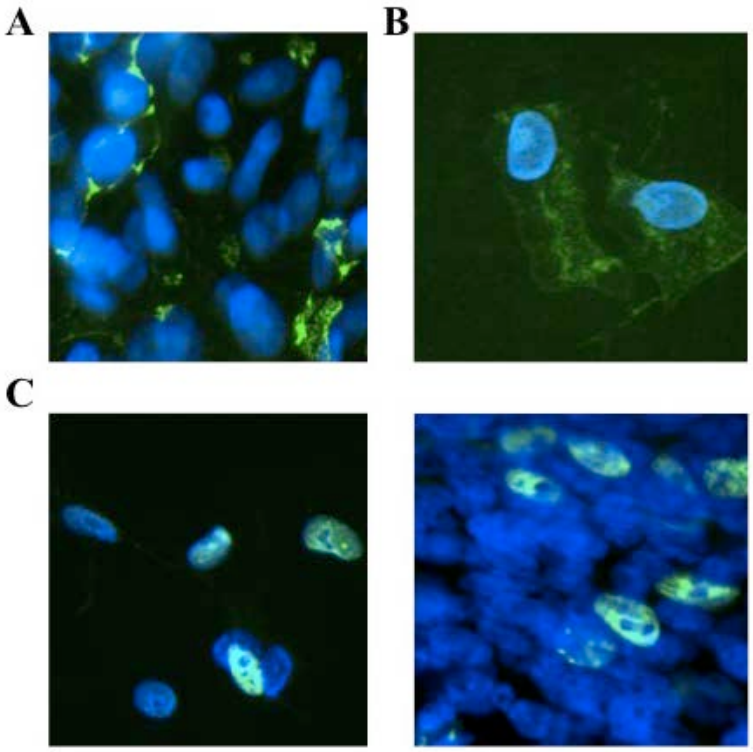

Figure 15. BKV TAg can be detected by immunofluorescence.

Vero cells were infected with BKV for 3 d before IF staining for DNA and TAg. Blue indicates the DAPI stained nuclear DNA, and green indicates pAB416 and Alexa Fluor 488 goat anti-mouse IgG (TAg). A. A mock infection probed with undiluted pAB416 demonstrates one type of background issue sometimes seen in this assay. B. BKV infected Vero cells stained with undiluted pAB416. In this case the cytoplasmic staining is not thought to indicate TAg expression, but high background levels. C. Infected Veros stained with pAB416 diluted 1:20. This dilution of antibody reduced background such that some, but not all, cells appeared to express nuclear TAg. The nucleus does not significantly change size at this stage in infection.

As shown in Figure 15C, very little cytopathic effect was visible from the BKV infection, in contrast to SV40, which causes nuclear swelling during infection (data not shown). BKV TAg was consistently detected in Vero cells, and the stocks were titered at $8x10^3$ ffu/mL. This low stock titer is an indication of the how much less efficient BKV is compared to SV40 (for reference, my SV40 stocks are consistently $1x10^7$ pfu/mL or greater, where pfu is a more stringent readout for viral particles than ffu). Given this low titer and infection efficiency, the expected 100-fold decrease in viral replication upon addition of inhibitor would have shown less than 1 infected cell per slide, invalidating this method of detection for the proposed experiments. However, future experiments could get around this limitation by using higher titer stocks, which may be possible to obtain if the virus is purified from the crude stock. Based on the data from these titrations, I suspect that the low efficiency of infection is due to tropism. The crude stock prepared from the Imperiale lab was prepared in human renal proximal tubule cells, which are the native host for BKV (Low et al., 2004). For each infection, the titer decreased about 25-fold, as demonstrated in Table 7. Since the viral stocks were passaged through Vero cells twice (one time to make the stock, and a second time in the titration), the apparent MOI is decreased by several hundred or a thousand-fold. Although Vero cells are competent for BKV replication, it has been suggested that HEK293 cells may be a better cell line for making crude stocks from (M. Jiang, personal communication).

Table 7. Titers of BKV stocks as determined by immunofluorescence.

Two different approaches were used in preparing stocks: 'fed' cells were supplemented with media 2 dpi, and 'unfed' were not. Both infections continued 14dpi until the crude stocks were harvested. Based on the known titer of the Imperiale lab stock, infections with each of these crude stocks were performed with identical volumes at an estimated MOI of 1. The infected and uninfected cells were counted to determine the relative infection.

Stock	**Relative infection (MOI=1)**
Imperiale	1:25 cells infected
'fed' stock	1:480 cells infected
'unfed' stock	1:1220 cells infected

Instead, to quantitatively address the activity of the compounds during infection, a more sensitive and quantitative qPCR detection method was used to assess the activity of bithionol and hexachlorophene on BKV replication. In this assay, a low titer infection was performed in Vero cells, and the DNA was quantified by qPCR, as performed for SV40 (Figure 16). Data were compared to a DMSO control, MAL2-11B and to cidofovir, which has been shown to inhibit BKV replication *in vitro* and has been used clinically (Farasati et al., 2005; Johnston et al., 2010). The results of this experiment showed that bithionol and hexachlorophene inhibit BKV replication by ~70% at a 30 μM, and this effect is comparable to the impact of MAL2-11B or cidofovir on BKV when used at much higher final concentrations (100 and 350 μM, respectively; Figure 16). Interestingly, hexachlorophene maintained its potent inhibition at 10 μM, but bithionol was significantly less effective at this lower concentration (Figure 16). A model to describe this phenomenon is provided in section 2.4. Together, these data indicate that the directed screening for TAg ATPase inhibitors can be used to identify inhibitors of polyomavirus infection. Among these inhibitors, two compounds were identified that are more potent than clinically evaluated anti-virals. Our data also indicate that second-round screening for inhibition SV40 replication via qPCR assay is a valid route to isolate inhibitors of BKV replication, which is significantly more laborious to propagate and analyze.

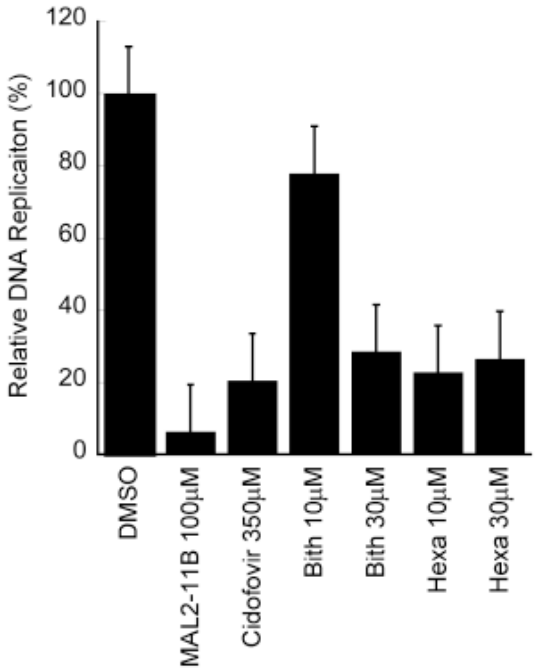

Figure 16. BKV DNA replication is inhibited by bithionol and hexachlorophene.

Both bithionol and hexachlorophene inhibit BKV DNA replication in Vero monkey kidney cells. The replication of BKV DNA was assessed after 5 d of infection with MAL2-11B, cidofovir, bithionol or hexachlorophene at the indicated concentrations, and the levels of viral DNA were quantified by qPCR as described in the section 2.2.4. The data were standardized to the DMSO control, +/- SE. Data represent the means of 12 experiments from four independent infections.

2.4 DISCUSSION

Previous screening strategies to identify polyomavirus inhibitors took advantage of indirect read-outs for viral infection, which led to the identification of ellagic acid and spiperone as inhibitors of TAg expression in SV40, BKV, and JCV infected cells (Goodwin et al., 2009). A preliminary analysis of these compounds indicated that they may block viral entry. While these efforts have identified inhibitors of viral propagation, target and off-target effects could not be ascertained. In contrast, I took advantage of my knowledge of polyomavirus biology to identify components of the viral life cycle that could be disrupted by small molecules. We then created an assay to target the TAg dependent activity. The assay takes advantage of the fact that TAg's ATPase activity is essential for viral replication (Castellino et al., 1997; Fanning et al., 2009), and that human cells lack a TAg homologue. The data presented in this Chapter indicate the success of this targeted, mechanism-based approach. Based on the excellent Z factor and signal-to-noise for the targeted screen (0.7 and 50, respectively), the specificity and structural similarities of the lead compounds, and the fact that the estimated therapeutic index for these compounds is >10 (Table 5), I am confident that more potent and efficacious inhibitors can be obtained via subsequent efforts with more diverse libraries.

My work was initiated to address the paucity of available therapeutics for polyomavirus infection. Previous work to identify compounds that inhibit polyomavirus led to the discovery of cidofovir, leflunomide (Farasati et al., 2005), and the quinolones (Ali et al., 2007). These agents have been used with some success in the clinic. Cidofovir inhibits BKV *in vitro* and is commonly used as a treatment for BKVAN (Farasati et al., 2005), but high creatine levels, which

are typical in nephropathy, contraindicate its use. In addition, there has been no controlled clinical study to suggest that the lower dosage levels used in BKVAN actually compromise viral replication beyond the impact of reducing immunosuppression (Hirsch and Randhawa, 2009). Similarly, the immunosuppressant used to treat rheumatoid arthritis, leflunomide, has been shown to decrease BKV replication *in vitro* but has not been rigorously examined in clinical trials (Faguer et al., 2007; Josephson et al., 2006a). A third class of compounds used for the treatment of BKVAN are the quinolones, including ciprofloxacin and ofloxacin. While these antibiotics have shown promise both *in vitro* and in the clinic (Leung et al., 2005; Randhawa, 2005), some patients cannot tolerate them, and they exhibit relatively low potency (Ali et al., 2007). In addition, our lab previously uncovered MAL2-11B as an inhibitor of SV40 and BKV replication, but this agent was neither obtained via directed screening efforts nor optimized as an anti-viral (Wright et al., 2009). The low solubility and efficacy of this compound requires further refinement if this scaffold is to be pursued as an anti-viral agent.

As described above, bithionol and hexachlorophene were included in the library used for our screen by virtue of the fact that they are FDA approved for other applications. Both compounds have been used as topical anti-microbials, but it is known that overexposure can be toxic (Kimbrough, 1973; Powell and Lampert, 1973). Under conditions in which the potential neurotoxic effects of these agents are not as problematic, bithionol and hexachlorophene also have veterinary applications as anti-parasitic and anti-fluke agents. In fact, these compounds may be of use for the veterinary treatment of Avian Polyomavirus, which can cause acute death in a wide range of psittacine birds (Katoh et al., 2010). Further, in geographical regions where fluke outbreaks in humans are more problematic, bithionol has been used to successfully clear

infections in humans after oral administration (Bacq et al., 1991; Kim, 1970; Lee and Kim, 2006; Price et al., 1993; Seo et al., 1982).

The correlation between SV40 inhibition and BKV inhibition confirms my hypothesis that the isolation of SV40 TAg ATPase and SV40 replication inhibitors can lead to the identification of inhibitors of other polyomaviruses. However, it was curious that bithionol and hexachlorophene inhibit BKV to a different extent when used at a final concentration of 10 μM, although their effects on the ATPase activity of TAg and on SV40 replication were essentially identical. This phenomenon may reflect bithionol's differential interactions between the SV40 and BKV TAgs, which—while highly conserved (74% identity)—are certainly not identical (see section 1.3). Alternatively, this difference may be a result of the different time courses needed to assess viral infection. Given that SV40 replication is assayed after two days, and BKV replication is assessed after five days, compensatory and/or off-target effects of one agent (but not the other) may accumulate over the duration of the infection. It is also worthwhile to note that while bithionol and hexachlorophene are structurally similar they may not interact identically with TAg. Indeed, their effects on the K_m for ATP in TAg are unique (Table 6). A recent report indicated that these agents inhibit glutamate dehydrogenase, but interestingly they bound somewhat differently to this hexameric enzyme when analyzed structurally (Li et al., 2009). Hexachlorophene binds the center core of the hexamer, while bithionol binds at the two-fold axis between pairs of subunits. Thus, it is possible that bithionol and hexachlorophene also interact differently with TAg, perhaps even at a site that is distinct from the ATP binding pocket. Indeed, even though the effects of bithionol and hexachlorophene on the V_{max} of TAg were not statistically significant (Table 6), it is possible that the compounds have pleiotropic effects on TAg: a primary binding site might be at or near the nucleotide pocket, as has been observed by

competitive inhibition of the NADPH binding enzyme 3-oxoacyl-ACP reductase (Wickramasinghe et al., 2006), whereas secondary binding may occur between monomers at the hexameric interfaces in TAg. This question can best be resolved via a structural analysis of bisphenol binding to TAg, an effort that is underway. Regardless, it is important to emphasize that whatever off-target effects these agents may possess, the magnitude of these interactions is insufficient to alter cell viability anywhere near the effective concentration needed to inhibit SV40 or BKV replication.

It should be noted that determining the molecular mechanism of these small molecules on TAg was pursued aggressively without success. Purified TAg was not amenable to native gel electrophoresis (data not shown), which may have allowed me to examine the oligomeric state of TAg in the presence of the inhibitory compounds. This may have been related to the fact that more recent preparations of pure TAg appeared to be insoluble in a simple pelleting assay, despite displaying robust ATPase activity (data not shown). Although minor changes to the purification protocol may be responsible for these changes, these also greatly improved protein yield, and did not hinder the proteins activity in a variety of other *in vitro* assays (see section 3.3.1). Limited proteolysis of TAg by proteinase K did suggest that bithionol and hexachlorophene did not induce major conformational changes in the protein (Figure 13). Based on our screening method, I believe that the anti-viral activity displayed by bithionol and hexachlorophene directly targets TAg, although it remains unclear how these compounds inhibit TAg either *in vitro* or during an infection.

Unfortunately, without a better understanding of the molecular mechanism, any explanation of the distinct results on DNA replication *in vitro* and in culture is speculation. However, given the known discrepancies in these assays, I will suggest some hypotheses for this

activity. It is known that the J domain of TAg is required for viral replication, but it appears to be dispensable in the *in vitro* system (Weisshart et al., 1996), so this is not the first time such a distinction has occurred. Although the ATPase activity of TAg is essential for replication of viral DNA, it is not clear that this is the rate-limiting step in either assay. In fact, there has not been a direct correlation between the concentrations of small molecules that inhibit TAg ATPase and that inhibit DNA replication *in vitro* (Huryn et al., 2011; Wright et al., 2009). Since it is known that DNA stimulates the ATPase activity of TAg (Giacherio and Hager, 1979), it is possible that the presence of DNA in the replication assay or during an infection overcomes the effect of the inhibitors. This may explain the lack of a correlation of the effects of the compounds between the *in vitro* DNA replication assay and the ATPase assay.

Overall, the experiments reported in this chapter document three important findings. First, we were able to design a high throughput screen to identify inhibitors of the SV40 TAg. This method was suitable for screening in 384-well plates and it may be co-opted in the future to screen larger and more diverse libraries. Second, we identified two FDA-approved compounds that inhibit both TAg ATPase activity and the replication of two polyomaviruses, SV40 and BKV. Third, we developed and verified the efficacy of qPCR assays that can be employed to perform secondary and tertiary screens to more rapidly verify the efficacies of polyomavirus inhibitors in future efforts. The recent explosion in the number of new polyomaviruses and the fact that the population of immunocompromised individuals is rising indicate that there is a dire need for new antiviral therapies. My work has not only provided a novel strategy to identify potent and specific polyomavirus inhibitors, but the two most promising candidates from this effort may now be re-formulated and tested for their effects in the clinic. In parallel, high

throughput screening efforts to identify even more potent inhibitors with improved therapeutic potential have been undertaken, and are discussed in Chapter 3.

3.0 HIGH THROUGHPUT SCREENING IDENTIFIES A BISPHENOL INHIBITOR OF SV40 LARGE T-ANTIGEN ATPASE ACTIVITY.

3.1 INTRODUCTION

Polyomaviruses (PyVs) are a family of non-enveloped viruses with double-stranded DNA genomes that are able to transform cells and promote tumor formation. There are ten PyVs that are known to infect humans; one of these, the Simian Virus 40 (SV40), was unknowingly introduced into the population as a contaminant of the original polio vaccine. The oncogenic SV40 is a well-characterized model used to examine the underlying mechanisms of growth control and cancer, and induces tumors in rodents, although it is not tumorigenic in humans (Pipas, 2009; Poulin and DeCaprio, 2006). Approximately 50-80% of humans are seropositive for one of these viruses, suggesting life-long infection (Kean et al., 2009).

Two other PyVs, JC Virus (JCV) and BK Virus (BKV), result in morbidity and mortality in immunocompromised patients (see section 1.4.2). JCV is a neurotropic polyomavirus and the causative agent of progressive multifocal leukoencephalopathy (PML), a demyelination disease of the central nervous system associated with a high mortality rate. BKV infects kidney epithelial cells, and lytic infection in immune-compromised patients can cause BKV or polyomavirus associated nephropathy, which is associated with high graft loss if not recognized early (Weinberg and Mian, 2010). Integration of Merkel Cell Virus (MCPyV) sequences into Merkel

cells (in skin) seems to be the cause of Merkel cell carcinomas (Shuda et al., 2009), and Trichodysplasia Spinulosa Virus (TSV) appears to be the cause of post-transplant trichodysplasia spinulosa (van der Meijden et al., 2010). Further studies are needed to confirm if the other 6 PyVs have a role in disease. Unfortunately, there is no specific treatment for polyomavirus related diseases (Johnston et al., 2010; Josephson et al., 2006b).

SV40 is an excellent model for studying the PyVs because the conditions for the replication of this virus in cell culture are well-characterized and because all PyVs encode a viral protein, the large T-antigen (TAg), which is essential for viral replication. TAg is a multidomain protein that is transcribed early after infection. Among other features, TAg contains an N-terminal J domain, the central Origin Binding Domain, and the C-terminal helicase domain. TAg forms a double hexamer that utilizes host cellular protein factors to coordinate bidirectional DNA replication (Bullock, 1997), in addition to binding to and inactivating p53 and the Rb tumor suppressor family of proteins. In 1997, it was reported that TAg encodes a functional J domain chaperone (reviewed in (Brodsky and Pipas, 1998). The N-terminal J domain, which stimulates the ATPase activity of the cellular hsp70 chaperone, is essential for both virion assembly and disruption of Rb-E2F-binding, and mutations that compromise this chaperone function block viral replication and cellular transformation. Lastly, the oncogenic potential of SV40, JCV, and BKV can be recapitulated by TAg alone (Bollag et al., 1989). TAg is conserved among polyomaviruses, (Simmons, 2000) and there is the possibility that inhibitors of SV40 TAg may be effective across the PyV family (Wright et al., 2009).

TAg is also an ATP-dependent helicase, which is an essential activity that facilitates the unwinding of DNA during viral replication (Stahl et al., 1986). ATP binding to the TAg ATPase domain stimulates TAg hexamerization and dodecamer assembly; the active dodecamer partially

melts the viral DNA and associates with proteins required for replication (reviewed in (Bullock, 1997). Therefore, chemical modulators of SV40 TAg ATPase activity might represent a new avenue to combat PyV-associated diseases. Mutations that reduce TAg's endogenous ATPase activity also block viral replication (Castellino et al., 1997). Previous efforts to identify PyV inhibitors employed *in vitro* assays that measured inhibition of TAg-mediated p53 interactions (Carbone et al., 2003) and TAg-mediated ATP hydrolysis, (Wright et al., 2009) and led to the identification of new TAg inhibitors. However, the existing inhibitors exhibit low potency and/or low specificity, and are not necessarily amenable to future chemical optimization strategies. Therefore, the isolation of novel TAg inhibitors with unique chemical scaffolds is vital, particularly as the incidence of PyV-associated diseases is rising (see section 1.4).

To this end, in collaboration with the Noah Lab at the Southern Research Institute we performed a high throughput screen (HTS) suitable for the discovery of novel PyV inhibitors. A biochemical, fluorescence-intensity assay using the ADP Hunter kit in a 1536-well microplate format was developed to measure TAg ATPase activity in the presence of potentially inhibitory small molecule compounds from the NIH/Molecular Libraries Probe Centers Network (MLPCN) compound collection. Hits from the primary screen were counter-screened for assay interference in the ADP Hunter Screen and for cytotoxicity. Secondary assays, which utilized quantitative, established techniques for target validation, allowed for the prioritization of 'hits' from the primary screen based on potency, cytotoxicity, and target specificity. Three small molecule modulators that inhibited the ATPase activity of TAg were identified using the HTS. Subsequent chemical refinement by the Golden Lab at Kansas University produced one compound (a bisphenol derivative) that was confirmed to interfere with the replication of SV40 in infected cells. Further chemical optimization derived a fourth effective biochemical inhibitor

of TAg ATPase activity (bisphenol A), but the use of this inhibitor for *in vitro* or *in vivo* investigations is complicated by its cytotoxicity.

3.2 MATERIALS AND METHODS

3.2.1 Recombinant TAg expression and purification

For this effort, the consistency and yield of TAg purification were improved. Starting with the previously described protocol (Cantalupo et al., 1999), the purification protocol was slightly modified. A total of $4x10^8$ Sf9 insect cells grown in Grace's Complete Media containing 10% FBS and Pen/Strep were infected with wild type-TAg expressing baculovirus and plated in 15 10-cm dishes (Gibco) for 45 h. The cells were harvested by scraping and washed in PBS-EDTA with protease inhibitors. The cocktail of protease inhibitors (Leupeptin at 2 μg/mL, Aprotinin at 2 μg/mL (Roche), soybean Trypsin inhibitor at 1 μg/mL (Roche), Pepstatin at 1 μg/mL, E64 at 1 μg/mL (Roche), TPCK at 1 μg/mL (Sigma), and PMSF at 1 mM) were added freshly to all buffers until the dialysis step. Modest improvements were made by decreasing the lysis volume to 15 mL, which was achieved by adding 1 mL Kelly's lysis buffer per 10 cm dish infected 0.2M LiCl, 20 mM Tris pH8.0, 1 mM EDTA, 0.5% NP40, and 1 mM DTT. The lysate was clarified using a 2 μm filter and then centrifuged for 30 min at 15,000 rpm, in an SS-34 rotor at 4°C. The lysate was loaded onto a PAb419-Protein G Sepharose Fast Flow column (GE Healthcare) at 10 mL/h using a peristaltic pump. The column was washed with 15 mLs of each of the three wash buffers. The first wash buffer contains 20 mM Tris pH 8.0, 0.5 M NaCl, 1 mM EDTA, 1% NP40, 10% glycerol, and 1mM DTT. DTT and protease inhibitors were freshly added. The

second wash buffer was the same as the first but lacks NP40, while the third wash buffer was identical to the second but adjusted to pH 9.0. TAg was eluted from the column with 20 mM CAPS pH 11.0, 0.5 M NaCl, 1 mM EDTA, 10% glycerol and 1 mM DTT directly into 0.5 M Tris pH 7.0, 1 mM EDTA, and 10% glycerol. Peak fractions were dialyzed into 10 mM Tris pH8.0, 1.0 mM EDTA, 100 mM NaCl, 10% glycerol, 1 mM DTT overnight at 4°C. These fractions were flash frozen in liquid nitrogen, and purity was confirmed by subjecting fractions to SDS-PAGE followed by Coomassie Brilliant blue stain and western blot with a TAg specific-antibody (described below). The activity of TAg was confirmed by steady state ATPase assay.

3.2.2 Expression and purification of PAb419 from hybridoma cells

PAb419 hybridoma cells express a TAg specific antibody that is ideal for purification of SV40 TAg (Cantalupo et al., 1999; Harlow et al., 1981). The culture was kept between 5 x 10^4 and 5 x 10^5 cells/mL in DMEM with 10% FBS, and since these cells are non-adherent, they were gently mixed prior to counting on a hemocytometer. Cells were diluted 1:10 or 1:20, and sub-cultured between 2-4 d. There was no need to remove the old medium, as this contained antibody. The hybridomas were expanded to at least ten T150 dishes (Falcon).

Once fully expanded, the culture was allowed to grow until the cells died (~14 d), because when the cells leave log phase, they over-express antibody and release it into the medium. Death can be induced by reducing serum levels, but this was not necessary. The media was collected from an expired culture, and spun at 100x*g* in a clinical centrifuge for 10 min at RT. The antibody-containing supernatant was harvested. If debris remained, an additional 10 min spin was used to clear the antibody solution prior to column purification. The typical yield was 20-50μg antibody/mL of cellular supernatant. This supernatant was either used directly for

detection of TAg by immunofluorescence or Western blot, or purified with Poros Protein A column (Invitrogen) if antibody was used for the column purification TAg.

To purify the antibody, 50-100 mL supernatant was loaded onto a 1-2 mL Poros Protein A column, and the column was run at 1 mL/min, or by gravity. The column was washed with 25 column volumes of PBS-Tween 20 (0.05%), and the antibody eluted in 0.1 M glycine-HCl, pH 2.5. The eluate can be dialyzed into another buffer or stored at this pH with 0.02% NaN_3 at 4°C to preserve for future use.

3.2.3 Screening Assay Validation Conditions

The early high throughput screen validation assays were conducted in 384-well black, clear-bottom microplates (#3712 Corning Inc., Corning, NY). Assay buffer consisted of 100 mM Tris-HCl, 20 mM KCl, 6 mM $MgCl_2$, and 0.1 mg/mL BSA, pH 7.4. Initially, 5 µL of test compound (single dose, 20 µM final concentration, as described below) in assay buffer with 5% DMSO was added to the respective plate wells. Purified TAg was diluted to a concentration of 14.4 ng/µL in assay buffer. A total of 15 µL of TAg (14.4 ng/µL, 216 ng total) in assay buffer was added to each well and allowed to incubate for 30 min at ambient temperature. Following incubation, 5 µL of 5mM ATP (A7699, Sigma-Aldrich, St. Louis, MO) in assay buffer was added to the respective wells, and incubated for 120 min at ambient temperature. Total reaction volume (without endpoint reagent) was 25 µL. Commercially available kits (e.g., Malachite Green Phosphate Assay Kit, POMG-25H, from BioAssay Systems, Hayward, CA and the ADP Hunter-Plus Kit [DiscoverX, Freemont, CA]) were used according to the manufacturer's instructions to measure ATP hydrolysis. Enzyme and buffer volumes were dispensed using a WellMate

(Matrix, Hudson, NH). Compounds were dispensed manually. The final DMSO concentration was 1.0%.

3.2.4 Pilot and Primary Assay Conditions

The assay was conducted in 1536-well black, clear-bottom microplates (#3891 Corning Inc., Corning, NY), and was used for both the full library single-dose screen and the confirmatory dose-response evaluation of hits. Assay buffer is listed above. Initially, 250 nL of test compound (single dose, 20 µM final concentration, as described below) in assay buffer supplemented with 5% DMSO was added to the respective plate wells. Purified TAg was diluted as above. A total of 750 nL of TAg (14.4 ng/µL, 10.8 ng total) in assay buffer was added to each well and allowed to incubate for 30 min at ambient temperature. Following incubation, 250 nL of 5 mM ATP in assay buffer was added to the respective wells, and incubated for 120 min at ambient temperature. Total reaction volume (without endpoint reagent) was 1.25 µL. Enzyme and buffer volumes were dispensed using a BioRAPTR FRD (Beckman Coulter, Fullerton, CA). Compounds were dispensed using an Echo 500 Series Liquid Handler (Labcyte, Sunnyvale, CA). The final DMSO concentration was 1.0%.

Endpoint readings: The endpoint method was by fluorescence detection, using the ADP Hunter Kit (Charter, 2006) and the manufacturer's instructions. The plates were bottom-read for fluorescence intensity using an Envision plate reader (Perkin Elmer, Waltham, MA) at an excitation/emission of 530/590 nm, respectively.

Controls and Compound Addition: The positive control (MAL2-11B; (Wright et al., 2009) was diluted in 4% DMSO/assay media and added to the control wells of each plate (250 nL at 5x concentration, for a final reaction concentration of 100 µM) before the addition of TAg.

The final concentration of MAL2-11B was 100 µM. Additional controls included full reaction wells (containing TAg, DMSO blank, and ATP), and background wells (containing assay buffer, DMSO blank, and TAg) on each plate. The final DMSO concentration was 1% for all plate wells.

3.2.5 Counter-Screens for cytotoxicity and assay interference

In each assay, compounds were added in dose-response format. The cytotoxicity assay was cell-based in 384-well plate format and used Madin-Darby Canine Kidney cells (MDCK, ATCC, Manassas, VA, CCL-34, passage 55). The cytotoxicity assay was conducted for 72 h, after which cell viability was determined using Cell-Titer Glo (Promega, Madison, WI) (Noah et al., 2007). To measure assay interference, the counter-screen was performed using the primary assay method (above), but without TAg (buffer only). A final concentration of 10 µM ADP was used instead of ATP, and the assay was read 10 min following the addition of the endpoint reagents.

3.2.6 DNA replication assays

DNA replication assays, using a reporter plasmid that contained the SV40 origin of replication, were performed as previously described (Wright et al., 2009) as well as in section 2.1.3.

3.2.7 Cell Culture

Madin-Darby Canine Kidney (MDCK) cells were obtained from American Type Culture Collection. African Green Monkey kidney cell line BSC-1 (ATCC, Manassas, VA, CCL-26) were used for the cytoprotection and viral load reduction assays. Cells were cultured in DMEM with 2 mM L-glutamine, 1X pen/strep, and 10% FBS. CV1 cells were cultured in MEM with 10% FBS and pen/strep. The cells were maintained at 37°C, 5.0% CO_2 to 90% confluence. The cells were trypsinized, and recovered. The trypsin was neutralized with culture media.

3.2.8 Preparation of SV40

SV40 stocks were prepared from the plasmid pSVB3. This plasmid contains the entire SV40 genome incorporated into the pBR322 backbone at a BamH1 site (Peden et al., 1980). pSVB3 was digested by BamH1, and then phenol:chloroform extracted. The clean DNA fragments were diluted to 3 μg/mL and ligated with T4 DNA ligase overnight at 15 °C. The low concentration of DNA in the ligation reaction favors circularization over concatamerization. The ligation reaction was heat killed and then transfected into CV1 with Lipofectamine (Invitrogen), according to manufacturers instructions. The media was changed the next day, and the transfection proceeded 6 d before the cells were freeze-thawed three times to lyse. This created a low titer viral stock, which was used to infect CV1 cells in 10 cm dishes. The CV1s were supplemented with 2mL of fresh media 2 dpi, and the infection continued a total 8 dpi, or until there was significant CPE. This viral stock was titered by plaque assay, as described in section 2.2.4. Typical yield was between $8x10^7$ and $1x10^8$ pfu/mL.

3.2.9 Cytoprotection assays

This assay was used to test the ability of compounds to protect from viral cytopathic effects (CPE). BSC-1 cells in DMEM with 10% FBS and 4mM L-glutamine (Assay Media) were plated in 96-well microplates at 15,000 cells/well. After 18 h, test compounds were diluted to a final concentration in the range of 200 - 1.6 µM as indicated, added to the cells, and incubated for 30 min. Afterward, 100 $TCLD_{50}$s (50% tissue culture lethal dose, the virus stock dilution that induces CPE in 50% of the cells at endpoint) of SV40 virus (prepared as described in section 3.2.9) were added to each well. Cell viability was determined after 120 h using Cell-Titer Glo (Promega, Madison, WI) (Noah et al., 2007).

3.2.10 Compound handling for the HTS effort

The NIH Molecular Libraries Probe Centers Network (MLPCN) compound library was used for the primary HTS screening. Compounds (stored in 100% DMSO) were diluted into Assay Media (see section 3.2.8) by automation and added to the plates in 5 µl volumes using a Biomek FX liquid handler (Beckman Coulter, Fullerton, CA). The final compound concentration used in primary, single-dose screening was 20 µM, with a final DMSO concentration of 1%.

3.2.11 Data acquisition and analysis

96 full reaction wells, 96 background wells, and 64 control drug wells per plate were used to calculate the Z' value (Zhang et al., 1999) for each plate and to normalize the data on a per plate basis. Results for each concentration of compound were expressed as percent inhibition (%

Inhibition), which was calculated as: 100*((Median Enzyme Control-High Dose Control Drug) - (Test well-High Dose Control Drug))/(Median Enzyme Control-High Dose Control Drug). The dose response data were analyzed using a four parameter logistic fit to the data (XLFit equation 205) with the maximum and minimum locked at 100 and 0. From these curves IC_{50} values were calculated for TAg and CC_{50} values were calculated for MDCK cell cytotoxicity. A Selectivity Index for compounds showing TAg inhibition was calculated as $SI = CC_{50}/EC_{50}$. Raw data were imported to Activity Base Data Management software (IDBS, Alameda, CA) for determination of Z, Z', S/B, S/N, and percent inhibition for assayed compounds. Compounds showing greater than 30% inhibition of TAg ATPase activity were considered "hits". Statistical calculations were made as follows: $Z = 1 - ((3\sigma R + 3\sigma B)/|\mu R - \mu B|)$, where μR is the mean reaction signal, σR is the standard deviation of the reaction signal, μB is the mean background control signal, and σB is the standard deviation of the background control signal. $Z' = 1 - ((3\sigma d + 3\sigma B)/|\mu d - \mu B|)$, where μd is the mean MAL2-11B control signal, σd is the standard deviation of the MAL2-11B control signal. Signal to background (S/B, fold increase) = $\mu R/\mu v$. Signal to noise (S/N) = $(\mu R - \mu B)/((\sigma R)2 + (\sigma B)2)1/2$ (Zhang et al., 1999). Each assay validation step was performed in triplicate with the exception of the pilot validation screens with 6,930 compounds, which was performed in duplicate.

3.2.12 Compound acquisition and/or synthesis

Many of the compounds were obtained from commercial sources. All compounds, regardless of source, were purified by silica gel chromatography and analyzed by LCMS and NMR. Bisphenol A (CAS# 80-05-7, 2,2-Bis(4-hydroxyphenyl)propane, SID 92277586) was acquired

commercially from TCI America. Silica gel chromatography was then performed with 1:1 hexanes/ethyl acetate as eluent, analyzed by LCMS at 214 nm and the structure was confirmed by proton and carbon NMR. ^{1}H NMR (400 MHz, DMSO-d6) d 1.55 ((s, 6H, CH3); 6.68 (d, J = 8.7 Hz, 4H); 7.01 (d, J = 8.7 Hz, 4H); 9.17 (s, 2H, ArOH); ^{13}C NMR (100 MHz, DMSO-d6) δ 154.9; 141.1; 127.3; 114.6; 40.9; 30.9; TLC Rf: 0.51 (1:1, hexanes:ethyl acetate). HPLC (Acquity BEH Shield C-18, 5-95% CH3CN in H2O): Retention time = 2.713 min; bisphenol A did not ionize.

3.3 RESULTS

3.3.1 Improving TAg purification protocol

To undertake a very high throughput screen (HTS) for TAg inhibitors, active TAg needed to be efficiently purified. Previously published purification protocols produced TAg relatively quickly (pure, dialyzed TAg was prepared 3 dpi) with yields of less than 1mg of protein (Cantalupo et al., 1999). In this method, TAg is expressed in Sf9 cells from a baculovirus stock, and purified over a monoclonal antibody column. Because TAg is very labile and requires specific phosphorylation events for robust activity (Chen et al., 1991; Hubner et al., 1997; McVey et al., 1989), I preferred to modify the previous protocol rather than redesign the purification scheme (Hoss et al., 1990). Factors that were considered to improve the yield were to improve expression, maximize binding to the antibody column, and minimize protein loss during washes.

As summarized in Table 8, I modified several variables in the purification. I determined that the recommended infection time of 45 h was ideal for TAg expression, and that the

particular viral stock used did not seem to greatly affect yield. Baculovirus stocks are not generally titered for this type of use because of the quick turnover (one expansion of the "stock" in ten 10-cm dishes results in enough baculovirus for two TAg preparations), but seem to have a similar viral yield when the appropriate protocol for expansion is followed (Cantalupo et al., 1999). However, I did choose to modify the lysis conditions. The column had a tendency to clog during the very slow load of the lysate, which is why the volume of Kelly's lysis buffer used was more than 1 mL/10 cm dish. However, anecdotal evidence suggested that resuspending the column to repair the clog seemed to negatively impact the yield and protein activity. I hypothesized that during the 2.5 hours the column was loading, proteins were aggregating on the column preventing efficient flow. By decreasing the volume of lysis buffer, the time required to load the lysate was decreased, as was the risk of clogging.

Next, I determined that the majority of the wash volume (recommended at 25 times the column volume) was not necessary, and the major protein washing off the column was TAg. Therefore, the wash volume was decreased to 10 mL without significantly impacting the purity of the final protein. While the time spent in dialysis did not seem to negatively affect the activity of the protein, I did determine that protein purified at a higher concentration was relatively more active than protein purified at a lower concentration. One factor that consistently impacted the outcome of the final protein concentration was the column, which lost affinity for TAg after about 7-10 purifications. Although the column can be stored for years, multiple uses resulted a decline in purification efficiency, which can be determined by detecting TAg in the third column wash buffer (Figure 17).

Overall, these changes to the protocol made modest changes to the expected yield of purification, but greatly increased the predictability of the protocol and decreased the overall

time needed to purify TAg. This facilitated the purification of the ~ 12 mgs that were required for the HTS performed by the Noah Lab.

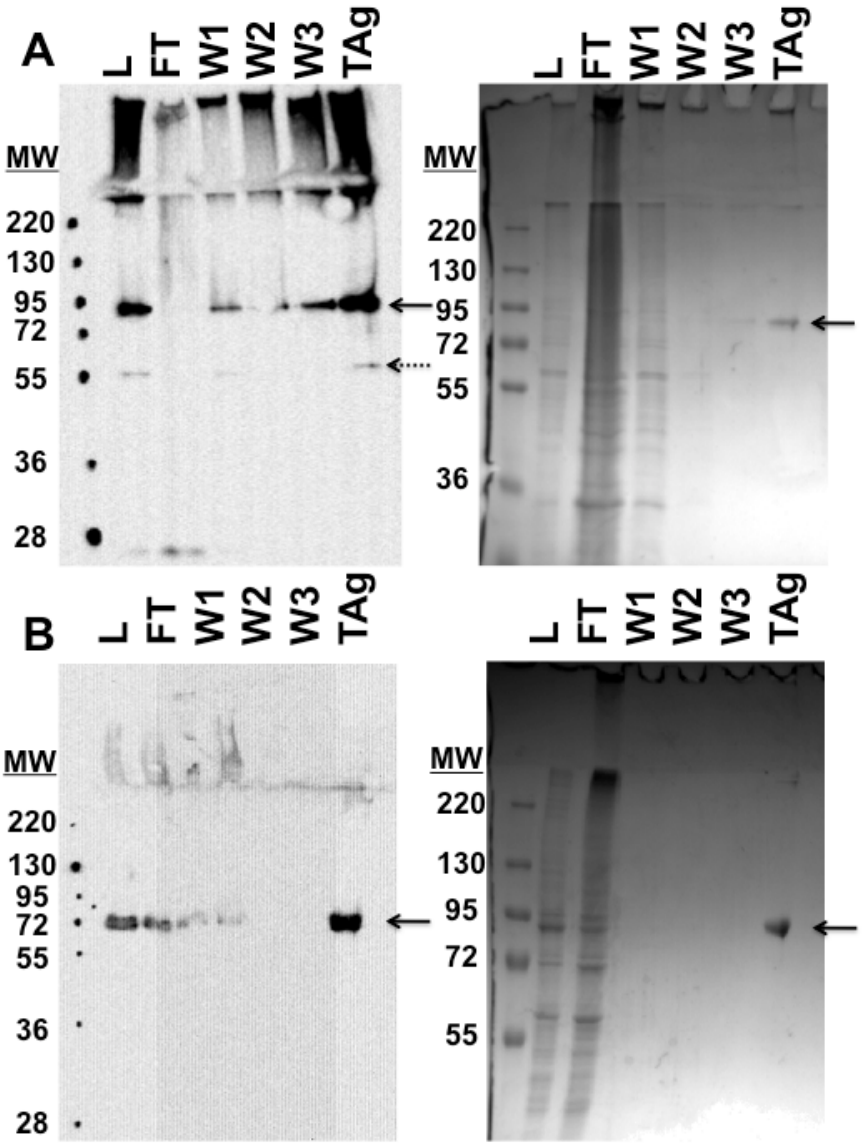

Figure 17. Modifications to TAg purification protocol improve yield.

Abbreviations are as follows: L- lysate, FT- column flow through, W1- Wash 1, W2- Wash 2, W3- Wash 3, TAg- purified TAg after dialysis. Arrow indicates full length TAg. Dashed arrow represents a contaminant that may be cleaved TAg or free antibody; the presence of this band is indicative of low activity in the final purified protein. A. Samples from the protocol initially used for TAg purification. Left panel is a Western blot with pAB419, and the right panel is a Coomassie Brilliant blue stained gel. It is clear that TAg is in W3 in both cases, and it is evident from the right panel that TAg is the major component of W3. B. After protocol modification and a new column, less TAg was lost in W3.

Table 8. Notes from TAg purification during optimization.

The following data highlight the changes made to the TAg purification protocol and the effect on outcomes. Among the variables tracked, the date of the baculovirus stock and the hours of this infection seemed not to make a significant difference. Reducing the volume of Kelly's Lysis Buffer (KLB) that was used to lyse the Sf9 cells seemed to affect column clogging during loading. The duration of dialysis did not seem to impact yield or activity, but the volume of the wash buffer used was minimized to a volume where minimal levels of any protein (and specifically TAg) were washed off. This had the greatest impact on TAg total yield and concentration. NR indicates not recorded.

Date of Prep	Viral stock	Hours infected	KLB Volume	Column clogged?	Dialysis (h)	Volume of washes (mL)	Yield (mgs)	[Tag] µg/µL
11/12/08		45	25		16	22	1	0.55
12/9/08	12/2/08	46	20	N	6	22	0.48	0.26
12/11/08	12/2/08	45	20	N	6	22	0.528	0.3
12/15/08	11/15/08	45	25	Y	4	10	0.96	0.4
12/18/08	12/2/08	45	15	N	16	11	1.21	0.55
1/21/09	11/15/08	45	15	N	17	11	1.38	0.46
1/24/09		45	15	N	5	11	1.54	0.7
1/26/09	11/27/08	45	10	N	15	10	NR	0.39
1/29/09		45	10	N	6	10	1.1	0.55

3.3.2 Primary Assay Development and Validation

In collaboration with the Noah lab, a biochemical assay to screen diverse compound libraries for efficacy against the ATPase activity of SV40 TAg was developed and validated. During assay development, the Noah lab defined the optimum endpoint detection method (fluorescence) and time, DMSO tolerance, optimum enzyme concentration, and confirmed equivalency to other established ATPase assays (e.g., in comparison to malachite green). They also confirmed the efficacy of a positive control, MAL2-11B (Wright et al., 2009), an inhibitor of the ATPase activity of TAg in this assay. They began with the adaptation and validation of the 96-well microplate assay format for TAg-mediated ATPase activity to a 384-well microplate format. This included quantification of HTS assay parameters such as coefficient of variation (CV), signal-to-background (S/B), signal-to-noise (S/N), Z-value, and establishment of the positive and negative control conditions, values, and compounds. The assay was linearly miniaturized into 1536-well microplates. HTS validation included a survey of any edge and liquid handling effects and reagent and read stability, and was completed by duplicate pilot screening of a 6,390 compound library. Each development step was performed in triplicate, and validation steps were performed in duplicate unless otherwise noted.

Malachite green can be used to determine the amount of free phosphate liberated as a product of TAg-mediated ATP hydrolysis. This assay method is based on the complex formed between malachite green molybdate and free orthophosphate under acidic conditions. Although this assay endpoint method provided sufficient reliability and S/B ratios for detection of TAg ATPase activity in 96-well microplate format, the limiting reagent in screening a large library of compounds (>300,000) was the amount of purified TAg available for screening. Because the

expression and purification of recombinant TAg was both economically and temporally costly, it was necessary to miniaturize the assay as much as possible while maximizing robustness and S/B.

A comparison of the malachite green assay and a commercially available product, the ADP Hunter kit (Charter et al., 2006) was also performed to measure inhibition of TAg-mediated ATPase activity, with the caveat that compounds that inhibit the reagent enzyme cascade or are themselves inherently fluorescent will result in a false signal. The fluorescent signal is red-shifted, minimizing potential interference from fluorescent compounds. Both assay methods were evaluated for S/B, Z, control drug interference, read stability, sensitivity, and DMSO tolerance. To do this, the Noah lab first compared the limits of detection (sensitivity) of both the malachite green and ADP Hunter assays. The limit of substrate detection for the ADP Hunter assay is two-fold lower than that seen using the malachite green assay (Figure 18). The ratio of signal-to-background (S/B) values at 1 µM substrate is 2.04 for ADP Hunter, and 1.06 for malachite green. The maximal S/B values are 19.33 (ADP Hunter) and 7.75 (malachite green). This indicated that ADP Hunter could be miniaturized further without losing signal, and prompted us to choose the ADP Hunter endpoint methods for all subsequent validation experiments.

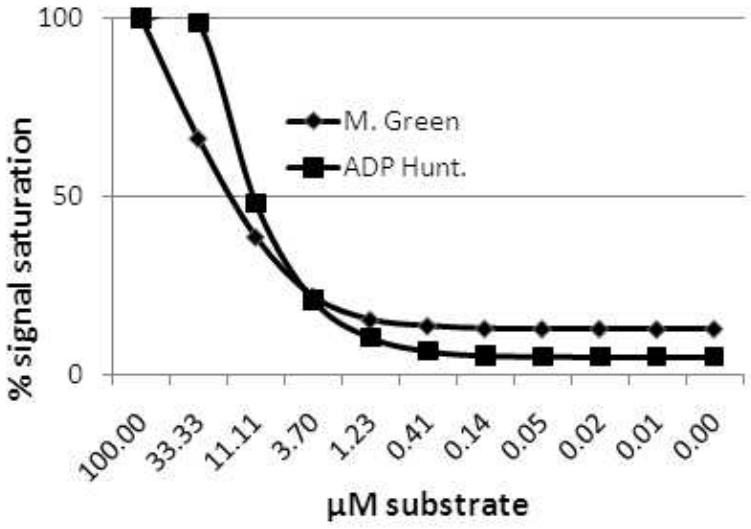

Figure 18. Comparison of assay sensitivity using the malachite green and ADP Hunter endpoint methods.

The graph shows the increase in assay signal with a titration of substrate (phosphate or ADP, respectively). The X-axis shows substrate concentration in µM, and the Y-axis shows the percentage of the maximum signal at each substrate concentration. Each point represents the mean from three assays. To simplify the figure, error bars are not shown; standard deviation for each point was < 2%.

We then determined assay sensitivity to DMSO. For large-scale screening, compound libraries are generally stored in DMSO, which at higher concentrations (>1%) may dramatically affect cellular membrane permeability and viability (Irvine et al., 1999). The assay tolerated DMSO concentrations up to 5% without an effect on the detection parameters. To promote increased compound solubility in the assay media, we standardized the assay to run in 1% DMSO for all subsequent primary screening. Additional experiments using the control compound MAL2-11B (at a final concentration of 100 µM) determined that DMSO did not interfere with the assay sensitivity (data not shown) (Wright et al., 2009). Lastly, the assay

background signal was highest in the absence of ATP but with TAg present, indicating that non-enzymatic ATP hydrolysis is only a minor contributor to background signal (data not shown). Instead, the higher background signal in the presence of TAg suggests that residual ADP was present in the purified TAg that contributed to a higher background signal. Because of this observation, ATP was omitted in the negative control wells (- reaction), but TAg was retained in order to reflect an accurate assay signal window. For the screening conditions a final reaction TAg concentration of 8.6 ng/µL was chosen, and a reaction time of 120 min, as longer incubations of the reaction did not result in an appreciable signal return (data not shown).

3.3.3 Pilot and Primary Screening

To complete assay validation, the Noah lab linearly reduced the well volume of the reaction for direct transference into a 1536-well microplate format and conducted a duplicate pilot screen of 6,390 compounds. Table 9 lists the pilot screen data. It shows that 68% of the hits that decreased fluorescence in each pilot screen more than 19% (which was the S/N threshold) correlated, indicating that the assay reliably identified potential ATPase inhibitors.

Table 9. Summary of the TAg ATPase HTS assay pilot validation and primary screen.

Pilot Screen Parameters	Screen 1	Screen 2
n compounds	6,390	6,390
mean Z [a,b]	0.69 ± 0.05	0.55 ± 0.06
mean S/B [a,b]	2.7	2.4
S/N [a,b]	24	27
pilot screen ≥ 19% inhibition hit rate[a,c]	0.58% (n = 37)	0.59% (n = 38)
≥ 19% inhibition hit rate correlation coeff.[c]		68%
Significance	p =	< 0.005
Primary Screen Parameters		
mean Z [a,b]	0.68+/- 0.04	
mean inhibition	2.04% +/- 5.36%	
mean S/B [a,b]	3.9	
≥ 44% inhibition hit rate[a,c]	0.81% (n = 2500)	
Dose response confirmation of ≥ 44% inhibition hit rate	48%	

[a]**Values for Z, S/B, S/N, and pilot screen hit rates are averaged from duplicate screens. Standard deviations are given as +/- values.**

[b]**Calculations for Z, S/B, and S/N are detailed in section 3.2.11.**

[c]**Hit rate is based on the number of compounds that inhibited fluorescent signal by > 44% in duplicate pilot and primary screens.**

The Noah lab followed the pilot validation with a full screen of the NIH Molecular Libraries Probe Centers Network compound collection (306,015 compounds), which was screened in single dose at a concentration of 20 μM. Primary screening data are also shown in Table 9. A total of 2153 hits that inhibited ATPase activity >44% were available for confirmation. These were screened in dose-response over a 625-fold concentration range (from 100 μM to 0.16 μM) for assay interference, cytotoxicity, and inhibition of ATPase activity. Assay interference counter-screening (using 10 μM ADP) was performed simultaneously with the confirmatory assay to exclude compounds that inhibit the coupling enzymes in the assay kit. Compounds that were positive in the counter-screen (inhibitory by assay interference) were considered inactive. Compounds that inhibited in the primary screen but had no effect in the counter-screen were considered active. Finally, a cytotoxicity screen of the hits in MDCK cells was performed. Of the 2153 compounds, 104 reduced TAg-mediated fluorescence without interfering with the assay itself or exhibiting extreme toxicity. The primary assay IC_{50} values for these compounds ranged from <0.16 μM to 53 μM.

3.3.4 Assay Hit Characterization by Secondary Assays

The 104 confirmed hits were further restricted by their degree of "drug-likeness," that is to what extent each compound looked non-toxic, cell permeable and amenable to chemical refinement. Compound promiscuity (the number of times hits were identified in other PubChem primary screens) was also surveyed, and compounds isolated as hits in >20% of assays were excluded from further consideration, as were chemical scaffolds that were not amenable to medicinal chemistry. Three compounds (Figure 19) were selected for further evaluation using targeted, mechanistic secondary assays (see Figures 19, 20 and 21). These compounds (PubChem SIDs 85281215, 85281217, and 85281218) were purchased from commercial sources, purified, and retested in the primary assay for confirmation of activity. The IC_{50} values for the three ranged from 7 µM to 27 µM, while the control compound MAL2-11B had an IC_{50} of 19.4 µM (Figure 19). To determine target specificity, I tested SIDs 85281215, 85281217, and 85281218 in a secondary biochemical assay for TAg-dependent DNA replication (Figure 20). In this assay, TAg recruits cellular machinery from the supplied HeLa cell lysate to polymerize trace radioisotope-labeled nucleotides into replicating DNA over time. Each compound was tested at 100, 300, and 800 µM. While all three compounds inhibited TAg dependent DNA replication at 800 µM (Figure 21), SID 85281215 is the most potent biochemical inhibitor of DNA polymerization, and DNA replication was absent at 300 µM.

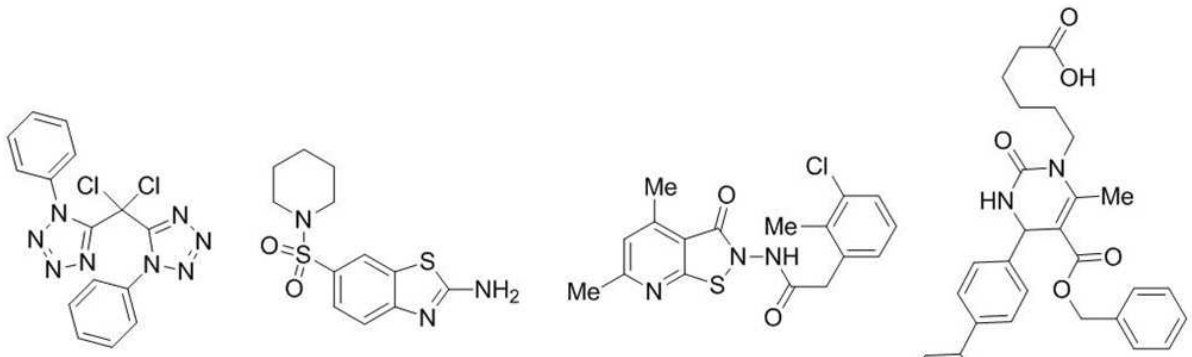

Entry	Pubchem SID or CID	1° Screen IC_{50} (μM)	2° Screen EC_{50} (μM)	2° Assay TC_{50} (μM)
1	SID 85281215	7.3	ND	34.0
2	SID 85281217	14.7	ND	200.0
3	SID 85281218	26.2	ND	64.0
4	CID 5461634 (Mal2-11B)	19.5	80.0	114.0

ND = not determined

Figure 19. Compounds confirmed as active against SV40 TAg ATPase activity in a biochemical assay.

Structures of the three primary assay hits and control compound MAL2-11B are depicted. The corresponding biochemical assay inhibitory concentrations (IC_{50}), the cell-based effective concentrations (EC_{50}), and the cytotoxic concentrations (TC_{50}) are tabulated for each compound. ND indicates that the values were not determined due to high compound cytotoxicity.

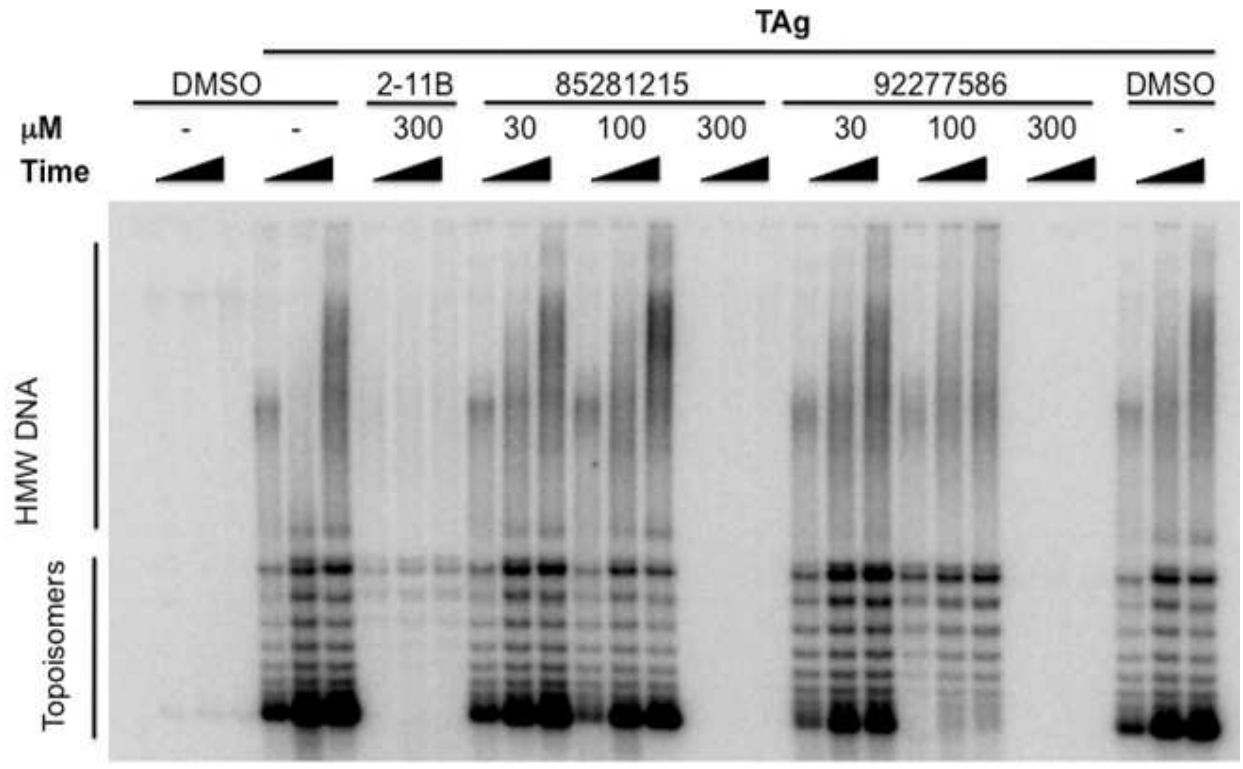

Figure 20. Specificity for TAg is demonstrated by TAg dependent *in vitro* DNA replication assays.

The figure compares the effects of increasing concentrations of MAL2-11B (2-11B), and SIDs 85281215 and 92277586 on TAg-dependent DNA replication. Products were analyzed by agarose gel electrophoresis. The increasing polymerization of high-molecular weight DNA (HMW DNA) is observed in uninhibited lanes, but is decreased where compound-mediated enzymatic inhibition occurs. The concentration of compound in μM is indicated at the top of the figure. Increasing reaction time (t=30, 60 or 90 min) is indicated by a black wedge.

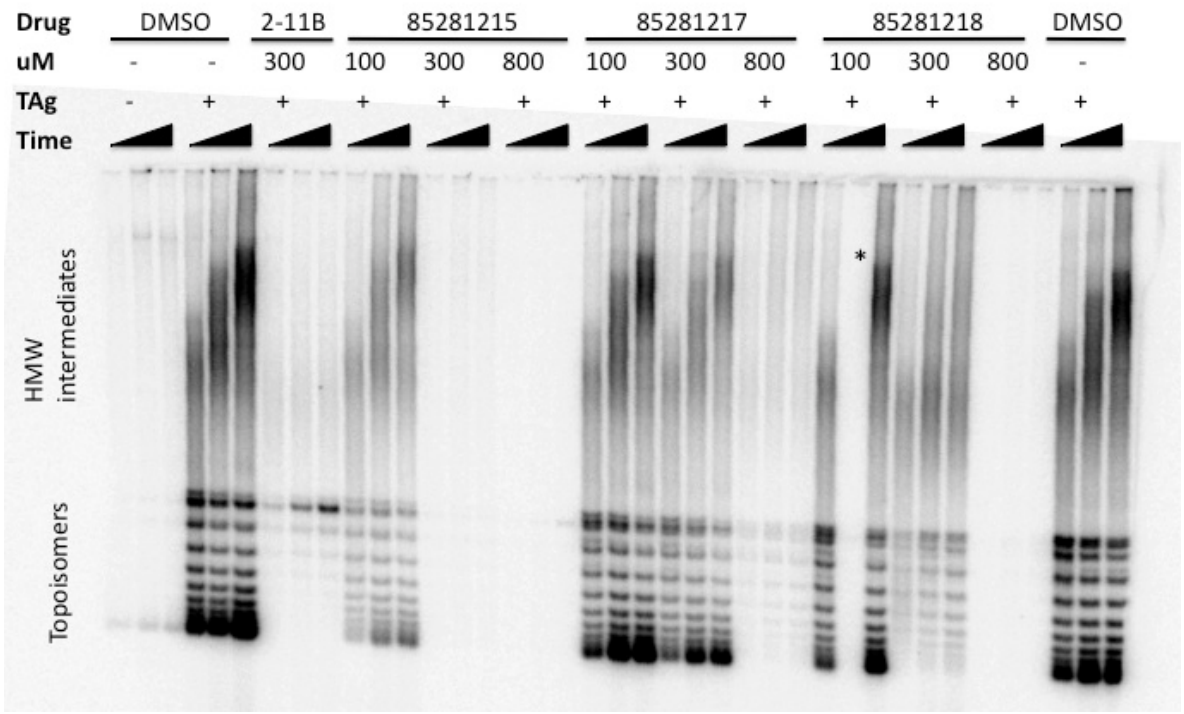

Figure 21. All three scaffolds inhibit TAg dependent *in vitro* DNA replication at high concentration, but to varying effects.

***In vitro* TAg dependent DNA replication was performed in the presence of the indicated compounds. TAg, DNA, HeLa cell lysate and a radiolabeled dCTP were mixed in the presence of an ATP regenerating system at 37°C for t=30, 60 or 90 min, as indicated by the black wedge. From each time point, the DNA was ethanol precipitated and resolved on an agarose gel. Incorporation of the radiolabel indicates DNA replication. This activity is TAg dependent, and has been shown to be dependent on the concentration of HeLa lysate and time (data not shown). (* indicates DNA lost during precipitation)**

To examine the selectivity and *in vitro* efficacy of these chemotypes, the Noah lab tested the ability of the three compounds, SIDs 85281215, 85281217, and 85281218, to protect against SV40 virus-induced cell death in a BSC-1 cell culture cytoprotection assay. Of the three, only SID 85281215 sustained cell viability (16%) in the cytoprotection assay, but the effect was limited due to observed cytotoxicity near the effective concentration (EC_{50}) (Figure 22). Cytoprotection assays also showed that the TC_{50} (toxic concentration) values for the test compounds ranged from 34 μM to greater than 200 μM (Figure 22).

3.3.5 Analog design and syntheses

Chemical optimization was initiated on compound SID 85281215 (5-[dichloro-(1-phenyltetrazol-5-yl)methyl]-1-phenyltetrazole). Systematic alteration of the dichloro-bis-tetrazole scaffold resulted in a steep structure-activity relationship (SAR) profile for an initial set of compounds. The series also required the use of challenging and unreliable chemistry to obtain analogs (J. Golden, personal communication); therefore, similarly tethered bis-aryl scaffolds were investigated. This effort was aimed at identifying structurally-related leads that could be derived from more accessible synthetic methods. In principle, this could provide a more tractable SAR and yield improved activity profiles. One of the several scaffolds that was surveyed belonged to the bisphenolic series of compounds. Bisphenol A (SID 92277586, or 4-[2-(4-hydroxyphenyl)propan-2-yl]phenol) was purchased as part of this exploratory SAR effort. The compound had an EC_{50} = 6.2 μM in the CPE assay and a TC_{50} = 7.9 μM (Figure 22), thus possessing a narrow therapeutic margin. To improve this profile, a standard SAR approach was undertaken to reveal the importance of various structural features of this scaffold. Bisphenol A is a symmetrical compound containing a geminal dimethyl linkage that tethers two identical 4-

substituted phenols. The impact of changing the substituted positions of the hydroxyl groups, replacing the phenolic hydroxyl groups, molecular desymmetrization by altering aryl substitution on one side, or modifying the linker was investigated (Table 10). Interestingly, these results confirm the separate SAR that was determined for the bisphenols identified in Chapter 2 (see section 2.2.2). After optimization efforts and by using the biochemical and *in vitro* assays described above, we identified SID 92277586 as the most effective TAg inhibitor. In the primary biochemical assay, this compound exhibited a comparably high IC_{50} of 41.4 µM (Table 10) but it showed somewhat better efficacy than either SID 85281215 or MAL2-11B in the DNA replication assay (some inhibitory at 100 µM, and complete inhibition at 300 µM, Figure 20), and in the cytoprotection assay (EC_{50} = 6.2, Figure 22). However, SID 92277586 still retained high cytotoxicity, with an SI (specificity index) of 1.3.

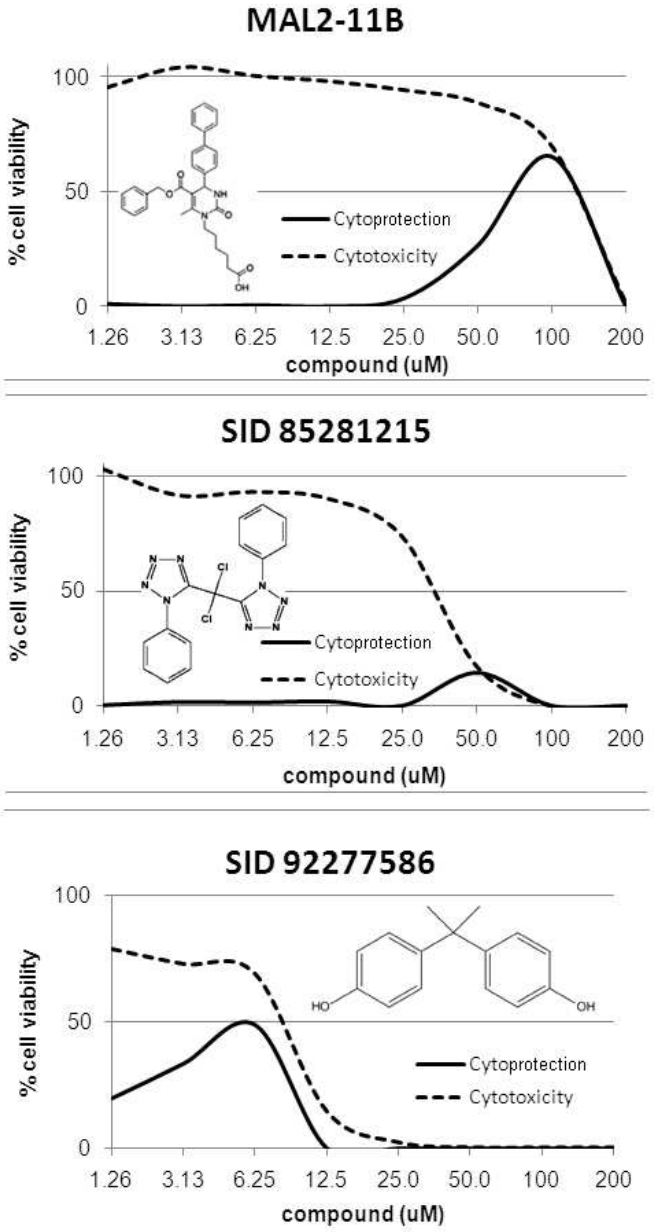

Figure 22. Cytoprotection and cytotoxicity of TAg inhibitors.

The indicated compounds were tested (200-1.26 µM) in cytoprotection assays using BSC-1 cells, and % cell viability was measured six d post-drug or post-viral infection. The dashed line represents cells in the presence of compound only (cytotoxicity), and the solid line represents infected cells with compound (cytoprotection). Compound structures are indicated for the two compounds identified in by this screen. The corresponding numerical EC_{50} and TC_{50} values are given in Figure 19.

Table 10. A structure activity relationship for bisphenol A and analogues.

Green highlights the modified portion of each structure. Compounds with a primary assay EC_{50} > 100 µM were not tested in secondary assays. ND indicates that no data was obtained during the experiment, either because the compounds had a primary assay EC_{50} > 100 µM or because the compound CC_{50} in the cytoprotection (CPE) assay was lower than the EC_{50}.

Entry	Pubchem SID	Structure	Primary assay EC_{50} µM	Secondary CPE assay EC_{50} µM	Cellular toxicity TC_{50} µM	Therapeutic index EC_{50}/CC_{50}
1	SID 92277586	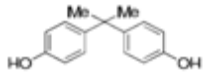	41.4	6.2	7.9	1.2
2	SID 96022078		>100	ND	ND	ND
3	SID 99206586	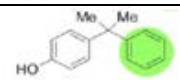	>100	ND	ND	ND
4	SID 99206566	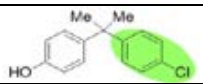	100.0	ND	71.2	ND
5	SID 93575587	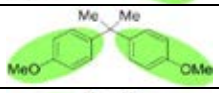	>100	ND	ND	ND
6	SID 99206560	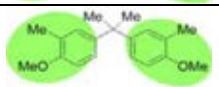	>100	ND	ND	ND
7	SID 99206561	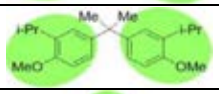	26.7	11.9	24.0	2.0
8	SID 96022079	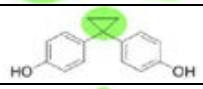	18.0	ND	196.0	ND
9	SID 99234230	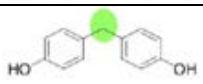	70.1	ND	>200	ND
10	SID 99234234	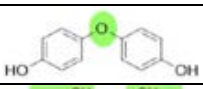	37.7	ND	9.9	ND
11	SID 99234233	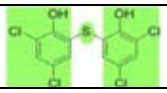	35.7	ND	21.2	ND

3.4 DISCUSSION

We employed a high throughput, biochemical assay as the primary screen to identify compounds that inhibit SV40 viral replication by targeting the SV40 large T antigen ATPase activity. During assay development we defined assay parameters and validated the screen. We performed a primary screen and several counter-screens, which resulted in the identification of scaffolds that inhibited TAg ATPase activity. Lastly, we performed secondary assays for specificity and *in vitro* efficacy.

We designed the biochemical HTS to address the lack of specific treatments for PyV-related diseases. I hypothesized that inhibitors of SV40 TAg might also be effective against more clinically-relevant PyVs based on the conserved and essential nature of this activity. Other small molecules that inhibit the chaperone and ATPase activities of TAg have been identified recently (Wright et al., 2009). One recently identified compound, MAL2-11B, also inhibits the replication of SV40 in infected cells; however due to its low potency, solubility and cell permeability, it is not suitable as a therapeutic. Nevertheless, this compound was used as the positive control for our primary screen (Wright et al., 2009).

Ultimately a desirable lead compound would be one that reduces the replication rate of the SV40 virus by specifically inhibiting the ATPase and DNA replication activity of TAg (with an EC_{50} more potent than MAL2-11B, i.e. < 10 µM), is non-toxic (SI > 10), and has a broad applicability for other PyVs, including those that afflict humans (i.e., JC and BK viruses). One of the three primary screen hits (85281215) showed minimal *in vitro* efficacy by inhibiting SV40-induced cell death in a BSC-1 cell model, but this compound was cytotoxic at a

concentration only slightly above the effective concentration. Further optimization of the bis-tetrazole scaffold (SID 85281215) resulted in an additional compound (SID 92277586) with high biochemical efficacy, moderate *in vitro* efficacy, and again, low selectivity. While these compounds are effective probes in a biochemical system, their inherent toxicity currently limits their use in cell-based systems. However, the chemical scaffolds are starting points for a continuing chemistry effort to synthesize related compounds with lower effective and higher toxic concentrations.

The four compounds identified as TAg inhibitors (SIDs 85281215, 85281217, 85281218, and 92277586) are part of the MLPCN library, and each has been screened in several hundred different assays and formats. This is a goal of the Molecular Libraries Program, which seeks to develop a database for characterization of compounds within the MLPCN chemical library (Wheeler et al., 2007). Table 11 summarizes the number of times these compounds were identified as hits versus the total number of assays in which they were screened. The table also shows target-specific assays in which all three compounds were identified. As determined via Pubchem (http://pubchem.ncbi.nlm.nih.gov/), these compounds have been shown to inhibit hydroxyprostaglandin dehydrogenase 15-(NAD) isoform 1; (AID:894) prostaglandin E receptor 2; (AID:160544) phosphopantetheinyl transferase; (AID:1819) Microtubule-associated protein tau aggregation; (AID:1475) Mint1; (AID:2093) and nuclear receptor ROR-gamma (AID:2139). These targets are similar in that they all possess DNA-binding or ligand-binding domains, although there is limited information available to link these characteristics. The observation that the three compounds identified in the primary screen as TAg ATPase inhibitors also have overlapping activity in six other targeted screens suggests that the compounds specifically inhibit the targets and do not operate in a non-specific manner.

Table 11. Summary of hit coincidence of TAg ATPase inhibitors.

Compound hits/screens	SID 85281215 - 37/353 [a] assays	SID 85281217 - 17/438 [a] assays	SID 85281218 - 29/339 [a] assays
Target	hydroxyprostaglandin dehydrogenase 15-(NAD) isoform 1	hydroxyprostaglandin dehydrogenase 15-(NAD) isoform 1	
	prostaglandin E receptor 2		prostaglandin E receptor 2
	phosphopantetheinyl transferase	phosphopantetheinyl transferase	phosphopantetheinyl transferase
	aldehyde dehydrogenase 1	aldehyde dehydrogenase 1	
	Microtubule-associated protein tau	Microtubule-associated protein tau	Microtubule-associated protein tau
	Mint1	Mint1	Mint1
	nuclear receptor ROR-gamma		nuclear receptor ROR-gamma

[a]Number of times compound was identified as an inhibitor/total number of assays in which the compound was screened.

Chemical optimization of SID 85281215 ultimately resulted in identification of SID 92277586, also known as bisphenol A (BPA), which has been shown to be estrogenic and cytotoxic at low concentrations (Erler and Novak, 2010). Bisphenol compounds have previously been identified as putative ATPase inhibitors, and antagonize Ca2+ influx via a mitochondrial ATPase (Ardon et al., 2009). Compounds of this type have also been shown to inhibit cell growth by acting as catalytic inhibitors of topoisomerase IIα (Liang et al., 2008). The convergence of these two activities may account for the biochemical and cytotoxicity assay results shown here for compounds 85281215 and 92277586. More recently, BPA was found to induce activation of ERK1/2 and transcriptionally regulate c-fos in human breast cancer cell

lines, thereby implicating the compound in carcinogenesis (Dong et al., 2011). Studies have reported the adverse effects of μM concentrations of BPA on the nervous system and, potentially, on neonatal brain development (Kim et al., 2007) as well as reproductive organ development (Richter et al., 2007). The use of the bisphenol scaffold as a potential therapeutic is discussed in section 4.3. Although the cytotoxicity of BPA in different cell types varies tremendously, the cytotoxicity of BPA in BSC-1 cells (African green monkey kidney epithelial cells) at ~10 μM suggests that it is particularly nephrotoxic (Table 10).

In summary, primary and secondary screening have led to the discovery of a bisphenol, BPA, that specifically inhibits the ATPase activity of SV40 large T antigen. Activity data from the confirmatory and secondary assays were analyzed to identify key scaffolds for additional SAR studies and probe optimization efforts. This BPA proved to be a more potent biochemical inhibitor of TAg ATPase activity than currently available molecules such as MAL2-11B, but had a low selectivity when tested *in vitro* for SV40 viral replication inhibition. Although the *in vitro/vivo* use of compounds identified by this particular screen is limited due to the cytotoxic effects, this screening algorithm itself was successful and could be applied to evaluate other small molecule libraries for inhibitors of TAg and consequently PyV replication.

4.0 CONCLUSIONS AND PERSPECTIVES

The recent discovery of new polyomavirus (PyV) family members (Allander et al., 2007; Feng et al., 2008; Gardner et al., 1971; Gaynor et al., 2007; Padgett et al., 1971; Schowalter et al., 2010; Scuda et al., 2011; van der Meijden et al., 2010) and the expansion of immunosuppressed populations (WHO, 2008) make PyV-related diseases a growing public health concern. All PyVs express a large T Antigen (TAg), which is conserved and essential for viral replication (section 1.3). This suggested that TAg may be PyV specific drug target. My dissertation work started with the hypothesis that inhibitors of the ATPase activity of SV40 TAg might inhibit the replication of other PyVs. Based on the promising preliminary results of a quinaldine red screen of the MS2000 library, a larger ADP Hunter screen of the NCI library was performed in parallel. Hits from both screens were characterized, and both screens identified bisphenols as inhibitors of TAg. In this chapter, I will make a comparison of the screening methods used in this dissertation and suggest further ways to use the resulting data. Next, I will discuss the applications of the compounds that were identified, and how this has lead to refinement of my starting hypothesis. Finally I will suggest the implications of this work for future efforts to identify PyV-inhibitors and therapeutics.

4.1 COMPARISON OF THE SCREENING METHODS USED AND OTHER APPLICATIONS OF THIS APPROACH

In the preceding chapters, I discussed two screens to identify inhibitors of TAg ATPase activity. My efforts represented a novel approach to identify PyVs inhibitors, in part because a high throughput format was used, but more importantly, because the target of hits from such screens is well defined. In contrast, other labs have suggested methods to identify PyVs inhibitors based on the detection of DNA replication, either during a normal infection or by using a reporter (Fradet-Turcotte et al., 2010; Murata et al., 2009). If used as a primary screen, this alternative method is likely to target host proteins that may result in unwanted side effects. For example, a description of the effects of Vitamin A (retinoic acid) on PyV replication suggested that this compound decreased both viral and cellular DNA replication (Russell and Blalock, 1984). Neither proposed method has yet been reported in a successful drug screen. Therefore, I chose to develop a targeted approach to minimize the potential off target effects.

TAg has other essential enzymatic activities, however the ATPase appears to be the best target for screening. While the J domain of TAg is another potential target, because it is also conserved and essential (section 1.3.1), J domain specific inhibitors have not yet been identified. Most inhibitors of J domain-dependent stimulation of hsp70 exert their effect directly on the Hps70 (Wisen et al., 2010). In fact, the relative specificity of MAL2-11B on TAg over other J domain containing proteins is unique (Wright et al., 2009). The difficulty in targeting distinct J domains results in part because the J domain contains only a 4 helical bundle that most likely adapt different conformations, and because of the high conservation of the J domain sequence between J domain containing proteins (Walsh et al., 2004). Another screen identified inhibitors of TAg's p53 binding using an ELISA based method, which were meant to be used to

treat PyV related cancers (Carbone et al., 2003). Although this is an interesting approach that may enable host cell responses to detect and destroy the virus, the method has not yet been miniaturized to accommodate screening of large libraries. Further, if inhibitors of TAg-p53 binding inhibit other p53 binding interaction, these may result in cytotoxic effects, which was not addressed in this study. Assays targeting these activities might make for interesting secondary screens.

In contrast, the ATPase domain of TAg is an ideal target for screening for several reasons. First, a variety of screening methods have been used to detect other ATPase or kinase inhibitors (Chang et al., 2008; Charter et al., 2006; Miyata et al., 2010), and these were adapted for our screen. Second, the activity of the ATPase domain is essential for DNA replication, which if sufficiently inhibited should be rate limiting during viral replication. Third, this domain is conserved and essential, allowing me to use SV40 TAg as a proxy TAg for other PyVs. However, a possible limitation of targeting this activity is that general ATPase inhibitors, or inhibitors of AAA+ ATPases, may be identified and need to be distinguished. An ideal inhibitor of TAg would need to be TAg specific, and not disrupt other essential AAA+ ATPases, such as p97 or the MCMs (Ju and Weihl, 2010; Koonin, 1993; Snider et al., 2008). Disrupting p97 activity was recently shown to affect an array of cellular targets, including impairing ERAD and autophagy while inducing caspase activity (Chou et al., 2011). In principle, this screening approach could identify TAg specific inhibitors, especially if followed by a counter-screen for p97 inhibitors.

Having performed two screens with the same target but different readouts raised some interesting questions. Is one method more advantageous? Do both screens identify similar inhibitors? The major distinction between the two screens is that ADP Hunter uses an indirect

enzymatic readout for ADP levels, in contrast to either malachite green or quinaldine red, which detect the presence of inorganic phosphate. The apparent equivalency of these two methods would suggest that similar, if not identical, compounds could be found in both screens and that screening sensitivities should be similar. Both methods reported similar Z-factors and hit rates, indicating objectively that the results of both screens should be similar in their ability to distinguish potent compounds. In a direct comparison of the two methods, the ADP Hunter screen appeared to be more sensitive than malachite green and this is why it was selected for the screen (Figure 18). However, ADP Hunter also made some compounds tested in this assay appear more potent, in particular MAL2-11B (which was determined to have an IC_{50} of 20 μM in contrast to the previously reported value of 50 μM; (Huryn et al., 2011). An advantage of the ADP Hunter screen is that the counter-screen (screening the compounds with the ADP Hunter enzymes in the absence of TAg) can quickly identify compounds that may have general affects on enzymes. One interesting consequence of this fact is that, although included in the library, the ADP Hunter screen did not identify bithionol and hexachlorophene as potent and specific inhibitors. As discussed further is section 4.3, this is likely because both have appeared to have general effects on ATPases and other enzymes and were identified as false positives by the counter-screen. Another difference was that the quinaldine red method was performed in 384 well plates, in contrast to the ADP Hunter screen which was performed in 1536 well plates, meaning that a quinaldine red screen would be slower, or require further refinement. Given the known advantages and disadvantages of both methods, there is not a clear reason to choose one method of ATPase inhibitor detection over another.

One of the important aspects of my work was the development of high throughput techniques used for these screens. It is likely that both methods will have further application in

identifying inhibitors of ATPases tied to other diseases, such as hsp70 in cancer. In particular, the quinaldine red screen represents a new approach that will prove useful for screening other ATP dependent processes. This method was developed to identify hsp70 inhibitors, and has not yet been widely used (Miyata et al., 2010). Although both screens have been used before on other ATPase targets (Charter et al., 2006; Miyata et al., 2010), to my knowledge the use of quinaldine red or ADP Hunter to identify anti-viral drugs represents a unique application of these methods.

The screen of 330,000 compounds discussed in Chapter 3 covers a significant portion of known chemical space. Therefore, I believe that there is minimal need to repeat high throughput screens with SV40 TAg until new libraries are developed. Alternatively, re-screening these libraries directly on the purified TAgs from other PyVs may circumvent some of the difficulties we have had in predicting which SV40 TAg inhibitors may inhibit other PyVs (see section 4.4).

4.2 FURTHER UTILITY FOR THE GENERATED SCREENING DATA

Although the described screening methods will only identify inhibitors that disrupt the ATPase activity of TAg, there are several ways this can happen. For example, a competitive inhibitor may bind in the place of ATP; or compounds may bind at a site that prevents the necessary conformational change that hydrolyzes ATP or that prevents the formation of the active site by inhibiting hexamer formation. Because we have identified compounds with similar scaffolds, I predict that all of the compounds act by a similar mechanism although my current efforts have not conclusively determined the mechanism of action of these compounds. The volume and

diversity of compounds available in the Molecular Libraries Probe Production Centers Network (MLPCN) is likely to provide scaffolds capable of operating through each these activities with some potency. Identifying such compounds may require less stringent cutoffs for identification of lead compounds, which would place a greater emphasis on chemical refinement of promising scaffolds.

One advantage of the high throughput screening approach described in Chapters 2 and 3 is that the existing data are available for re-analysis. Since very stringent cut-offs for the compounds were used (IC_{50} less than MAL2-11B), in light of the subsequent results, it may prove advantageous to reconsider the hits identified using different criteria, perhaps selecting less potent compounds that may be more amenable for chemical refinement to improve bioavailability or specific bioactivity. Notably, the screen described in Chapter 3 examined one of the largest chemical libraries available without identifying a compound with more therapeutic potential than MAL2-11B. In addition, the chemical refinement of compound 85281215 proved to be a major obstacle, suggesting that having multiple scaffolds to refine may help future efforts.

The results of the ADP Hunter screen (Chapter 3) have been uploaded to Pubchem (http://pubchem.ncbi.nlm.nih.gov/), making this data available for other researchers. For example, those looking for specific ATPase inhibitors may select against compounds that also inhibit TAg. Alternatively, compounds could be selected for desirable secondary effects, in particular if I were to reanalyze the results of the ADP Hunter Screen. For example, the Pubchem interface makes it possible to find compounds that have been identified in multiple screens, such as hsp70 inhibitors or p53 activators. One of the reasons that MAL2-11B is effective is that inhibits both the ATPase activity of TAg and the hsp70 (Wright et al., 2008;

Wright et al., 2009), which may suggest that other compounds that can be selected with multiple targets may be advantageous. While doing such comparisons is straightforward for the screen described in Chapter 3, the results of which have been loaded to Pubchem, investigation of specific chemical structures is also possible for hits from the screen described in Chapter 2. This may be one way to select for compounds with a bipartite effect that may make them more potent viral inhibitors.

4.3 APPLICATIONS OF THE IDENTIFIED POLYOMAVIRUS INHIBITORS

As a result of the two performed screens, I identified compounds that inhibit both TAg activity *in vitro* and PyV replication. Bithionol and hexachlorophene are among the most potent PyV inhibitors identified. It is interesting that our second screen (Chapter 3) also identified a bisphenol inhibitor, in this case Bisphenol A. The structure activity relationship defined in both Chapter 2 and Chapter 3 suggests that some bisphenols exert a unique effect on TAg that is dependent on specific structural features. Are bisphenols a class of TAg inhibitors? Perhaps, but in general, bisphenols are known to interact with and modulate the activity of many proteins, which is further discussed below.

Even though the data presented in Chapters 2 and 3 suggests that there is a unique structure activity relationship between the bisphenol compounds and their effect on TAg (Figure 7 and Table 10), we were disappointed to identify a scaffold that lacks therapeutic value. Both bithionol and hexachlorophene have been FDA approved for human use, and in some cases can be administered orally. However, these effects are due to the antiseptic and promiscuous effects on multiple, diverse targets, including but not limited to, Glyceraldehyde 3-phosphate

dehydrogenase, NFκB, and caspases 3/7, and β-catenin via the E3 Siah-1 (Li et al., 2009; Miller et al., 2010; Min et al., 2009). The diversity of bisphenol targets is thought to be responsible for the antiseptic and anthelmintic effects of these compounds (Takeuchi et al., 1985; Wickramasinghe et al., 2006). Given that these small molecules interact with a wide variety of targets, it is not possible to make the case for TAg specificity. In fact, the details of the bisphenol structure activity relationship further limit the opportunities for future chemical refinement towards specificity. Because there are few R groups on this small scaffold that are not essential for the unique TAg interaction, there are not many remaining sites available for modification. This chemical limitation suggests that this compound cannot be improved in terms of drug-like qualities.

The many off target effects of bisphenols discourages their use in clinical settings, even of a modified compound based on the bisphenol scaffold. Hexachlorophene had been favored as a preoperative topical antiseptic and in the delivery room and in other obstetric applications, but a rash of fatal accidents involving young children discouraged its use (Canzonetti and Dalley, 1952; Kimbrough, 1973). Instead, the compound bithionol was used as a replacement in similar settings (Powell and Lampert, 1973). While bithionol has been used in humans to treat blood flukes, especially in southern Asia, it is known to have many off target effects (see Figures 8 and 9) which can result in side effects (Bacq et al., 1991; Kim, 1970; Price et al., 1993; Seo et al., 1982). Both compounds have also been used in veterinary settings, perhaps because the neurological effects, which include blindness, are less noticeable in the cattle, sheep and rodents (Corbett and Goose, 1971; Udall, 1972). Because of the known pathogenicity of the avian PyVs (see section 1.1.4), either bithionol or hexachlorophene may be viable choices for the treatment of birds that cannot be vaccinated. Bisphenol A is known as an environmental

toxin with wide ranging effects on development stemming from endocrine disruption (Ardon et al., 2009; Erler and Novak, 2010; Richter et al., 2007; Rubin, 2011; vom Saal et al., 2007). In the face of the public pushback against this ubiquitous compound, which is commonly used to make polycarbonate plastics, it seems unlikely to be useful even in a veterinary setting (Sharpe, 2010). Though not as thoroughly investigated as endocrine disruptors, it is unclear whether bithionol and hexachlorophene may have similar effects on development, which would discourage either long-term use or administration of high dosages of any of these compounds.

Despite these limitations, these compounds may fill a need for topical polyomavirus inhibitors. As described above, both bithionol and hexachlorophene are approved for topical use (Canzonetti and Dalley, 1952; Powell and Lampert, 1973). Interestingly, four of the most recently discovered PyVs appear to have a skin tropism: Merkel Cell Polyomavirus (MCPyV), Human Polyomavirus 6 and 7 (HPyV6, HPyV7) and Trichodysplasia Spinulosa Virus (TSV). Since both TSV and MCPyV are associated with disease, this suggests that a topical therapeutic may be valuable. Unfortunately, when tested on a MCPyV cell culture system, neither bithionol nor hexachlorophene inhibited growth of Merkel Cell Carcinoma (MCC) cells (R. Arora and Y. Chang, personal communication). I hypothesize that this is because the MCC cell lines express a truncated TAg, which lacks the ATPase domain. The effects of these compounds have not yet been tested on TSV in part because this disease is very rare and there is not yet an *in vitro* replication system for this virus. However, both compounds would be reasonable candidates for treatment of these or other PyVs that infect skin.

Although the therapeutic potential of all the compounds identified in these screens is probably limited, as mentioned in Chapter 3, any of the described compounds may prove to be valuable tools for chemical genetics. One such example would be to use these compounds to

characterize TAg specific *in vitro* activities, such as the role of TAg in DNA replication. As described in Chapter 1, a very well characterized and minimal system for *in vitro* TAg-dependent DNA replication has been developed (see section 1.2.2). However, there are some known, but not well understood, differences between this system and DNA replication in cell culture. One example of this distinction is the requirement for a functional J domain to replicate DNA *in vivo*, but not *in vitro* (Weisshart et al., 1996). It seemed conspicuous that of the many compounds tested in this assay, none appeared to be active inhibitors of *in vitro* replication at concentrations below 300 μM (Figures 11, 20 and 21). Therefore, these compounds, including all three bisphenols as well as SIDs 85281215, 85281217 and 85281218, may provide a tool to understand the differences between DNA replication *in vitro* and *in vivo*. Although the lack of inhibition of *in vitro* DNA replication may simply reflect the lack of potency of these compounds, this result was surprising since these compounds were more potent in assays of TAg ATPase activity.

One aspect of the disparity between ATPase inhibition and DNA replication inhibition is that TAg ATPase activity may not be rate-limiting during DNA replication, especially in the *in vitro* DNA replication assay. Another consideration is that in the unsynchronized cell lysate used in these assays (Figures 11, 20 and 21), only a small population of the TAg in the reaction may be recruiting the active necessary factors required for DNA replication. This suggests the effects of these compounds may be more evident in the highly purified system (Waga et al., 1994), and the use of such inhibitors may inform our understanding of the role of the ATPase domain during replication. For example, DNA is known to stimulate the ATPase activity of TAg (Giacherio and Hager, 1979), and it is possible that the presence of DNA (which is not included in our screening system) may overcome the effects of an inhibitor. For example, the

recent structure of TAg bound to single stranded DNA implicated unpredicted residues in DNA binding, which is an indication of the structural differences between monomeric TAg, and TAg in complex with DNA (Meinke et al., 2011). These structural differences may mitigate binding by some inhibitors or change the kinetics of the ATPase reaction. Overall, a better understanding the relationship between ATP hydrolysis, DNA binding and DNA unwinding is important to understand effects on viral replication, and the described compounds may provide tools for this characterization.

A skeptical reading of these findings would suggest that TAg will not be amenable to small molecule inhibition; the enzymatic activity of TAg is minimal and the compounds identified so far have problematic off target effects. However, I remain confident that TAg can be a drug target, because the ATPase activity of TAg is one of the few essential enzymatic activities encoded by the virus. I am currently investigating the potential for a synergistic effect of the bisphenols in addition to cidofovir, a known PyV inhibitor (see section 1.4.2.5). While we are optimistic that using lower doses of both drugs in combination may improve their overall efficacies while minimizing toxicity, synergism may prove more evident when examined with a different combination of TAg inhibitors. Future drug screens should take advantage of synergistic effects by pairing drug treatment with either bithionol or hexachlorophene.

4.4 REFINEMENT OF THE HYPOTHESIS: INHIBITORS OF SV40 TAG MAY INHIBIT REPLICATION OF OTHER PYVS, BUT WITH DIFFERENT POTENCIES

The described work supported the hypothesis that inhibitors of SV40 TAg can be inhibitors of PyV replication, but my results also led to a refinement of this hypothesis. I also predicted that due to the slow replication of BKV, compounds that have a modest effect on SV40 would have a greater effect on BKV or other PyVs. The relatively low viral yield, especially when BKV is replicating in Vero cells, indicates that the virus is not replicating at maximal efficiency. Therefore, I expected modest inhibition of TAg activities would make viral replication much less efficient; however, this was not the case. The compounds that were tested in both viruses appeared less potent on BKV than was predicted from the SV40 replication data (compare Figures 10 and 16). It was also interesting that bithionol and hexachlorophene did not have the expected identical effects on BKV replication (see Appendix B for another example of this disparate effect between SV40 and BKV replication). It is not clear if this difference reflects the biology of these two viruses or an indication that the compounds that I have identified act via different mechanisms.

A frequent reviewer comment is that because BKV is "slower" there is more time to overcome the effects of the compound over the course of the infection. This explanation perhaps provides a longer time course for the host cell to clear the drug, but still seems to be an insufficient explanation. For example, this comment does not explain the different potency of bithionol and hexachlorophene on BKV, which were expected to have identical potencies in the BKV assays based on the identical potency on SV40 replication. The demonstrated inhibition of BKV is an order of magnitude less than the inhibition of SV40 replication (compare Figures 10 and 16). Drug clearing is unlikely to be the explanation for these results, since in this assay

compounds were supplemented every 48 h during the infection (Figure 16). While the replication rate may be the basis of this difference, it is unclear how this rate results in the distinct effects of compounds on SV40 and BKV. As mentioned in section 2.4, the observed difference in compound potencies endorses the continued use of large library screens to identify relevant scaffolds that may be amenable to chemical refinement, or at least to provide multiple hits to test in relevant assays. I have only directly compared the effects of PyV inhibitors between SV40 and BKV. It seems possible, if not likely, that there may be a similar distinction in potencies as compounds are tested on other PyV replication systems.

As mentioned above, screening for TAg ATPase inhibitors remains a promising way to target PyV replication while minimizing off target effects. However, as the disparate effects of TAg inhibitors on different PyVs highlights, a better approach may be to screen the inhibitors on purified TAg from the PyV of interest. The conservation of TAgs would suggest that inhibitors of any TAg should inhibit the entire family. The major limitation for studies on PyVs is that replication systems have not been developed for most of these viruses yet. Expressing and purifying TAgs from other PyVs for chemical inhibitor screening will certainly be a rapid way to confirm whether SV40 TAg inhibitors have effects on the entire viral family, expanding the utility of this approach. JC TAg has been purified using a similar method employed in the purification of SV40 TAg (Bollag et al., 1996), suggesting analogous techniques could be used with other PyV TAgs. Additionally, use of an exogenous DNA replication assay in cell culture that does not require viral replication may provide a secondary counter screen for such efforts (Boichuk et al., 2010; Gjorup et al., 1994).

4.5 RECOMMENDATIONS FOR FURTHER IDENTIFICATION OF PYV INHIBITORS AND THERAPEUTICS

One fundamental question that remains is how therapeutics for PyVs should be identified. A parallel issue to this is that of the 330,000 compounds screened, an ideal therapeutic was not identified. At a minimum, this suggests that potent TAg specific inhibitors are not abundant in existing libraries. Future efforts to identify TAg or PyV inhibitors will need to find approaches to address this challenge, either by using different libraries or focusing on a different target. As described in Chapter 1, since the majority of activities required for viral replication are performed by host factors, the viral targets for such compounds are relatively limited. Indeed, even the essential enzymatic activities of the major screening target, TAg, are limited.

Limited viral targets are one reason that general antivirals, which support cellular recognition of Pathogen Associated Molecular Patterns (PAMPs) or inhibit such activities, may be advantageous (Unterholzner and Bowie, 2008). Unfortunately, PyVs do not show several of the common PAMPs that would trigger an innate immune response; DNA replication is nuclear rather than cytoplasmic, there are no free DNA ends or dsRNA and there are very limited viral antigens and no viral envelope proteins, all of which are known to induce Toll-like receptors (Mogensen, 2009; Unterholzner and Bowie, 2008). Yet, there are features of PyV replication that are shared with other viral pathogens, such as inappropriate initiation of S-phase or endoreduplication, which may serve as better and more broad targets. For example, compounds that target an activity that is not essential to a resting cell but is essential for viral replication, such as Bub1 activity might be uniquely potent (Hein et al., 2009). DNA methylation (indicated by CpG doublets) is another common feature of viral DNA, which can protect the genome from being clipped (Goorha et al., 1984). In PyVs, the presence of these doublets is not highly

conserved, suggesting that compounds that inhibit DNA methylation or support host recognition of this pattern may not inhibit the entire family equally (Subramanian, 1982). As another example, it has been shown that specific post-translational modifications regulate TAg activity, such as essential phosphorylation and acetylation (McVey et al., 1989; Poulin et al., 2004). It may be possible to modulate the kinases or acetylases responsible for this activity with minimal impact on host cell function. Others have suggested that directly stimulating TLRs, in this case TLR3 in SV40 transformed cells, may promote an immune response directed at the viral antigens (Lowe et al., 2010). Recent work characterizing transcriptional regulation in TAg expressing cells indicated that TAg activates Interferon stimulated genes, including Stat1 independent of interferon, suggesting that TAg is also modulating innate immune responses (Cantalupo et al., 2009; Rathi et al., 2010; Rathi et al., 2009). Applying a general antiviral to PyV-related diseases is how cidofovir and leflunomide came into favor (see section 1.4.2.5).

This returns to the issue that the compounds that are currently favored for the treatment of PyV are not PyV specific, nor are they yet supported by sufficient evidence to justify their use in clinical settings (see section 1.4.2.5). For some compounds, this is a matter of expanding multi-center trials to collect sufficient data (Farasati et al., 2005; Tan and Koralnik, 2010). Performing the necessary clinical trials to test the use of compounds that have been shown to inhibit PyV replication *in vitro* may be the fastest way to establish a therapeutic standard for PyV diseases. In addition, other antiviral drugs that are known to inhibit viral DNA replication, which likely share similar PAMPs, in particular for papilloma or herpes virus, should be tested in a PyV replication system. It has also been suggested that a PyV vaccine for humans, using virus-like particles or inactivated virus, such as has been used for birds (Ritchie et al., 1998a;

Ritchie et al., 1998b), may be a viable prophylactic for the at risk populations (K. Peden, personal communication).

One missing piece that would support my investigations is an understanding of what causes pathogenicity in PyVs. PyVs are widely distributed, and can be detected at relatively high levels without pathogenicity. Perhaps the best quantitated example of the distinction between viral levels that are pathogenic or benign is the detection of TSV (van der Meijden et al., 2010). In this paper, researchers documented a viral titer of $2x10^5$ copies per cell in the symptomatic patient, while after treatment, when symptoms were reduced, the viral titer was 10^4 copies per cell in this same patient (van der Meijden et al., 2010). This 20-fold reduction may indicate that a modest effect of an inhibitor allows the host immune system to control viral replication and symptoms. This evidence should encourage the investigation of compounds that have a modest but specific effect on viral replication.

Another approach may be to investigate the sequence specific changes that make PyVs pathogenic. Limited single nucleotide polymorphisms (SNPs) have been identified for BKV, which have not yet been correlated with patient outcome or pathogenicity (Luo et al., 2009). Additionally, monitoring of viral sequences from patients has suggested that changes in the non-coding control region may be associated with increased pathogenicity (Broekema et al., 2010; Sharma et al., 2007). It is not yet clear if this is the only site of rearrangement and if these genetic changes lead to pathogenicity. More recent analysis of patient samples suggested that individual patients are infected with a surprising diversity of viral genotypes for a DNA virus, especially since DNA viruses that recruit the host polymerase are predicted to have a low mutation rate similar to mutation rates during eukaryotic replication (P. Randhawa, personal communication). This evidence suggests either that there may be specific sequence changes

that result in virulence, or that viral diversity gives rise to virulence by allowing for rapid adaptation to the responding host environment (although the quasispecies model is more common in RNA viruses; (Lauring and Andino, 2010). In the end, understanding the roles of diverse genotypes in pathogenic PyV infection will be important to understanding virulence, and may present a new target to prevent virulence.

4.6 SUMMARY AND CONCLUSIONS

There have been several valuable contributions of my work to the field of PyV biology. These include identifying a screenable target activity (the ATPase activity of TAg), adapting high throughput methods to identify TAg inhibitors, identifying bisphenols as a general scaffold for PyV inhibitors and refining the activity of this structure, and proving that inhibitors of SV40 replication can also inhibit BKV replication. This work provides important tools for further characterization of PyV inhbitors and presents candidate compounds to use chemical genetics to explore PyV replication. In sum, this work supports the continued use of SV40 as a model for PyV replication, since assays for replication are best established in SV40, facilitating characterization of the compound before assays are performed on slower replicating viruses.

APPENDIX A

INHIBITION OF SIMIAN VIRUS 40 REPLICATION BY TARGETING THE MOLECULAR CHAPERONE FUNCTION AND ATPASE ACTIVITY OF T ANTIGEN

This work was performed in collaboration with the Wipf Lab at the University of Pittsburgh, and is published (Wright et al., 2009).

Previous work by a graduate student in the Brodsky lab, Dr. Christine Wright, had identified a small molecule scaffold that targets hsp70 activity, and resulted in decreased proliferation of cancer cells (Wright et al., 2008). As part of this study, the J domain of TAg was tested with the hsp70 in the presence of the inhibitor. It became clear that this compound could inhibit both the endogenous ATPase activity of the TAg and the ability to enhance hsp70's ATPase activity. The characterization of this activity was the subject of a 2009 *Virus Research* manuscript (Wright et al., 2009).

A.1 RESULTS

Dr. Wright demonstrated that MAL2-11B could inhibit both endogenous TAg activity, as well as the ability of TAg to stimulate hsp70. It was assumed that this was a J domain dependent activity, because Dr. Wright demonstrated this effect was less potent with other J domains, suggesting J domain specificity. Using known TAg mutants, I demonstrated that the J domain was essential for this activity, and that the detected activity was not from endogenous TAg activity. Specifically, I took advantage of an ATPase defective mutant known as 5061, and a point mutation (D44N) in the HPD motif of the J domain, which renders the J domain incapable of stimulating hsp70 activity (Castellino et al., 1997; Srinivasan et al., 1997). Both purified mutants were provided by the Pipas lab. These data showed that hsp70 is maximally stimulated by wild type TAg, and by 5061, suggesting that the ATPase activity in this assay was not from TAg (Figure 23). The D44N mutant showed activity most similar to wt-hsp70 alone, further supporting the notion that the stimulation shown in these assays was from the J domain of TAg, not the endogenous TAg ATPase activity. These data further suggested that MAL2-11B acted by inhibiting the activity of the J domain of TAg.

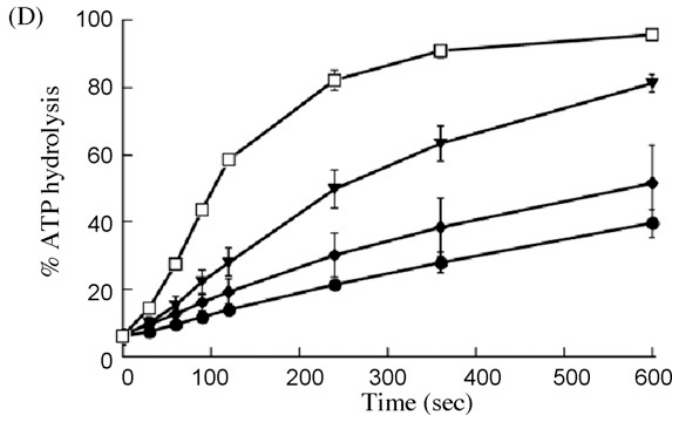

Figure 23. Stimulation of hsp70 ATPase activity is dependent on the TAg J domain in a single turnover ATPase assay.

Filled circles, hsp70 alone; Open squares, Tag; Inverted filled triangles, TAg mutant 5061; Filled diamonds, D44N TAg. Error bars represent standard deviations of the data; n=3.

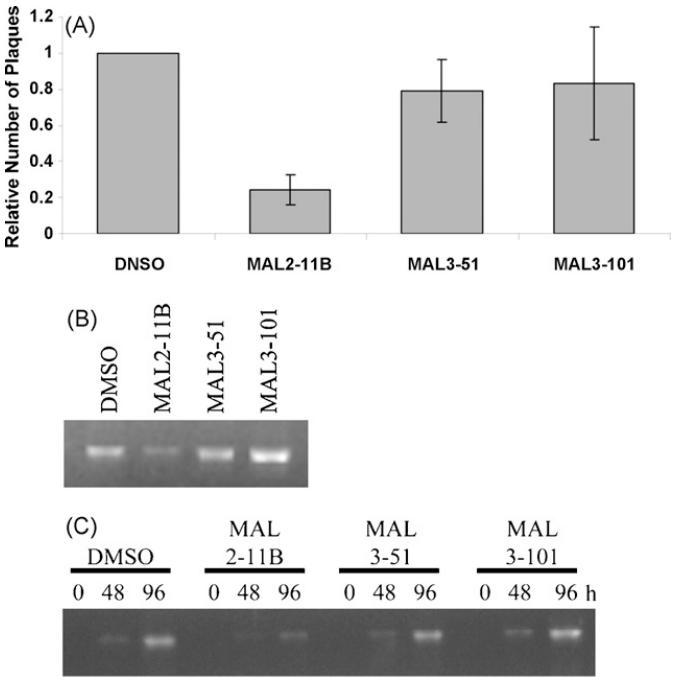
(A)
Relative Number of Plaques
1.2
1
0.8
0.6
0.4
0.2
0
DNSO
MAL2-11B
MAL3-51
MAL3-101
(B)
DMSO
MAL2-11B
MAL3-51
MAL3-101
(C)
DMSO
MAL 2-11B
MAL 3-51
MAL 3-101
0 48 96 0 48 96 0 48 96 0 48 96 h

Figure 24. MAL2-11B inhibits SV40 DNA replication.

(A) MAL2-11B reduces viral propagation in plaque assays. The number of plaques visualized in duplicate reactions was averaged and the results were normalized to the DMSO control. The results of three independent experiments were then averaged and the means of the reactions ± the standard deviations of the data are shown. MAL2-11B compared to the DMSO control, $p < 0.0002$. (B) MAL2-11B inhibits SV40 DNA replication 48 h after treatment. Viral DNA was isolated from SV40-infected cells 48 h after treatment with 100 μM of the indicated compounds and digested with BamHI, and the products were visualized after resolution on an ethidium bromide-stained agarose gel. The fact that the product corresponded to viral DNA was confirmed based units size (5.2 kb after BamH1 digestion) and by the fact that internal primers specific to SV40 DNA yielded the expected product after PCR (data not shown). (C) Time course of the effects of MAL2-11B, MAL3-101, and MAL3-51 on SV40 DNA synthesis. DNA was isolated at the indicated times (in h) and analyzed as described in part (B). Note: More material was loaded than in part (B) in order to better visualize the time-dependent increase in SV40 DNA. To control for the DNA loaded in these gels, we used a real-time PCR analysis to detect the amount of the actin gene in the same samples used in part (B) (see section 2.2.4). The amount of actin DNA in the DMSO control was set to "1.0", and based on this analysis the relative amounts of total DNA analyzed were: DMSO, 1.0; MAL2-11B, 3.4; MAL3-51, 4.0; MAL3-101, 4.0.

Dr. Wright next demonstrated that MAL2-11B inhibits replication of viral DNA in infected cells. She did this by harvesting DNA from infected BSC40 cells that had been treated with the compounds of interest. This DNA was linearized and visualized on an agarose gel (Figure 24A and B). In response to a reviewer's comment, I was able to confirm these results, first by confirming that this was viral DNA by obtaining a PCR product using SV40 specific primers and this harvested DNA as a template, which indicated that the visualized DNA in Figure 24B was of viral origin. Second, I demonstrated that the effect of the tested compounds was not simply due to a delay in viral DNA replication. I performed a time course of infection and harvested DNA at 0, 48 and 96 hpi. The DNA was visualized on an agarose gel (Figure 24C), and quantitated by quantitative PCR. I also showed that similar amounts of each sample were visualized on the gel in Figure 24B by detecting trace amounts of actin DNA by qPCR.

Another lingering question was whether the effect of the compound was on TAg or a more general stress response or possibly due to programmed cell death. While Dr. Wright demonstrated that MAL2-11B did decrease TAg expression, I showed that this compound did not increase hsp70 expression, which would indicate a stress response (Figure 25A). I further demonstrated by Western blot that MAL2-11B did not induce PARP cleavage, which would have been an indication of an apoptotic response (Figure 25B(Pieper et al., 1999)).

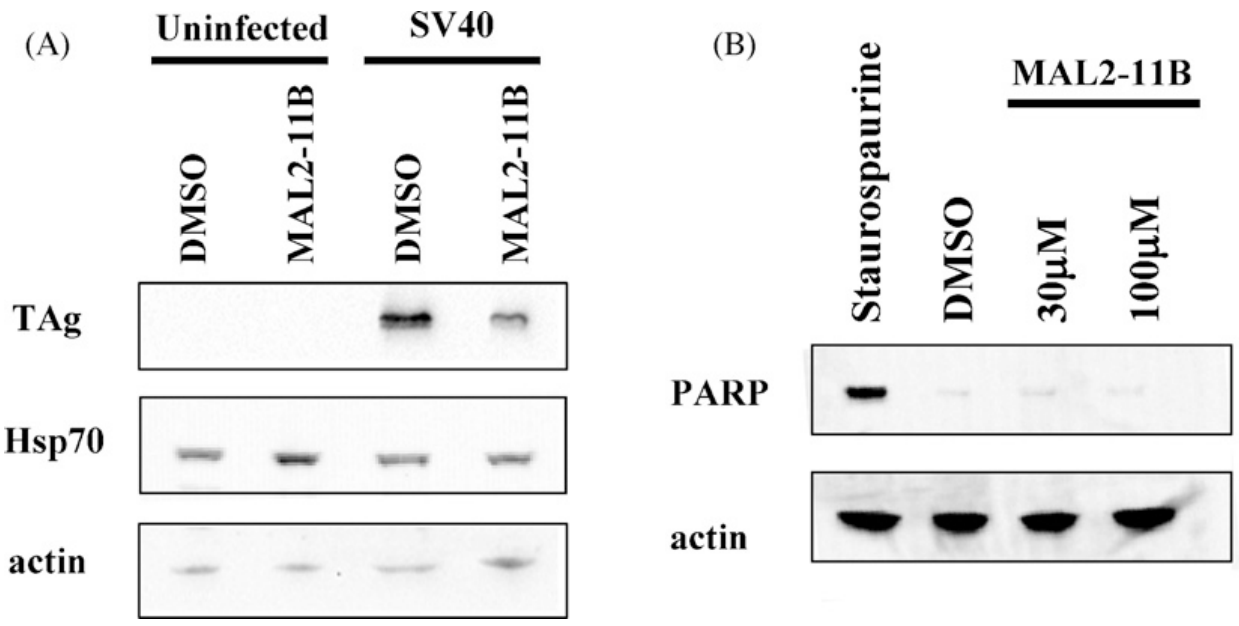

Figure 25. MAL2-11B reduces TAg expression without inducing apoptosis.

A. Freshly confluent BSC40 cells were infected with SV40 for 2 h and subsequently treated with 100 μM MAL2-11B for 48 h. Control cells that were uninfected, but treated with DMSO or MAL2-11B, were also examined. The cells were lysed and an equal amount of total cellular protein was resolved on a polyacrylamide gel. After transfer to nitrocellulose the blots were decorated with the indicated antisera. B. Cells were treated as described in (A), except that 1 μM staurosporine was added for 4 h, where indicated, and the indicated concentrations of MAL2-11B were included in the medium for 48 h. Lysates were resolved, transferred to nitrocellulose, and probed with anti-PARP or anti-actin antibody.

APPENDIX B

CHEMICAL REFINEMENT OF THE MAL2-11B SCAFFOLD IDENTIFIES A BKV INHIBITOR AND RAISES QUESTIONS ABOUT COMPARISONS BETWEEN PYVS

This work was originally published in collaboration with at the Wipf lab at the University of Pittsburgh (Huryn et al., 2011). These results raise an interesting question about PyV biology.

Previous work in our lab identified the MAL2-11B scaffold as an interesting inhibitor of TAg and polyomavirus replication (Wright et al., 2009). Specifically, MAL2-11B was shown both to inhibit endogenous TAg ATPase activity, as well as the ability of TAg to stimulate hsp70 activity. This results in inhibition of both SV40 and BKV replication in cell culture. Although MAL2-11B itself has limitations, including low cell permeability and potency, this bipartite effect may be improved by scaffold optimization. To explore this idea, derivatives of this scaffold were developed by the Wipf lab and tested by Alex Ireland, an undergraduate researcher, in our *in vitro* assays. I then examined the effects of the compounds on viral replication in cell culture.

B.1 METHODS FOR VALIDATING THE MAL2-11B DERIVATIVES.

Purification of T Antigen : Purification of the SV40 large T Antigen (TAg) was as previously reported (Cantalupo et al., 1999; Wright et al., 2009). In brief, a baculovirus expressing TAg was used to infect Sf9 cells, which were harvested and lysed. The lysate was purified over a Protein G Sepharose Fast-Flow column covalently crosslinked to the monoclonal antibody PAb419, which recognizes TAg (Harlow et al., 1981). After washing, the enriched protein was released with base and dialyzed into buffer containing 10 mM Tris pH 8.0, 1 mM EDTA, 100 mM NaCl, 10% glycerol and 1 mM DTT.

Steady state ATPase assay : The ATPase activity of TAg was measured using a previously described method (Cyr et al., 1992; Wright et al., 2009). Protein and compound were incubated for 15 min on ice before the addition of a mix of radiolabeled and non-radiolabeled ATP to a final concentration of 50 μM. The reaction was shifted to 30 °C, and 3 μL aliquots were removed and the reaction was quenched every 15 min for 60 min. ADP was resolved from ATP by TLC in a LiAc/formic acid-containing solvent and the TLC was exposed to a phosphoimager plate. Data were analyzed on a Fujifilm BAS-2500 phosphoimager and quantified using Imageguage software v.4.

BKV DNA replication assay : Vero cells were a generous gift from the McClane lab (University of Pittsburgh, School of Medicine). BKV crude stocks were a gift from the Imperiale lab (University of Michigan). Vero cells were grown at 37 ºC in 5% CO_2 in DMEM containing 10% FBS.

To determine the effect of the compounds on BKV replication, a qPCR assay based on methods reported previously (Murata et al., 2009; Randhawa et al., 2005b) was performed. In brief, a low titer of BKV was used to infect low confluence Vero cells for 1 h. The media was

then replaced with DMEM containing the desired compound and 0.3% DMSO. The infection continued until 5 dpi, when the culture was lysed by freeze-thaw and the viral content was assayed by qPCR. To perform the qPCR assay, a mix of primers (Wright et al., 2009) and Taqman probe (IDT) were assembled with PerfeCta qPCR SuperMix, ROX (Quanta Biosciences) in MicroAmp plates (ABI) and amplified by a *7300* Real-Time PCR System. Absolute quantification was performed using pBKV (Dalrymple and Beemon, 1990) as a reference for BKV. This plasmid contains the entire viral genome cloned into a BamH1 site, and serves as a control. The DNA was initially melted at 95 ºC for 1 min and cycled between 95º for 15 sec and 60ºC for 1 min. Data were quantified by 7300 System SDS version 1.3.1 (ABI) and are reported relative to the DMSO control.

B.2 RESULTS

Derivatives of MAL2-11B were prepared to test whether changes to the linker region might improve efficacy and solubility of this scaffold. While several of the compounds tested did not have any effect, the tetrazol derivative, referred to in the manuscript as compound **32**, was slightly more potent than MAL2-11B in the ATPase assay (Figure 26 A and B). I next characterized this effect on BKV by qPCR assay (Figure 26 C). While it is clear that both MAL2-11B and **32** inhibit BKV replication, we were surprised that there was not a distinct effect of these two compounds.

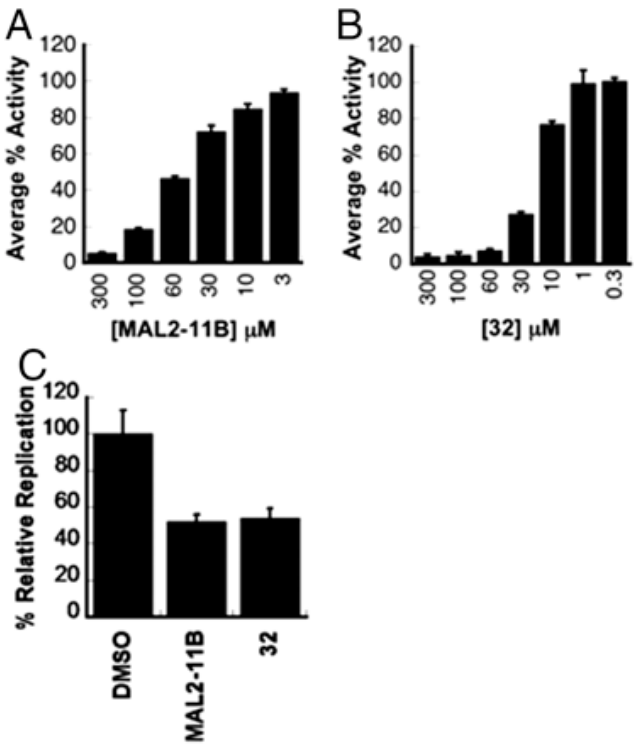

Figure 26. Effect of MAL2-11B and the tetrazol derivative on TAg and BKV replication.

Steady-state ATPase assays with purified T-antigen were performed as described (B.1) in the presence of the indicated concentrations of (*A*) MAL2-11B or (*B*) 32**. Data represent the means of at least three determinations ± SD. (*C*) The replication of the BK virus and viral DNA content were assessed in the presence of the indicated supplements. MAL2-11B and** 32 **were used at a final concentration of 100 μM. Data represent the means of two independent infections, each performed in triplicate, ± SEM; $p \leq 0.007$ for DMSO vs. the compound treated samples.**

B.3 CONCLUSIONS AND FUTURE DIRECTIONS

The driving hypothesis of this work has been that inhibitors of SV40 TAg will inhibit the replication of PyVs in general. I had also assumed that due to its slower replication and decreased TAg expression, that BKV would be more sensitive to TAg inhibitors than SV40. Therefore I expected the tetrazol, **32**, to be a significantly more potent inhibitor of BKV. I was surprised by the result that both MAL2-11B and **32** were less potent on BKV than anticipated based on previous work with SV40 (Wright et al., 2009). This was in part because it implies that BKV is not more sensitive to inhibitors than SV40, and also that a two-fold improvement in TAg inhibition *in vitro* may not have a significant effect on viral replication. There certainly are differences in the biology of BKV and SV40 that can explain these data. As mentioned above, BKV infections are much slower than SV40, and while the reason for this is not clear, during this time, compounds may be metabolized by the cell or bind off-targets, leaving TAg free to replicate BKV. To minimize this phenomena, the media and compounds were refreshed during the infection. Perhaps another explanation is that there are some fundamental differences between SV40 and BKV TAgs. Our lab has not yet developed a system to purify other TAgs, but *in vitro* testing of compounds on these other TAgs might provide more evidence about the differences we see when infecting with different viruses.

While previous research on TSV made us optimistic that the effects of a compound need only modestly effect viral replication to dramatically improve pathology (van der Meijden et al., 2010), my results also suggest that modest improvements in antiviral effect may be more difficult to obtain with TAg inhibitors. While ATPase activity is essential for viral replication, it is not likely to be the rate limited step in viral replication (Rohaly et al., 2010). This suggests that to dramatically reduce viral replication, TAg activity must be severely curtailed, or

compounds that target other viral activities may need to be used in combination with TAg inhibitors.

Nevertheless, a bipartite effect may prove to be more important that initially thought. Further derivatives of the tetrazol, **32**, are being synthesized by the Wipf lab, and I look forward to testing them in our assays. These results certainly confirm that we can quickly produce the data necessary to characterize such compounds. Although my evidence suggests that these compounds may need to be significantly improved in potency to have a future as a therapeutic, this line of research may serve to elucidate some of the subtle differences between BKV and SV40 replication. Perhaps more importantly, the MAL2-11B scaffold is more amenable to chemical refinement than the other compounds identified in this dissertation (e.g. the bisphenols or SID 85281215, see Chapters 2 and 3 respectively).

BIBLIOGRAPHY

Aaronson, S.A., and Todaro, G.J. (1968). Basis for the acquisition of malignant potential by mouse cells cultivated in vitro. Science *162*, 1024-1026.

Abend, J.R., Low, J.A., and Imperiale, M.J. (2010). Global effects of BKV infection on gene expression in human primary kidney epithelial cells. Virology *397*, 73-79.

Abrahams, P.J., Mulder, C., Van De Voorde, A., Warnaar, S.O., and van der Eb, A.J. (1975). Transformation of primary rat kidney cells by fragments of simian virus 40 DNA. J Virol *16*, 818-823.

Ahuja, D., Saenz-Robles, M.T., and Pipas, J.M. (2005). SV40 large T antigen targets multiple cellular pathways to elicit cellular transformation. Oncogene *24*, 7729-7745.

AID:894. PubChem Bioassay Database; AID= 894 qHTS Assay for Inhibitors of HPGD (15-Hydroxyprostaglandin Dehydrogenase) http://pubchemncbinlmnihgov/assay/assaycgi?aid=894. National Center for Biotechnology Information. Accessed on June 16, 2011

AID:1475. Pubchem Bioassay Database; AID= 1475 Quantitative High-Throughput Screen for Inhibitors of Tau Fibril Formation. http://pubchemncbinlmnihgov/assay/assaycgi?aid=1475. National Center for Biotechnology Information. Accessed on June 16, 2011

AID:1819. PubChem Bioassay Database; AID= 1819 Probe Development Summary of Inhibitors of Bacillus subtilis Sfp phosphopantetheinyl transferase (PPTase). http://pubchemncbinlmnihgov/assay/assaycgi?aid=1819. National Center for Biotechnology Information. Accessed on June 16, 2011

AID:2093. Pubchem Bioassay Database; AID= 2093 Summary assay for inhibitors of Mint1. http://pubchemncbinlmnihgov/assay/assaycgi?aid=2093. National Center for Biotechnology Information. Accessed on June 16, 2011

AID:2139. Pubchem Bioassay Database; AID= 2139 Summary of probe development efforts to identify novel modulators of the Retinoic acid receptor-related Orphan Receptors (ROR). http://pubchemncbinlmnihgov/assay/assaycgi?aid=2139. National Center for Biotechnology Information. Accessed on June 16, 2011

AID:160544. PubChem Bioassay Database; AID= 160544 Functional activity in RAT-1cells, transiently-transfected with human Prostaglandin E receptor EP1 http://pubchemncbinlmnihgov/assay/assaycgi?aid=160544. National Center for Biotechnology Information. Accessed on June 16, 2011

Aksamit, A.J. (2001). Treatment of non-AIDS progressive multifocal leukoencephalopathy with cytosine arabinoside. J Neurovirol *7*, 386-390.

Ali, S.H., Chandraker, A., and DeCaprio, J.A. (2007). Inhibition of Simian virus 40 large T antigen helicase activity by fluoroquinolones. Antivir Ther *12*, 1-6.

Ali, S.H., Kasper, J.S., Arai, T., and DeCaprio, J.A. (2004). Cul7/p185/p193 binding to simian virus 40 large T antigen has a role in cellular transformation. J Virol *78*, 2749-2757.

Allander, T., Andreasson, K., Gupta, S., Bjerkner, A., Bogdanovic, G., Persson, M.A., Dalianis, T., Ramqvist, T., and Andersson, B. (2007). Identification of a third human polyomavirus. J Virol *81*, 4130-4136.

Amin, A.A., Murakami, Y., and Hurwitz, J. (1994). Initiation of DNA replication by simian virus 40 T antigen is inhibited by the p107 protein. J Biol Chem *269*, 7735-7743.

Anders, D.G., and Consigli, R.A. (1983). Chemical cleavage of polyomavirus major structural protein VP1: identification of cleavage products and evidence that the receptor moiety resides in the carboxy-terminal region. J Virol *48*, 197-205.

Ardon, F., Rodriguez-Miranda, E., Beltran, C., Hernandez-Cruz, A., and Darszon, A. (2009). Mitochondrial inhibitors activate influx of external Ca(2+) in sea urchin sperm. Biochim Biophys Acta *1787*, 15-24.

Ashkenazi, A., and Melnick, J.L. (1963). Tumorigencity of simian papovavirus SV40 and of virus-transformed cells. J Natl Cancer Inst *30*, 1227-1265.

Avantaggiati, M.L., Carbone, M., Graessmann, A., Nakatani, Y., Howard, B., and Levine, A.S. (1996). The SV40 large T antigen and adenovirus E1a oncoproteins interact with distinct isoforms of the transcriptional co-activator, p300. EMBO J *15*, 2236-2248.

Bacq, Y., Besnier, J.M., Duong, T.H., Pavie, G., Metman, E.H., and Choutet, P. (1991). Successful treatment of acute fascioliasis with bithionol. Hepatology *14*, 1066-1069.

Bargonetti, J., Reynisdottir, I., Friedman, P.N., and Prives, C. (1992). Site-specific binding of wild-type p53 to cellular DNA is inhibited by SV40 T antigen and mutant p53. Genes Dev *6*, 1886-1898.

Basse, G., Mengelle, C., Kamar, N., Guitard, J., Ribes, D., Esposito, L., and Rostaing, L. (2007). Prospective evaluation of BK virus DNAemia in renal transplant patients and their transplant outcome. Transplant Proc *39*, 84-87.

Bechert, C.J., Schnadig, V.J., Payne, D.A., and Dong, J. (2010). Monitoring of BK viral load in renal allograft recipients by real-time PCR assays. Am J Clin Pathol *133*, 242-250.

Becker, J.C., Houben, R., Ugurel, S., Trefzer, U., Pfohler, C., and Schrama, D. (2009). MC polyomavirus is frequently present in Merkel cell carcinoma of European patients. J Invest Dermatol *129*, 248-250.

Bedi, A., Miller, C.B., Hanson, J.L., Goodman, S., Ambinder, R.F., Charache, P., Arthur, R.R., and Jones, R.J. (1995). Association of BK virus with failure of prophylaxis against hemorrhagic cystitis following bone marrow transplantation. J Clin Oncol *13*, 1103-1109.

Bellard, M., Oudet, P., Germond, J.E., and Chambon, P. (1976). Subunit structure of simian-virus-40 minichromosome. Eur J Biochem *70*, 543-553.

Berg, P. (2004). Paul Berg - Autobiography. In Nobel Lectures (Stockholm, The Nobel Foundation).

Berger, L.C., Smith, D.B., Davidson, I., Hwang, J.J., Fanning, E., and Wildeman, A.G. (1996). Interaction between T antigen and TEA domain of the factor TEF-1 derepresses simian virus 40 late promoter in vitro: identification of T-antigen domains important for transcription control. J Virol *70*, 1203-1212.

Berk, A.J., and Sharp, P.A. (1978). Spliced early mRNAs of simian virus 40. Proc Natl Acad Sci U S A *75*, 1274-1278.

Bernhoff, E., Gutteberg, T.J., Sandvik, K., Hirsch, H.H., and Rinaldo, C.H. (2008). Cidofovir inhibits polyomavirus BK replication in human renal tubular cells downstream of viral early gene expression. Am J Transplant *8*, 1413-1422.

Bernhoff, E., Tylden, G.D., Kjerpeseth, L.J., Gutteberg, T.J., Hirsch, H.H., and Rinaldo, C.H. (2010). Leflunomide inhibition of BK virus replication in renal tubular epithelial cells. J Virol *84*, 2150-2156.

Bharucha, V.A., Peden, K.W., and Tennekoon, G.I. (1994). SV40 large T antigen with c-Jun down-regulates myelin P0 gene expression: a mechanism for papovaviral T antigen-mediated demyelination. Neuron *12*, 627-637.

Bialasiewicz, S., Rockett, R., Whiley, D.W., Abed, Y., Allander, T., Binks, M., Boivin, G., Cheng, A.C., Chung, J.Y., Ferguson, P.E., *et al.* (2010). Whole-genome characterization and genotyping of global WU polyomavirus strains. J Virol *84*, 6229-6234.

Bialasiewicz, S., Whiley, D.M., Lambert, S.B., Wang, D., Nissen, M.D., and Sloots, T.P. (2007). A newly reported human polyomavirus, KI virus, is present in the respiratory tract of Australian children. J Clin Virol *40*, 15-18.

Binet, I., Nickeleit, V., Hirsch, H.H., Prince, O., Dalquen, P., Gudat, F., Mihatsch, M.J., and Thiel, G. (1999). Polyomavirus disease under new immunosuppressive drugs: a cause of renal graft dysfunction and graft loss. Transplantation *67*, 918-922.

Black, P.H., and Rowe, W.P. (1963). An Analysis of Sv40-Induced Transformation of Hamster Kidney Tissue in Vitro. I. General Characteristics. Proc Natl Acad Sci U S A *50*, 606-613.

Black, P.H., and Rowe, W.P. (1964). Viral Studies of Sv40 Tumorigenesis in Hamsters. J Natl Cancer Inst *32*, 253-265.

Bocchetta, M., Di Resta, I., Powers, A., Fresco, R., Tosolini, A., Testa, J.R., Pass, H.I., Rizzo, P., and Carbone, M. (2000). Human mesothelial cells are unusually susceptible to simian virus 40-mediated transformation and asbestos cocarcinogenicity. Proc Natl Acad Sci U S A *97*, 10214-10219.

Bochkareva, E., Martynowski, D., Seitova, A., and Bochkarev, A. (2006). Structure of the origin-binding domain of simian virus 40 large T antigen bound to DNA. EMBO J *25*, 5961-5969.

Bochman, M.L., and Schwacha, A. (2010). The Saccharomyces cerevisiae Mcm6/2 and Mcm5/3 ATPase active sites contribute to the function of the putative Mcm2-7 'gate'. Nucleic Acids Res *38*, 6078-6088.

Bofill-Mas, S., Formiga-Cruz, M., Clemente-Casares, P., Calafell, F., and Girones, R. (2001). Potential transmission of human polyomaviruses through the gastrointestinal tract after exposure to virions or viral DNA. J Virol *75*, 10290-10299.

Boichuk, S., Hu, L., Hein, J., and Gjoerup, O.V. (2010). Multiple DNA damage signaling and repair pathways deregulated by simian virus 40 large T antigen. J Virol *84*, 8007-8020.

Bolen, J.B., and Consigli, R.A. (1980). Separation of neutralizing and hemagglutination-inhibiting antibody activities and specificity of antisera to sodium dodecyl sulfate-derived polypeptides of polyoma virions. J Virol *34*, 119-129.

Bollag, B., Chuke, W.F., and Frisque, R.J. (1989). Hybrid genomes of the polyomaviruses JC virus, BK virus, and simian virus 40: identification of sequences important for efficient transformation. J Virol *63*, 863-872.

Bollag, B., Mackeen, P.C., and Frisque, R.J. (1996). Purified JC virus T antigen derived from insect cells preferentially interacts with binding site II of the viral core origin under replication conditions. Virology *218*, 81-93.

Boren, E.J., Cheema, G.S., Naguwa, S.M., Ansari, A.A., and Gershwin, M.E. (2008). The emergence of progressive multifocal leukoencephalopathy (PML) in rheumatic diseases. J Autoimmun *30*, 90-98.

Brade, L., Muller-Lantzsch, N., and zur Hausen, H. (1981). B-lymphotropic papovavirus and possibility of infections in humans. J Med Virol *6*, 301-308.

Bradley, M.K., Griffin, J.D., and Livingston, D.M. (1982). Relationship of oligomerization to enzymatic and DNA-binding properties of the SV40 large T antigen. Cell *28*, 125-134.

Brockman, W.W. (1978). Transformation of BALB/c-3T3 cells by tsA mutants of simian virus 40: temperature sensitivity of the transformed phenotype and retransofrmation by wild-type virus. J Virol *25*, 860-870.

Brodsky, J.L., and Pipas, J.M. (1998). Polyomavirus T antigens: molecular chaperones for multiprotein complexes. J Virol *72*, 5329-5334.

Broekema, N.M., Abend, J.R., Bennett, S.M., Butel, J.S., Vanchiere, J.A., and Imperiale, M.J. (2010). A system for the analysis of BKV non-coding control regions: application to clinical isolates from an HIV/AIDS patient. Virology *407*, 368-373.

Brugge, J.S., and Butel, J.S. (1975). Role of simian virus 40 gene A function in maintenance of transformation. J Virol *15*, 619-635.

Bullock, P.A. (1997). The initiation of simian virus 40 DNA replication in vitro. Crit Rev Biochem Mol Biol *32*, 503-568.

Butel, J.S., Jarvis, D.L., and Maxwell, S.A. (1989). SV40 T-antigen as a dual oncogene: structure and function of the plasma membrane-associated population. Ann N Y Acad Sci *567*, 104-121.

Butin-Israeli, V., Drayman, N., and Oppenheim, A. (2010). Simian virus 40 infection triggers a balanced network that includes apoptotic, survival, and stress pathways. J Virol *84*, 3431-3442.

Campbell, K.S., Mullane, K.P., Aksoy, I.A., Stubdal, H., Zalvide, J., Pipas, J.M., Silver, P.A., Roberts, T.M., Schaffhausen, B.S., and DeCaprio, J.A. (1997). DnaJ/hsp40 chaperone domain of SV40 large T antigen promotes efficient viral DNA replication. Genes Dev *11*, 1098-1110.

Cantalupo, P., Doering, A., Sullivan, C.S., Pal, A., Peden, K.W., Lewis, A.M., and Pipas, J.M. (2005). Complete nucleotide sequence of polyomavirus SA12. J Virol *79*, 13094-13104.

Cantalupo, P., Saenz-Robles, M.T., and Pipas, J.M. (1999). Expression of SV40 large T antigen in baculovirus systems and purification by immunoaffinity chromatography. Methods Enzymol *306*, 297-307.

Cantalupo, P.G., Saenz-Robles, M.T., Rathi, A.V., Beerman, R.W., Patterson, W.H., Whitehead, R.H., and Pipas, J.M. (2009). Cell-type specific regulation of gene expression by simian virus 40 T antigens. Virology *386*, 183-191.

Canzonetti, A.J., and Dalley, M.M. (1952). Bacteriologic survey of scrub technics with special emphasis on Phisoderm with 3 per cent hexachlorophene. Ann Surg *135*, 228-233.

Carbone, M., Rudzinski, J., and Bocchetta, M. (2003). High throughput testing of the SV40 Large T antigen binding to cellular p53 identifies putative drugs for the treatment of SV40-related cancers. Virology *315*, 409-414.

Carmichael, G., Schaffhausen, B.S., Mandel, G., Liang, T.J., and Benjamin, T.L. (1984). Transformation by polyoma virus is drastically reduced by substitution of phenylalanine for tyrosine at residue 315 of middle-sized tumor antigen. Proc Natl Acad Sci U S A *81*, 679-683.

Castellino, A.M., Cantalupo, P., Marks, I.M., Vartikar, J.V., Peden, K.W., and Pipas, J.M. (1997). trans-Dominant and non-trans-dominant mutant simian virus 40 large T antigens show distinct responses to ATP. J Virol *71*, 7549-7559.

Cettomai, D., and McArthur, J.C. (2009). Mirtazapine use in human immunodeficiency virus-infected patients with progressive multifocal leukoencephalopathy. Arch Neurol *66*, 255-258.

Chang, L., Bertelsen, E.B., Wisen, S., Larsen, E.M., Zuiderweg, E.R., and Gestwicki, J.E. (2008). High-throughput screen for small molecules that modulate the ATPase activity of the molecular chaperone DnaK. Anal Biochem *372*, 167-176.

Charter, N.W., Kauffman, L., Singh, R., and Eglen, R.M. (2006). A generic, homogenous method for measuring kinase and inhibitor activity via adenosine 5'-diphosphate accumulation. J Biomol Screen *11*, 390-399.

Charter, N.W., Kauffman, L., Singh, R., Eglen, R.M. (2006). A Generic, Homogenous Method for Measuring Kinase and Inhibitor Activity via Adenosine 5'-Diphosphate Accumulation. J Biomol Screen *11*, 390-399.

Chen, C.H., Wen, M.C., Wang, M., Lian, J.D., Wu, M.J., Cheng, C.H., Shu, K.H., and Chang, D. (2001). A regulatory region rearranged BK virus is associated with tubulointerstitial nephritis in a rejected renal allograft. J Med Virol *64*, 82-88.

Chen, X.S., Stehle, T., and Harrison, S.C. (1998). Interaction of polyomavirus internal protein VP2 with the major capsid protein VP1 and implications for participation of VP2 in viral entry. EMBO J *17*, 3233-3240.

Chen, Y.R., Lees-Miller, S.P., Tegtmeyer, P., and Anderson, C.W. (1991). The human DNA-activated protein kinase phosphorylates simian virus 40 T antigen at amino- and carboxy-terminal sites. J Virol *65*, 5131-5140.

Chiang, A.N., Valderramos, J.C., Balachandran, R., Chovatiya, R.J., Mead, B.P., Schneider, C., Bell, S.L., Klein, M.G., Huryn, D.M., Chen, X.S., *et al.* (2009). Select pyrimidinones inhibit the propagation of the malarial parasite, Plasmodium falciparum. Bioorg Med Chem *17*, 1527-1533.

Chiang, L.C., Silnutzer, J., Pipas, J.M., and Barnes, D.W. (1985). Selection of transformed cells in serum-free media. In Vitro Cell Dev Biol *21*, 707-712.

Chong, J.L., Wenzel, P.L., Saenz-Robles, M.T., Nair, V., Ferrey, A., Hagan, J.P., Gomez, Y.M., Sharma, N., Chen, H.Z., Ouseph, M., *et al.* (2009). E2f1-3 switch from activators in progenitor cells to repressors in differentiating cells. Nature *462*, 930-934.

Chou, T.F., Brown, S.J., Minond, D., Nordin, B.E., Li, K., Jones, A.C., Chase, P., Porubsky, P.R., Stoltz, B.M., Schoenen, F.J., *et al.* (2011). Reversible inhibitor of p97, DBeQ, impairs both ubiquitin-dependent and autophagic protein clearance pathways. Proc Natl Acad Sci U S A *108*, 4834-4839.

Chromy, L.R., Oltman, A., Estes, P.A., and Garcea, R.L. (2006). Chaperone-mediated in vitro disassembly of polyoma- and papillomaviruses. J Virol *80*, 5086-5091.

Chromy, L.R., Pipas, J.M., and Garcea, R.L. (2003). Chaperone-mediated in vitro assembly of Polyomavirus capsids. Proc Natl Acad Sci U S A *100*, 10477-10482.

Clever, J., Dean, D.A., and Kasamatsu, H. (1993). Identification of a DNA binding domain in simian virus 40 capsid proteins Vp2 and Vp3. J Biol Chem *268*, 20877-20883.

Cole, C. (1996). Polyomavirinae: The Viruses and Their Replication. In Feilds Virology, B.N. Fields, D.M. Knipe, and P.M. Howley, eds. (Philadelphia, PA, Lippincott - Raven Publishers).

Cole, C.N., Crawford, L.V., and Berg, P. (1979). Simian virus 40 mutants with deletions at the 3' end of the early region are defective in adenovirus helper function. J Virol *30*, 683-691.

Cole, C.N., and Stacy, T.P. (1987). Biological properties of simian virus 40 host range mutants lacking the COOH-terminus of large T antigen. Virology *161*, 170-180.

Corbett, J.R., and Goose, A.J. (1971). The biochemical mode of action of the fasciolicides nitroxynil, hexachlorophane and oxyclozanide. Biochem J *121*, 41P.

Cory, A.H., Owen, T.C., Barltrop, J.A., and Cory, J.G. (1991). Use of an aqueous soluble tetrazolium/formazan assay for cell growth assays in culture. Cancer Commun *3*, 207-212.

Cotsiki, M., Lock, R., Cheng, Y., Williams, G., Zhao, J., Perera, D., Freire, R., Entwistle, A., Golemis, E., Roberts, T., *et al.* (2004). Simian virus 40 large T antigen targets the spindle assembly checkpoint protein Bub1. Proc Natl Acad Sci U S A *101*, 947-952.

Craig, E.A., Huang, P., Aron, R., and Andrew, A. (2006). The diverse roles of J-proteins, the obligate Hsp70 co-chaperone. Rev Physiol Biochem Pharmacol *156*, 1-21.

Crawford, L., Dulbecco, R., Fried, M., Montagnier, L., and Stoker, M. (1964). Cell Transformation by Different Forms of Polyoma Virus DNA. Proc Natl Acad Sci U S A *52*, 148-152.

Cyr, D.M., Lu, X., and Douglas, M.G. (1992). Regulation of Hsp70 function by a eukaryotic DnaJ homolog. J Biol Chem *267*, 20927-20931.

Dalianis, T., Ramqvist, T., Andreasson, K., Kean, J.M., and Garcea, R.L. (2009). KI, WU and Merkel cell polyomaviruses: a new era for human polyomavirus research. Semin Cancer Biol *19*, 270-275.

Dalrymple, S.A., and Beemon, K.L. (1990). BK virus T antigens induce kidney carcinomas and thymoproliferative disorders in transgenic mice. J Virol *64*, 1182-1191.

Damania, B., and Pipas, J. (2009). Introduction. In DNA Tumor Viruses, B. Damania, and J. Pipas, eds. (New York, NY, Springer Science+Business Media), pp. xvii-xxvi.

Dang, X., Bialasiewicz, S., Nissen, M.D., Sloots, T.P., Koralnik, I.J., and Tan, C.S. (2011). Infrequent Detection of KI, WU and MC Polyomaviruses in Immunosuppressed Individuals with or without Progressive Multifocal Leukoencephalopathy. PLoS One *6*, e16736.

Daniels, R., Sadowicz, D., and Hebert, D.N. (2007). A very late viral protein triggers the lytic release of SV40. PLoS Pathog *3*, e98.

Danna, K., and Nathans, D. (1971). Specific cleavage of simian virus 40 DNA by restriction endonuclease of Hemophilus influenzae. Proc Natl Acad Sci U S A *68*, 2913-2917.

Danna, K.J., Sack, G.H., Jr., and Nathans, D. (1973). Studies of simian virus 40 DNA. VII. A cleavage map of the SV40 genome. J Mol Biol *78*, 363-376.

De Clercq, E. (2002). Cidofovir in the treatment of poxvirus infections. Antiviral Res *55*, 1-13.

De Clercq, E., Sakuma, T., Baba, M., Pauwels, R., Balzarini, J., Rosenberg, I., and Holy, A. (1987). Antiviral activity of phosphonylmethoxyalkyl derivatives of purine and pyrimidines. Antiviral Res *8*, 261-272.

De Luca, A., Ammassari, A., Pezzotti, P., Cinque, P., Gasnault, J., Berenguer, J., Di Giambenedetto, S., Cingolani, A., Taoufik, Y., Miralles, P., *et al.* (2008). Cidofovir in addition to antiretroviral treatment is not effective for AIDS-associated progressive multifocal leukoencephalopathy: a multicohort analysis. AIDS *22*, 1759-1767.

De Luca, A., Giancola, M.L., Cingolani, A., Ammassari, A., Gillini, L., Murri, R., and Antinori, A. (1999). Clinical and virological monitoring during treatment with intrathecal cytarabine in patients with AIDS-associated progressive multifocal leukoencephalopathy. Clin Infect Dis *28*, 624-628.

de Villiers, J., Olson, L., Tyndall, C., and Schaffner, W. (1982). Transcriptional 'enhancers' from SV40 and polyoma virus show a cell type preference. Nucleic Acids Res *10*, 7965-7976.

DeAngelis, T., Chen, J., Wu, A., Prisco, M., and Baserga, R. (2006). Transformation by the simian virus 40 T antigen is regulated by IGF-I receptor and IRS-1 signaling. Oncogene *25*, 32-42.

Deb, S., DeLucia, A.L., Baur, C.P., Koff, A., and Tegtmeyer, P. (1986). Domain structure of the simian virus 40 core origin of replication. Mol Cell Biol *6*, 1663-1670.

Deb, S., Tsui, S., Koff, A., DeLucia, A.L., Parsons, R., and Tegtmeyer, P. (1987). The T-antigen-binding domain of the simian virus 40 core origin of replication. J Virol *61*, 2143-2149.

DeCaprio, J.A. (2009). How the Rb tumor suppressor structure and function was revealed by the study of Adenovirus and SV40. Virology *384*, 274-284.

DeCaprio, J.A., Ludlow, J.W., Figge, J., Shew, J.Y., Huang, C.M., Lee, W.H., Marsilio, E., Paucha, E., and Livingston, D.M. (1988). SV40 large tumor antigen forms a specific complex with the product of the retinoblastoma susceptibility gene. Cell *54*, 275-283.

DeLeo, A.B., Jay, G., Appella, E., Dubois, G.C., Law, L.W., and Old, L.J. (1979). Detection of a transformation-related antigen in chemically induced sarcomas and other transformed cells of the mouse. Proc Natl Acad Sci U S A *76*, 2420-2424.

Dhar, R., Subramanian, K.N., Pan, J., and Weissman, S.M. (1977). Structure of a large segment of the genome of simian virus 40 that does not encode known proteins. Proc Natl Acad Sci U S A *74*, 827-831.

Dharnidharka, V.R., Cherikh, W.S., and Abbott, K.C. (2009). An OPTN analysis of national registry data on treatment of BK virus allograft nephropathy in the United States. Transplantation *87*, 1019-1026.

Dong, S., Terasaka, S., and Kiyama, R. (2011). Bisphenol A induces a rapid activation of Erk1/2 through GPR30 in human breast cancer cells. Environ Pollut *159*, 212-218.

Dulbecco, R. (1975). Renato Dulbecco - Autobiography. In Nobel Lectures, W. Odelberg, ed. (Stockholm, The Nobel Foundation).

Dulbecco, R., Hartwell, L.H., and Vogt, M. (1965). Induction of Cellular DNA Synthesis by Polyoma Virus. Proc Natl Acad Sci U S A *53*, 403-410.

Dulbecco, R., and Vogt, M. (1963). Evidence for a Ring Structure of Polyoma Virus DNA. Proc Natl Acad Sci U S A *50*, 236-243.

Dyson, N., Bernards, R., Friend, S.H., Gooding, L.R., Hassell, J.A., Major, E.O., Pipas, J.M., Vandyke, T., and Harlow, E. (1990). Large T antigens of many polyomaviruses are able to form complexes with the retinoblastoma protein. J Virol *64*, 1353-1356.

Eash, S., Querbes, W., and Atwood, W.J. (2004). Infection of vero cells by BK virus is dependent on caveolae. J Virol *78*, 11583-11590.

Eckner, R., Ludlow, J.W., Lill, N.L., Oldread, E., Arany, Z., Modjtahedi, N., DeCaprio, J.A., Livingston, D.M., and Morgan, J.A. (1996). Association of p300 and CBP with simian virus 40 large T antigen. Mol Cell Biol *16*, 3454-3464.

Eddy, B.E., Borman, G.S., Berkeley, W.H., and Young, R.D. (1961). Tumors induced in hamsters by injection of rhesus monkey kidney cell extracts. Proc Soc Exp Biol Med *107*, 191-197.

Elfaitouri, A., Hammarin, A.L., and Blomberg, J. (2006). Quantitative real-time PCR assay for detection of human polyomavirus infection. J Virol Methods *135*, 207-213.

Eliyahu, D., Raz, A., Gruss, P., Givol, D., and Oren, M. (1984). Participation of p53 cellular tumour antigen in transformation of normal embryonic cells. Nature *312*, 646-649.

Elphick, G.F., Querbes, W., Jordan, J.A., Gee, G.V., Eash, S., Manley, K., Dugan, A., Stanifer, M., Bhatnagar, A., Kroeze, W.K., *et al.* (2004). The human polyomavirus, JCV, uses serotonin receptors to infect cells. Science *306*, 1380-1383.

Engels, E.A., Frisch, M., Goedert, J.J., Biggar, R.J., and Miller, R.W. (2002). Merkel cell carcinoma and HIV infection. Lancet *359*, 497-498.

Engsig, F.N., Hansen, A.B., Omland, L.H., Kronborg, G., Gerstoft, J., Laursen, A.L., Pedersen, C., Mogensen, C.B., Nielsen, L., and Obel, N. (2009). Incidence, clinical presentation, and outcome of progressive multifocal leukoencephalopathy in HIV-infected patients during the highly active antiretroviral therapy era: a nationwide cohort study. J Infect Dis *199*, 77-83.

Erler, C., and Novak, J. (2010). Bisphenol a exposure: human risk and health policy. J Pediatr Nurs *25*, 400-407.

Faguer, S., Hirsch, H.H., Kamar, N., Guilbeau-Frugier, C., Ribes, D., Guitard, J., Esposito, L., Cointault, O., Modesto, A., Lavit, M., *et al.* (2007). Leflunomide treatment for polyomavirus BK-associated nephropathy after kidney transplantation. Transpl Int *20*, 962-969.

Fairman, M.P., and Stillman, B. (1988). Cellular factors required for multiple stages of SV40 DNA replication in vitro. EMBO J *7*, 1211-1218.

Fanning, E., and Zhao, K. (2009). SV40 DNA replication: from the A gene to a nanomachine. Virology *384*, 352-359.

Fanning, E., Zhao, X., and Jiang, X. (2009). Polyomavirus Life Cycle. In DNA Tumor Viruses, B. Damania, and J.M. Pipas, eds. (New York, NY, Springer New York).

Farasati, N.A., Shapiro, R., Vats, A., and Randhawa, P. (2005). Effect of leflunomide and cidofovir on replication of BK virus in an in vitro culture system. Transplantation *79*, 116-118.

Feng, H., Shuda, M., Chang, Y., and Moore, P.S. (2008). Clonal integration of a polyomavirus in human Merkel cell carcinoma. Science *319*, 1096-1100.

Fewell, S.W., Pipas, J.M., and Brodsky, J.L. (2002). Mutagenesis of a functional chimeric gene in yeast identifies mutations in the simian virus 40 large T antigen J domain. Proc Natl Acad Sci U S A *99*, 2002-2007.

Fewell, S.W., Smith, C.M., Lyon, M.A., Dumitrescu, T.P., Wipf, P., Day, B.W., and Brodsky, J.L. (2004). Small molecule modulators of endogenous and co-chaperone-stimulated Hsp70 ATPase activity. J Biol Chem *279*, 51131-51140.

Fiers, W., Contreras, R., Haegemann, G., Rogiers, R., Van de Voorde, A., Van Heuverswyn, H., Van Herreweghe, J., Volckaert, G., and Ysebaert, M. (1978). Complete nucleotide sequence of SV40 DNA. Nature *273*, 113-120.

Finlay, C.A., Hinds, P.W., and Levine, A.J. (1989). The p53 proto-oncogene can act as a suppressor of transformation. Cell *57*, 1083-1093.

Fradet-Turcotte, A., Morin, G., Lehoux, M., Bullock, P.A., and Archambault, J. (2010). Development of quantitative and high-throughput assays of polyomavirus and papillomavirus DNA replication. Virology *399*, 65-76.

Frearson, P.M., Kit, S., and Dubbs, D.R. (1966). Induction of dihydrofolate reductase activity by SV40 and polyoma virus. Cancer Res *26*, 1653-1660.

Friend, S.H., Bernards, R., Rogelj, S., Weinberg, R.A., Rapaport, J.M., Albert, D.M., and Dryja, T.P. (1986). A human DNA segment with properties of the gene that predisposes to retinoblastoma and osteosarcoma. Nature *323*, 643-646.

Fujimura, F.K., Deininger, P.L., Friedmann, T., and Linney, E. (1981). Mutation near the polyoma DNA replication origin permits productive infection of F9 embryonal carcinoma cells. Cell *23*, 809-814.

Fung, Y.K., Murphree, A.L., T'Ang, A., Qian, J., Hinrichs, S.H., and Benedict, W.F. (1987). Structural evidence for the authenticity of the human retinoblastoma gene. Science *236*, 1657-1661.

Furuse, Y., Suzuki, A., Kishi, M., Galang, H.O., Lupisan, S.P., Olveda, R.M., and Oshitani, H. (2010). Detection of novel respiratory viruses from influenza-like illness in the Philippines. J Med Virol *82*, 1071-1074.

Gardner, S.D., Field, A.M., Coleman, D.V., and Hulme, B. (1971). New human papovavirus (B.K.) isolated from urine after renal transplantation. Lancet *1*, 1253-1257.

Garneski, K.M., Warcola, A.H., Feng, Q., Kiviat, N.B., Leonard, J.H., and Nghiem, P. (2009). Merkel cell polyomavirus is more frequently present in North American than Australian Merkel cell carcinoma tumors. J Invest Dermatol *129*, 246-248.

Gasnault, J., Taoufik, Y., Goujard, C., Kousignian, P., Abbed, K., Boue, F., Dussaix, E., and Delfraissy, J.F. (1999). Prolonged survival without neurological improvement in patients with AIDS-related progressive multifocal leukoencephalopathy on potent combined antiretroviral therapy. J Neurovirol *5*, 421-429.

Gaynor, A.M., Nissen, M.D., Whiley, D.M., Mackay, I.M., Lambert, S.B., Wu, G., Brennan, D.C., Storch, G.A., Sloots, T.P., and Wang, D. (2007). Identification of a novel polyomavirus from patients with acute respiratory tract infections. PLoS Pathog *3*, e64.

Ge, H., and Manley, J.L. (1990). A protein factor, ASF, controls cell-specific alternative splicing of SV40 early pre-mRNA in vitro. Cell *62*, 25-34.

Gerber, P., and Kirschstein, R.L. (1962). SV40-induced ependymomas in newborn hamsters. I. Virus-tumor relationships. Virology *18*, 582-588.

Germond, J.E., Hirt, B., Oudet, P., Gross-Bellark, M., and Chambon, P. (1975). Folding of the DNA double helix in chromatin-like structures from simian virus 40. Proc Natl Acad Sci U S A *72*, 1843-1847.

Gershon, D., Hausen, P., Sachs, L., and Winocour, E. (1965). On the mechanism of polyoma virus-induced synthesis of cellular DNA. Proc Natl Acad Sci U S A *54*, 1584-1592.

Gething, M.J., and Sambrook, J. (1992). Protein folding in the cell. Nature *355*, 33-45.

Giacherio, D., and Hager, L.P. (1979). A poly(dT)-stimulated ATPase activity associated with simian virus 40 large T antigen. J Biol Chem *254*, 8113-8116.

Giacherio, D., and Hager, L.P. (1980). A specific DNA unwinding activity associated with SV40 large T antigen. J Biol Chem *255*, 8963-8966.

Gidoni, D., Scheller, A., Barnet, B., Hantzopoulos, P., Oren, M., and Prives, C. (1982). Different forms of simian virus 40 large tumor antigen varying in their affinities for DNA. J Virol *42*, 456-466.

Gilbert, J., and Benjamin, T. (2004). Uptake pathway of polyomavirus via ganglioside GD1a. J Virol *78*, 12259-12267.

Gilden, R.V., Carp, R.I., Taguchi, F., and Defend, V. (1965). The Nature and Localization of the Sv 40-Induced Complement-Fixing Antigen. Proc Natl Acad Sci U S A *53*, 684-692.

Giraldi, C., Noto, A., Tenuta, R., Greco, F., Perugini, D., Dodaro, S., Spadafora, M., Lo Bianco, A.M., Savino, O., Papalia, T., *et al.* (2007). Prospective study of BKV nephropathy in 117 renal transplant recipients. New Microbiol *30*, 127-130.

Girardi, A.J., Jensen, F.C., and Koprowski, H. (1965). Sv40-Induced Tranformation of Human Diploid Cells: Crisis and Recovery. J Cell Physiol *65*, 69-83.

Gjoerup, O., and Chang, Y. (2010). Update on human polyomaviruses and cancer. Adv Cancer Res *106*, 1-51.

Gjorup, O.V., Rose, P.E., Holman, P.S., Bockus, B.J., and Schaffhausen, B.S. (1994). Protein domains connect cell cycle stimulation directly to initiation of DNA replication. Proc Natl Acad Sci U S A *91*, 12125-12129.

Goodwin, E.C., Atwood, W.J., and DiMaio, D. (2009). High-throughput cell-based screen for chemicals that inhibit infection by simian virus 40 and human polyomaviruses. J Virol *83*, 5630-5639.

Goorha, R., Granoff, A., Willis, D.B., and Murti, K.G. (1984). The role of DNA methylation in virus replication: inhibition of frog virus 3 replication by 5-azacytidine. Virology *138*, 94-102.

Gordon-Shaag, A., Yosef, Y., Abd El-Latif, M., and Oppenheim, A. (2003). The abundant nuclear enzyme PARP participates in the life cycle of simian virus 40 and is stimulated by minor capsid protein VP3. J Virol *77*, 4273-4282.

Gotz, C., Koenig, M.G., Issinger, O.G., and Montenarh, M. (1995). A casein-kinase-2-related protein kinase is tightly associated with the large T antigen of simian virus 40. Eur J Biochem *233*, 327-334.

Graffi, A., Schramm, T., Graffi, I., Bierwolf, D., and Bender, E. (1968). Virus-associated skin tumors of the Syrian hamster: preliminary note. J Natl Cancer Inst *40*, 867-873.

Gray, F., Chretien, F., Vallat-Decouvelaere, A.V., and Scaravilli, F. (2003). The changing pattern of HIV neuropathology in the HAART era. J Neuropathol Exp Neurol *62*, 429-440.

Griffith, J.D. (1975). Chromatin structure: deduced from a minichromosome. Science *187*, 1202-1203.

Gross, L. (1953). A filterable agent, recovered from Ak leukemic extracts, causing salivary gland carcinomas in C3H mice. Proc Soc Exp Biol Med *83*, 414-421.

Grundhoff, A., and Sullivan, C.S. (2011). Virus-encoded microRNAs. Virology *411*, 325-343.

Guerriero, C.J., Weixel, K.M., Bruns, J.R., and Weisz, O.A. (2006). Phosphatidylinositol 5-kinase stimulates apical biosynthetic delivery via an Arp2/3-dependent mechanism. J Biol Chem *281*, 15376-15384.

Habel, K., Jensen, F., Pagano, J.S., and Koprowski, H. (1965). Specific Complement-Fixing Tumor Antigen in Sv40-Transformed Human Cells. Proc Soc Exp Biol Med *118*, 4-9.

Hahn, W.C., Counter, C.M., Lundberg, A.S., Beijersbergen, R.L., Brooks, M.W., and Weinberg, R.A. (1999). Creation of human tumour cells with defined genetic elements. Nature *400*, 464-468.

Hahn, W.C., Dessain, S.K., Brooks, M.W., King, J.E., Elenbaas, B., Sabatini, D.M., DeCaprio, J.A., and Weinberg, R.A. (2002). Enumeration of the simian virus 40 early region elements necessary for human cell transformation. Mol Cell Biol *22*, 2111-2123.

Halami, M.Y., Dorrestein, G.M., Couteel, P., Heckel, G., Muller, H., and Johne, R. (2010). Whole-genome characterization of a novel polyomavirus detected in fatally diseased canary birds. J Gen Virol *91*, 3016-3022.

Hall, C.D., Dafni, U., Simpson, D., Clifford, D., Wetherill, P.E., Cohen, B., McArthur, J., Hollander, H., Yainnoutsos, C., Major, E., *et al.* (1998). Failure of cytarabine in progressive multifocal leukoencephalopathy associated with human immunodeficiency virus infection. AIDS Clinical Trials Group 243 Team. N Engl J Med *338*, 1345-1351.

Harlow, E., Crawford, L.V., Pim, D.C., and Williamson, N.M. (1981). Monoclonal antibodies specific for simian virus 40 tumor antigens. J Virol *39*, 861-869.

Harris, K.F., Chang, E., Christensen, J.B., and Imperiale, M.J. (1998). BK virus as a potential co-factor in human cancer. Dev Biol Stand *94*, 81-91.

Harris, K.F., Christensen, J.B., and Imperiale, M.J. (1996). BK virus large T antigen: interactions with the retinoblastoma family of tumor suppressor proteins and effects on cellular growth control. J Virol *70*, 2378-2386.

Hartley, J.W., and Rowe, W.P. (1964). New Papovavirus Contaminating Shope Papillomata. Science *143*, 258-260.

Hartwell, L. (2001). Leland Hartwell - Autobiography. In Nobel Lectures, T. Frängsmyr, ed. (Stockholm, The Nobel Foundation).

Hartwell, L.H., Vogt, M., and Dulbecco, R. (1965). Induction of cellular DNA synthesis by polyoma virus. II. Increase in the rate of enzyme synthesis after infection with polyoma virus in mouse kidney cells. Virology *27*, 262-272.

Haycox, C.L., Kim, S., Fleckman, P., Smith, L.T., Piepkorn, M., Sundberg, J.P., Howell, D.N., and Miller, S.E. (1999). Trichodysplasia spinulosa--a newly described folliculocentric viral infection in an immunocompromised host. J Investig Dermatol Symp Proc *4*, 268-271.

Hein, J., Boichuk, S., Wu, J., Cheng, Y., Freire, R., Jat, P.S., Roberts, T.M., and Gjoerup, O.V. (2009). Simian virus 40 large T antigen disrupts genome integrity and activates a DNA damage response via Bub1 binding. J Virol *83*, 117-127.

Herbig, U., Weisshart, K., Taneja, P., and Fanning, E. (1999). Interaction of the transcription factor TFIID with simian virus 40 (SV40) large T antigen interferes with replication of SV40 DNA in vitro. J Virol *73*, 1099-1107.

Hermannstadter, A., Ziegler, C., Kuhl, M., Deppert, W., and Tolstonog, G.V. (2009). Wild-type p53 enhances efficiency of simian virus 40 large-T-antigen-induced cellular transformation. J Virol *83*, 10106-10118.

Hill, A.B. (1965). The Environment and Disease: Association or Causation? Proc R Soc Med *58*, 295-300.

Hilton, R., and Tong, C.Y. (2008). Antiviral therapy for polyomavirus-associated nephropathy after renal transplantation. J Antimicrob Chemother *62*, 855-859.

Hinds, P., Finlay, C., and Levine, A.J. (1989). Mutation is required to activate the p53 gene for cooperation with the ras oncogene and transformation. J Virol *63*, 739-746.

Hinzpeter, M., and Deppert, W. (1987). Analysis of biological and biochemical parameters for chromatin and nuclear matrix association of SV40 large T antigen in transformed cells. Oncogene *1*, 119-129.

Hirsch, H.H., Knowles, W., Dickenmann, M., Passweg, J., Klimkait, T., Mihatsch, M.J., and Steiger, J. (2002). Prospective study of polyomavirus type BK replication and nephropathy in renal-transplant recipients. N Engl J Med *347*, 488-496.

Hirsch, H.H., and Randhawa, P. (2009). BK virus in solid organ transplant recipients. Am J Transplant *9 Suppl 4*, S136-146.

Hirsch, H.H., and Steiger, J. (2003). Polyomavirus BK. Lancet Infect Dis *3*, 611-623.

Horowitz, J.M., Yandell, D.W., Park, S.H., Canning, S., Whyte, P., Buchkovich, K., Harlow, E., Weinberg, R.A., and Dryja, T.P. (1989). Point mutational inactivation of the retinoblastoma antioncogene. Science *243*, 937-940.

Hoss, A., Moarefi, I., Scheidtmann, K.H., Cisek, L.J., Corden, J.L., Dornreiter, I., Arthur, A.K., and Fanning, E. (1990). Altered phosphorylation pattern of simian virus 40 T antigen expressed in insect cells by using a baculovirus vector. J Virol *64*, 4799-4807.

Hou, J., and Major, E.O. (1998). The efficacy of nucleoside analogs against JC virus multiplication in a persistently infected human fetal brain cell line. J Neurovirol *4*, 451-456.

Houben, R., Adam, C., Baeurle, A., Hesbacher, S., Grimm, J., Angermeyer, S., Henzel, K., Hauser, S., Elling, R., Brocker, E.B., *et al.* (2011). An intact retinoblastoma protein binding site in merkel cell polyomavirus large T antigen is required for promoting growth of merkel cell carcinoma cells. Int J Cancer.

Houben, R., Shuda, M., Weinkam, R., Schrama, D., Feng, H., Chang, Y., Moore, P.S., and Becker, J.C. (2010). Merkel cell polyomavirus-infected Merkel cell carcinoma cells require expression of viral T antigens. J Virol *84*, 7064-7072.

Huang, H., Zhao, K., Arnett, D.R., and Fanning, E. (2010). A specific docking site for DNA polymerase {alpha}-primase on the SV40 helicase is required for viral primosome activity, but helicase activity is dispensable. J Biol Chem *285*, 33475-33484.

Hubner, S., Xiao, C.Y., and Jans, D.A. (1997). The protein kinase CK2 site (Ser111/112) enhances recognition of the simian virus 40 large T-antigen nuclear localization sequence by importin. J Biol Chem *272*, 17191-17195.

Huryn, D.M., Brodsky, J.L., Brummond, K.M., Chambers, P.G., Eyer, B., Ireland, A.W., Kawasumi, M., Laporte, M.G., Lloyd, K., Manteau, B., *et al.* (2011). Organic Synthesis Toward Small-Molecule Probes and Drugs Special Feature: Chemical methodology as a source of small-molecule checkpoint inhibitors and heat shock protein 70 (Hsp70) modulators. Proc Natl Acad Sci U S A *108*, 6757-6762.

Imperiale, M.J., and Major, E.O. (2007). Polyomaviruses. In Field's Virology, D.M. Knipe, P.M. Howley, D.E. Griffin, R.A. Lamb, M.A. Martin, B. Roizman, and S.E. Straus, eds. (Philadelphia, Lippincott Williams & Wilkins).

Irvine, J.D., Takahashi, L., Lockhart, K., Cheong, J., Tolan, J.W., Selick, H.E., and Grove, J.R. (1999). MDCK (Madin-Darby canine kidney) cells: A tool for membrane permeability screening. J Pharm Sci *88*, 28-33.

Ishimi, Y., Sugasawa, K., Hanaoka, F., Eki, T., and Hurwitz, J. (1992). Topoisomerase II plays an essential role as a swivelase in the late stage of SV40 chromosome replication in vitro. J Biol Chem *267*, 462-466.

Izzedine, H., Launay-Vacher, V., and Deray, G. (2005). Antiviral drug-induced nephrotoxicity. Am J Kidney Dis *45*, 804-817.

Jay, G., Nomura, S., Anderson, C.W., and Khoury, G. (1981). Identification of the SV40 agnogene product: a DNA binding protein. Nature *291*, 346-349.

Jenkins, J.R., Rudge, K., and Currie, G.A. (1984). Cellular immortalization by a cDNA clone encoding the transformation-associated phosphoprotein p53. Nature *312*, 651-654.

Jensen, F., Koprowski, H., and Ponten, J.A. (1963). Rapid Transformation of Human Fibroblast Cultures by Simian Virus. Proc Natl Acad Sci U S A *50*, 343-348.

Jiang, M., Abend, J.R., Johnson, S.F., and Imperiale, M.J. (2009a). The role of polyomaviruses in human disease. Virology *384*, 266-273.

Jiang, M., Abend, J.R., Tsai, B., and Imperiale, M.J. (2009b). Early events during BK virus entry and disassembly. J Virol *83*, 1350-1358.

Johne, R., Buck, C.B., Allander, T., Atwood, W.J., Garcea, R.L., Imperiale, M.J., Major, E.O., Ramqvist, T., and Norkin, L.C. (2011). Taxonomical developments in the family Polyomaviridae. Arch Virol.

Johne, R., and Muller, H. (2007). Polyomaviruses of birds: etiologic agents of inflammatory diseases in a tumor virus family. J Virol *81*, 11554-11559.

Johne, R., Wittig, W., Fernandez-de-Luco, D., Hofle, U., and Muller, H. (2006). Characterization of two novel polyomaviruses of birds by using multiply primed rolling-circle amplification of their genomes. J Virol *80*, 3523-3531.

Johnston, O., Jaswal, D., Gill, J.S., Doucette, S., Fergusson, D.A., and Knoll, G.A. (2010). Treatment of polyomavirus infection in kidney transplant recipients: a systematic review. Transplantation *89*, 1057-1070.

Johnston, S.D., Yu, X.M., and Mertz, J.E. (1996). The major transcriptional transactivation domain of simian virus 40 large T antigen associates nonconcurrently with multiple components of the transcriptional preinitiation complex. J Virol *70*, 1191-1202.

Josephson, M.A., Gillen, D., Javaid, B., Kadambi, P., Meehan, S., Foster, P., Harland, R., Thistlethwaite, R.J., Garfinkel, M., Atwood, W., *et al.* (2006a). Treatment of renal allograft polyoma BK virus infection with leflunomide. Transplantation *81*, 704-710.

Josephson, M.A., Williams, J.W., Chandraker, A., and Randhawa, P.S. (2006b). Polyomavirus-associated nephropathy: update on antiviral strategies. Transpl Infect Dis *8*, 95-101.

Ju, J.S., and Weihl, C.C. (2010). Inclusion body myopathy, Paget's disease of the bone and fronto-temporal dementia: a disorder of autophagy. Hum Mol Genet *19*, R38-45.

Kakizuka, A. (2008). Roles of VCP in human neurodegenerative disorders. Biochem Soc Trans *36*, 105-108.

Kalderon, D., Richardson, W.D., Markham, A.F., and Smith, A.E. (1984a). Sequence requirements for nuclear location of simian virus 40 large-T antigen. Nature *311*, 33-38.

Kalderon, D., Roberts, B.L., Richardson, W.D., and Smith, A.E. (1984b). A short amino acid sequence able to specify nuclear location. Cell *39*, 499-509.

Kalderon, D., and Smith, A.E. (1984). In vitro mutagenesis of a putative DNA binding domain of SV40 large-T. Virology *139*, 109-137.

Kantola, K., Sadeghi, M., Ewald, M.J., Weissbrich, B., Allander, T., Lindau, C., Andreasson, K., Lahtinen, A., Kumar, A., Norja, P., *et al.* (2010). Expression and serological characterization of polyomavirus WUPyV and KIPyV structural proteins. Viral Immunol *23*, 385-393.

Katinka, M., Yaniv, M., Vasseur, M., and Blangy, D. (1980). Expression of polyoma early functions in mouse embryonal carcinoma cells depends on sequence rearrangements in the beginning of the late region. Cell *20*, 393-399.

Katoh, H., Ogawa, H., Ohya, K., and Fukushi, H. (2010). A review of DNA viral infections in psittacine birds. J Vet Med Sci *72*, 1099-1106.

Kean, J.M., and Garcea, R. (2009). Polyomaviruses and Disease. In DNA Tumor Viruses, B. Damania, and J. Pipas, eds. (New York, NY, Springer Science+Business Media, LLC), pp. 53-74.

Kean, J.M., Rao, S., Wang, M., and Garcea, R.L. (2009). Seroepidemiology of human polyomaviruses. PLoS Pathog *5*, e1000363.

Kelley, W.L., and Georgopoulos, C. (1997). The T/t common exon of simian virus 40, JC, and BK polyomavirus T antigens can functionally replace the J-domain of the Escherichia coli DnaJ molecular chaperone. Proc Natl Acad Sci U S A *94*, 3679-3684.

Khalili, K., White, M.K., Sawa, H., Nagashima, K., and Safak, M. (2005). The agnoprotein of polyomaviruses: a multifunctional auxiliary protein. J Cell Physiol *204*, 1-7.

Khanna, N., Elzi, L., Mueller, N.J., Garzoni, C., Cavassini, M., Fux, C.A., Vernazza, P., Bernasconi, E., Battegay, M., and Hirsch, H.H. (2009). Incidence and outcome of progressive multifocal leukoencephalopathy over 20 years of the Swiss HIV Cohort Study. Clin Infect Dis *48*, 1459-1466.

Khopde, S., and Simmons, D.T. (2008). Simian virus 40 DNA replication is dependent on an interaction between topoisomerase I and the C-terminal end of T antigen. J Virol *82*, 1136-1145.

Khoury, G., Martin, M.A., Lee, T.N., Danna, K.J., and Nathans, D. (1973). A map of simian virus 40 transcription sites expressed in productively infected cells. J Mol Biol *78*, 377-389.

Kierstead, T.D., and Tevethia, M.J. (1993). Association of p53 binding and immortalization of primary C57BL/6 mouse embryo fibroblasts by using simian virus 40 T-antigen mutants bearing internal overlapping deletion mutations. J Virol *67*, 1817-1829.

Kilham, L. (1952). Isolation in suckling mice of a virus from C3H mice harboring Bittner milk agent. Science *116*, 391-392.

Kim, H.Y., Ahn, B.Y., and Cho, Y. (2001). Structural basis for the inactivation of retinoblastoma tumor suppressor by SV40 large T antigen. EMBO J *20*, 295-304.

Kim, J.S. (1970). Treatment of Paragonimus westermani infections with bithionol. Am J Trop Med Hyg *19*, 940-942.

Kim, K., Son, T.G., Kim, S.J., Kim, H.S., Kim, T.S., Han, S.Y., and Lee, J. (2007). Suppressive effects of bisphenol A on the proliferation of neural progenitor cells. J Toxicol Environ Health A *70*, 1288-1295.

Kimbrough, R.D. (1973). Review of the toxicity of hexachlorophene, including its neurotoxicity. J Clin Pharmacol *13*, 439-444.

Kimura, G., and Dulbecco, R. (1973). A temperature-sensitive mutant of simian virus 40 affecting transforming ability. Virology *52*, 529-534.

Kimura, G., and Itagaki, A. (1975). Initiation and maintenance of cell transformation by simian virus 40: a viral genetic property. Proc Natl Acad Sci U S A *72*, 673-677.

Kirschstein, R.L., and Gerber, P. (1962). Ependymomas produced after intracerebral inoculation of SV40 into new-born hamsters. Nature *195*, 299-300.

Kit, S., Piekarski, L.J., and Dubbs, D.R. (1967). DNA polymerase induced by Simian virus 40. J Gen Virol *1*, 163-173.

Klein, G., Powers, A., and Croce, C. (2002). Association of SV40 with human tumors. Oncogene *21*, 1141-1149.

Klockmann, U., and Deppert, W. (1983). Acylated simian virus 40 large T-antigen: a new subclass associated with a detergent-resistant lamina of the plasma membrane. EMBO J *2*, 1151-1157.

Knudson, A.G., Jr. (1971). Mutation and cancer: statistical study of retinoblastoma. Proc Natl Acad Sci U S A *68*, 820-823.

Kondo, M., Kojima, S., Kato, K., and Matsuyama, T. (1998). Late-onset hemorrhagic cystitis after hematopoietic stem cell transplantation in children. Bone Marrow Transplant *22*, 995-998.

Koonin, E.V. (1993). A common set of conserved motifs in a vast variety of putative nucleic acid-dependent ATPases including MCM proteins involved in the initiation of eukaryotic DNA replication. Nucleic Acids Res *21*, 2541-2547.

Koprowski, H., Ponten, J., Jensen, F., Ravdin, R.G., Moorhead, P., and Saksela, E. (1963). Transformation of cultures of human tissue infected with simian virus SV40. Acta Unio Int Contra Cancrum *19*, 362-367.

Kress, M., May, E., Cassingena, R., and May, P. (1979). Simian virus 40-transformed cells express new species of proteins precipitable by anti-simian virus 40 tumor serum. J Virol *31*, 472-483.

Kress, M., Resche-Rigon, M., and Feunteun, J. (1982). Phosphorylation pattern of large T antigens in mouse cells infected by simian virus 40 wild type or deletion mutants. J Virol *43*, 761-771.

Kunisaki, K.M., and Janoff, E.N. (2009). Influenza in immunosuppressed populations: a review of infection frequency, morbidity, mortality, and vaccine responses. Lancet Infect Dis *9*, 493-504.

Kunitake, T., Kitamura, T., Guo, J., Taguchi, F., Kawabe, K., and Yogo, Y. (1995). Parent-to-child transmission is relatively common in the spread of the human polyomavirus JC virus. J Clin Microbiol *33*, 1448-1451.

Lane, D.P., and Crawford, L.V. (1979). T antigen is bound to a host protein in SV40-transformed cells. Nature *278*, 261-263.

Lanford, R.E., and Butel, J.S. (1984). Construction and characterization of an SV40 mutant defective in nuclear transport of T antigen. Cell *37*, 801-813.

Lange-Mutschler, J., and Henning, R. (1984). Cell surface binding simian virus 40 large T antigen becomes anchored and stably linked to lipid of the target cells. Virology *136*, 404-413.

Lauring, A.S., and Andino, R. (2010). Quasispecies theory and the behavior of RNA viruses. PLoS Pathog *6*, e1001005.

Lazarus, H.M., Sporn, M.B., Smith, J.M., and Henderson, W.R. (1967). Purification of T antigen from nuclei of simian virus 40-induced hamster tumors. J Virol *1*, 1093-1095.

Lee, O.J., and Kim, T.H. (2006). Indirect evidence of ectopic pancreatic fascioliasis in a human. J Gastroenterol Hepatol *21*, 1631-1633.

Lee, S.H., Eki, T., and Hurwitz, J. (1989). Synthesis of DNA containing the simian virus 40 origin of replication by the combined action of DNA polymerases alpha and delta. Proc Natl Acad Sci U S A *86*, 7361-7365.

Lee, S.H., and Hurwitz, J. (1990). Mechanism of elongation of primed DNA by DNA polymerase delta, proliferating cell nuclear antigen, and activator 1. Proc Natl Acad Sci U S A *87*, 5672-5676.

Lee, W.H., Bookstein, R., Hong, F., Young, L.J., Shew, J.Y., and Lee, E.Y. (1987). Human retinoblastoma susceptibility gene: cloning, identification, and sequence. Science *235*, 1394-1399.

Leung, A.Y., Chan, M.T., Yuen, K.Y., Cheng, V.C., Chan, K.H., Wong, C.L., Liang, R., Lie, A.K., and Kwong, Y.L. (2005). Ciprofloxacin decreased polyoma BK virus load in patients who underwent allogeneic hematopoietic stem cell transplantation. Clin Infect Dis *40*, 528-537.

Levine, A.J. (2009). The common mechanisms of transformation by the small DNA tumor viruses: The inactivation of tumor suppressor gene products: p53. Virology *384*, 285-293.

Li, D., Zhao, R., Lilyestrom, W., Gai, D., Zhang, R., DeCaprio, J.A., Fanning, E., Jochimiak, A., Szakonyi, G., and Chen, X.S. (2003). Structure of the replicative helicase of the oncoprotein SV40 large tumour antigen. Nature *423*, 512-518.

Li, J.J., and Kelly, T.J. (1984). Simian virus 40 DNA replication in vitro. Proc Natl Acad Sci U S A *81*, 6973-6977.

Li, M., Smith, C.J., Walker, M.T., and Smith, T.J. (2009). Novel inhibitors complexed with glutamate dehydrogenase: allosteric regulation by control of protein dynamics. J Biol Chem *284*, 22988-23000.

Liang, H., Wu, X., Yalowich, J.C., and Hasinoff, B.B. (2008). A three-dimensional quantitative structure-activity analysis of a new class of bisphenol topoisomerase IIalpha inhibitors. Mol Pharmacol *73*, 686-696.

Liberek, K., Marszalek, J., Ang, D., Georgopoulos, C., and Zylicz, M. (1991). Escherichia coli DnaJ and GrpE heat shock proteins jointly stimulate ATPase activity of DnaK. Proc Natl Acad Sci U S A *88*, 2874-2878.

Liddington, R.C., Yan, Y., Moulai, J., Sahli, R., Benjamin, T.L., and Harrison, S.C. (1991). Structure of simian virus 40 at 3.8-A resolution. Nature *354*, 278-284.

Lill, N.L., Tevethia, M.J., Eckner, R., Livingston, D.M., and Modjtahedi, N. (1997). p300 family members associate with the carboxyl terminus of simian virus 40 large tumor antigen. J Virol *71*, 129-137.

Lilyestrom, W., Klein, M.G., Zhang, R., Joachimiak, A., and Chen, X.S. (2006). Crystal structure of SV40 large T-antigen bound to p53: interplay between a viral oncoprotein and a cellular tumor suppressor. Genes Dev *20*, 2373-2382.

Lin, H.J., Upson, R.H., and Simmons, D.T. (1992). Nonspecific DNA binding activity of simian virus 40 large T antigen: evidence for the cooperation of two regions for full activity. J Virol *66*, 5443-5452.

Linzer, D.I., and Levine, A.J. (1979). Characterization of a 54K dalton cellular SV40 tumor antigen present in SV40-transformed cells and uninfected embryonal carcinoma cells. Cell *17*, 43-52.

Liu, X., Hein, J., Richardson, S.C., Basse, P.H., Toptan, T., Moore, P.S., Gjoerup, O.V., and Chang, Y. (2011a). Merkel cell polyomavirus large T antigen disrupts lysosome clustering by translocating human Vam6p from the cytoplasm to the nucleus. J Biol Chem *286*, 17079-17090.

Liu, X., Hein, J., Richardson, S.C., Basse, P.H., Toptan, T., Moore, P.S., Gjoerup, O.V., and Chang, Y. (2011b). Merkel cell polyomavirus large T antigen disrupts lysosome clustering by translocating human VAM6P to the nucleus. J Biol Chem.

Low, J., Humes, H.D., Szczypka, M., and Imperiale, M. (2004). BKV and SV40 infection of human kidney tubular epithelial cells in vitro. Virology *323*, 182-188.

Low, J.A., Magnuson, B., Tsai, B., and Imperiale, M.J. (2006). Identification of gangliosides GD1b and GT1b as receptors for BK virus. J Virol *80*, 1361-1366.

Lowe, D.B., Shearer, M.H., Aldrich, J.F., Winn, R.E., Jumper, C.A., and Kennedy, R.C. (2010). Role of the innate immune response and tumor immunity associated with simian virus 40 large tumor antigen. J Virol *84*, 10121-10130.

Luo, C., Bueno, M., Kant, J., Martinson, J., and Randhawa, P. (2009). Genotyping schemes for polyomavirus BK, using gene-specific phylogenetic trees and single nucleotide polymorphism analysis. J Virol *83*, 2285-2297.

Luo, X., Sanford, D.G., Bullock, P.A., and Bachovchin, W.W. (1996). Solution structure of the origin DNA-binding domain of SV40 T-antigen. Nat Struct Biol *3*, 1034-1039.

Macpherson, I., and Montagnier, L. (1964). Agar Suspension Culture for the Selective Assay of Cells Transformed by Polyoma Virus. Virology *23*, 291-294.

Magnuson, B., Rainey, E.K., Benjamin, T., Baryshev, M., Mkrtchian, S., and Tsai, B. (2005). ERp29 triggers a conformational change in polyomavirus to stimulate membrane binding. Mol Cell *20*, 289-300.

Mansilla-Soto, J., Yoon-Robarts, M., Rice, W.J., Arya, S., Escalante, C.R., and Linden, R.M. (2009). DNA structure modulates the oligomerization properties of the AAV initiator protein Rep68. PLoS Pathog *5*, e1000513.

Martin, R.G., and Chou, J.Y. (1975). Simian virus 40 functions required for the establishment and maintenance of malignant transformation. J Virol *15*, 599-612.

Marzocchetti, A., Tompkins, T., Clifford, D.B., Gandhi, R.T., Kesari, S., Berger, J.R., Simpson, D.M., Prosperi, M., De Luca, A., and Koralnik, I.J. (2009). Determinants of survival in progressive multifocal leukoencephalopathy. Neurology *73*, 1551-1558.

Mastrangelo, I.A., Hough, P.V., Wall, J.S., Dodson, M., Dean, F.B., and Hurwitz, J. (1989). ATP-dependent assembly of double hexamers of SV40 T antigen at the viral origin of DNA replication. Nature *338*, 658-662.

Maxwell, S.A., Ames, S.K., Sawai, E.T., Decker, G.L., Cook, R.G., and Butel, J.S. (1991). Simian virus 40 large T antigen and p53 are microtubule-associated proteins in transformed cells. Cell Growth Differ *2*, 115-127.

Mayer, M.P., and Bukau, B. (2005). Hsp70 chaperones: cellular functions and molecular mechanism. Cell Mol Life Sci *62*, 670-684.

Mazzarelli, J.M., Atkins, G.B., Geisberg, J.V., and Ricciardi, R.P. (1995). The viral oncoproteins Ad5 E1A, HPV16 E7 and SV40 TAg bind a common region of the TBP-associated factor-110. Oncogene *11*, 1859-1864.

McVey, D., Brizuela, L., Mohr, I., Marshak, D.R., Gluzman, Y., and Beach, D. (1989). Phosphorylation of large tumour antigen by cdc2 stimulates SV40 DNA replication. Nature *341*, 503-507.

Meinke, G., Bullock, P.A., and Bohm, A. (2006). Crystal structure of the simian virus 40 large T-antigen origin-binding domain. J Virol *80*, 4304-4312.

Meinke, G., Phelan, P.J., Fradet-Turcotte, A., Bohm, A., Archambault, J., and Bullock, P.A. (2011). Structure-based analysis of the interaction between the simian virus 40 T-antigen origin binding domain and single-stranded DNA. J Virol *85*, 818-827.

Melendy, T., and Stillman, B. (1993). An interaction between replication protein A and SV40 T antigen appears essential for primosome assembly during SV40 DNA replication. J Biol Chem *268*, 3389-3395.

Mercer, W.E., Nelson, D., Hyland, J.K., Croce, C.M., and Baserga, R. (1983). Inhibition of SV40-induced cellular DNA synthesis by microinjection of monoclonal antibodies. Virology *127*, 149-158.

Miller, S.C., Huang, R., Sakamuru, S., Shukla, S.J., Attene-Ramos, M.S., Shinn, P., Van Leer, D., Leister, W., Austin, C.P., and Xia, M. (2010). Identification of known drugs that act as inhibitors of NF-kappaB signaling and their mechanism of action. Biochem Pharmacol *79*, 1272-1280.

Min, H.J., Cho, I.R., Srisuttee, R., Park, E.H., Cho, D.H., Ahn, J.H., Lee, I.S., Johnston, R.N., Oh, S., and Chung, Y.H. (2009). Hexachlorophene suppresses beta-catenin expression by up-regulation of Siah-1 in EBV-infected B lymphoma cells. Cancer Lett *276*, 136-142.

Minguez, J.M., Kim, S.Y., Giuliano, K.A., Balachandran, R., Madiraju, C., Day, B.W., and Curran, D.P. (2003). Synthesis and biological assessment of simplified analogues of the potent microtubule stabilizer (+)-discodermolide. Bioorg Med Chem *11*, 3335-3357.

Mitchell, P.J., Wang, C., and Tjian, R. (1987). Positive and negative regulation of transcription in vitro: enhancer-binding protein AP-2 is inhibited by SV40 T antigen. Cell *50*, 847-861.

Miyata, Y., Chang, L., Bainor, A., McQuade, T.J., Walczak, C.P., Zhang, Y., Larsen, M.J., Kirchhoff, P., and Gestwicki, J.E. (2010). High-throughput screen for Escherichia coli heat shock protein 70 (Hsp70/DnaK): ATPase assay in low volume by exploiting energy transfer. J Biomol Screen *15*, 1211-1219.

Mogensen, T.H. (2009). Pathogen recognition and inflammatory signaling in innate immune defenses. Clin Microbiol Rev *22*, 240-273, Table of Contents.

Monaco, M.C., Jensen, P.N., Hou, J., Durham, L.C., and Major, E.O. (1998). Detection of JC virus DNA in human tonsil tissue: evidence for site of initial viral infection. J Virol *72*, 9918-9923.

Montagnier, L. (2008). Luc Montagnier - Autobiography. In The Nobel Lectures, K. Grandin, ed. (Stockholm, The Nobel Foundation).

Montenarh, M., and Henning, R. (1982). The binding of simian virus 40 large T antigen to the polyphosphate backbone of nucleic acids. Biochim Biophys Acta *697*, 322-329.

Mukherjee, S., Kler, S., Oppenheim, A., and Zlotnick, A. (2010). Uncatalyzed assembly of spherical particles from SV40 VP1 pentamers and linear dsDNA incorporates both low and high cooperativity elements. Virology *397*, 199-204.

Muller, H., and Nitschke, R. (1986). A polyoma-like virus associated with an acute disease of fledgling budgerigars (Melopsittacus undulatus). Med Microbiol Immunol *175*, 1-13.

Murakami, Y., Wobbe, C.R., Weissbach, L., Dean, F.B., and Hurwitz, J. (1986). Role of DNA polymerase alpha and DNA primase in simian virus 40 DNA replication in vitro. Proc Natl Acad Sci U S A *83*, 2869-2873.

Murata, H., Peden, K., and Lewis, A.M., Jr. (2008). Identification of a mutation in the SV40 capsid protein VP1 that influences plaque morphology, vacuolization, and receptor usage. Virology *370*, 343-351.

Murata, H., Teferedegne, B., Lewis, A.M., Jr., and Peden, K. (2009). A quantitative PCR assay for SV40 neutralization adaptable for high-throughput applications. J Virol Methods *162*, 236-244.

Myers, R.M., Kligman, M., and Tjian, R. (1981). Does simian virus 40 T antigen unwind DNA? J Biol Chem *256*, 10156-10160.

Nathans, D. (1978). Daniel Nathans - Autobiography. In The Nobel Lectures, W. Odelberg, ed. (Stockholm, The Nobel Foundation).

Neske, F., Blessing, K., Prottel, A., Ullrich, F., Kreth, H.W., and Weissbrich, B. (2009). Detection of WU polyomavirus DNA by real-time PCR in nasopharyngeal aspirates, serum, and stool samples. J Clin Virol *44*, 115-118.

Neu, U., Stehle, T., and Atwood, W.J. (2009). The Polyomaviridae: Contributions of virus structure to our understanding of virus receptors and infectious entry. Virology *384*, 389-399.

Neuwald, A.F., Aravind, L., Spouge, J.L., and Koonin, E.V. (1999). AAA+: A class of chaperone-like ATPases associated with the assembly, operation, and disassembly of protein complexes. Genome Res *9*, 27-43.

Nickeleit, V., Hirsch, H.H., Binet, I.F., Gudat, F., Prince, O., Dalquen, P., Thiel, G., and Mihatsch, M.J. (1999). Polyomavirus infection of renal allograft recipients: from latent infection to manifest disease. J Am Soc Nephrol *10*, 1080-1089.

Noah, J.W., Severson, W., Noah, D.L., Rasmussen, L., White, E.L., and Jonsson, C.B. (2007). A cell-based luminescence assay is effective for high-throughput screening of potential influenza antivirals. Antiviral Res *73*, 50-59.

Norkin, L.C., and Kuksin, D. (2005). The caveolae-mediated sv40 entry pathway bypasses the golgi complex en route to the endoplasmic reticulum. Virol J *2*, 38.

Oda, K., and Dulbecco, R. (1968a). Induction of cellular mRNA synthesis in BSC-1 cells infected by SV40. Virology *35*, 439-444.

Oda, K., and Dulbecco, R. (1968b). Regulation of transcription of the SV40 DNA in productively infected and in transformed cells. Proc Natl Acad Sci U S A *60*, 525-532.

OPTN (2009). Annual Report of the U.S. Organ Procurement and Transplantation Network and the Scientific Registry of Transplant Recipients: Transplant Data 2000-2009 (United Network for Organ Sharing, Richmond, VA; University Renal Research and Education Association, Ann Arbor, MI).

Osborn, M., and Weber, K. (1975). Simian virus 40 gene A function and maintenance of transformation. J Virol *15*, 636-644.

Oudet, P., Gross-Bellard, M., and Chambon, P. (1975). Electron microscopic and biochemical evidence that chromatin structure is a repeating unit. Cell *4*, 281-300.

Padgett, B.L., Rogers, C.M., and Walker, D.L. (1977). JC virus, a human polyomavirus associated with progressive multifocal leukoencephalopathy: additional biological characteristics and antigenic relationships. Infect Immun *15*, 656-662.

Padgett, B.L., Walker, D.L., ZuRhein, G.M., Eckroade, R.J., and Dessel, B.H. (1971). Cultivation of papova-like virus from human brain with progressive multifocal leucoencephalopathy. Lancet *1*, 1257-1260.

Pallas, D.C., Shahrik, L.K., Martin, B.L., Jaspers, S., Miller, T.B., Brautigan, D.L., and Roberts, T.M. (1990). Polyoma small and middle T antigens and SV40 small t antigen form stable complexes with protein phosphatase 2A. Cell *60*, 167-176.

Parada, L.F., Land, H., Weinberg, R.A., Wolf, D., and Rotter, V. (1984). Cooperation between gene encoding p53 tumour antigen and ras in cellular transformation. Nature *312*, 649-651.

Pastrana, D.V., Tolstov, Y.L., Becker, J.C., Moore, P.S., Chang, Y., and Buck, C.B. (2009). Quantitation of human seroresponsiveness to Merkel cell polyomavirus. PLoS Pathog *5*, e1000578.

Peden, K.W., and Pipas, J.M. (1985). Site-directed mutagenesis of the simian virus 40 large T-antigen gene: replication-defective amino acid substitution mutants that retain the ability to induce morphological transformation. J Virol *55*, 1-9.

Peden, K.W., and Pipas, J.M. (1992). Simian virus 40 mutants with amino-acid substitutions near the amino terminus of large T antigen. Virus Genes *6*, 107-118.

Peden, K.W., Pipas, J.M., Pearson-White, S., and Nathans, D. (1980). Isolation of mutants of an animal virus in bacteria. Science *209*, 1392-1396.

Peinemann, F., de Villiers, E.M., Dorries, K., Adams, O., Vogeli, T.A., and Burdach, S. (2000). Clinical course and treatment of haemorrhagic cystitis associated with BK type of human polyomavirus in nine paediatric recipients of allogeneic bone marrow transplants. Eur J Pediatr *159*, 182-188.

Pelkmans, L., Kartenbeck, J., and Helenius, A. (2001). Caveolar endocytosis of simian virus 40 reveals a new two-step vesicular-transport pathway to the ER. Nat Cell Biol *3*, 473-483.

Pellikainen, J.M., and Kosma, V.M. (2007). Activator protein-2 in carcinogenesis with a special reference to breast cancer--a mini review. Int J Cancer *120*, 2061-2067.

Pennica, D., Goeddel, D.V., Hayflick, J.S., Reich, N.C., Anderson, C.W., and Levine, A.J. (1984). The amino acid sequence of murine p53 determined from a c-DNA clone. Virology *134*, 477-482.

Pershouse, M.A., Heivly, S., and Girtsman, T. (2006). The role of SV40 in malignant mesothelioma and other human malignancies. Inhal Toxicol *18*, 995-1000.

Persico-DiLauro, M., Martin, R.G., and Livingston, D.M. (1977). Interaction of Simian Virus 40 chromatin with Simian Virus 40 T-antigen. J Virol *24*, 451-460.

Pho, M.T., Ashok, A., and Atwood, W.J. (2000). JC virus enters human glial cells by clathrin-dependent receptor-mediated endocytosis. J Virol *74*, 2288-2292.

Pieper, A.A., Verma, A., Zhang, J., and Snyder, S.H. (1999). Poly (ADP-ribose) polymerase, nitric oxide and cell death. Trends Pharmacol Sci *20*, 171-181.

Pipas, J.M. (1985). Mutations near the carboxyl terminus of the simian virus 40 large tumor antigen alter viral host range. J Virol *54*, 569-575.

Pipas, J.M. (1992). Common and unique features of T antigens encoded by the polyomavirus group. J Virol *66*, 3979-3985.

Pipas, J.M. (2009). SV40: Cell transformation and tumorigenesis. Virology *384*, 294-303.

Pipas, J.M., Peden, K.W., and Nathans, D. (1983). Mutational analysis of simian virus 40 T antigen: isolation and characterization of mutants with deletions in the T-antigen gene. Mol Cell Biol *3*, 203-213.

Ponten, J., Jensen, F., and Koprowski, H. (1963). Morphological and virological investigation of human tissue cultures transformed with SV40. J Cell Comp Physiol *61*, 145-163.

Poulin, D.L., and DeCaprio, J.A. (2006). The carboxyl-terminal domain of large T antigen rescues SV40 host range activity in trans independent of acetylation. Virology *349*, 212-221.

Poulin, D.L., Kung, A.L., and DeCaprio, J.A. (2004). p53 targets simian virus 40 large T antigen for acetylation by CBP. J Virol *78*, 8245-8253.

Powell, H.C., and Lampert, P.W. (1973). Bithionol: a possible substitute for hexachlorophene. Pediatrics *52*, 859-861.

Prelich, G., Kostura, M., Marshak, D.R., Mathews, M.B., and Stillman, B. (1987). The cell-cycle regulated proliferating cell nuclear antigen is required for SV40 DNA replication in vitro. Nature *326*, 471-475.

Price, T.A., Tuazon, C.U., and Simon, G.L. (1993). Fascioliasis: case reports and review. Clin Infect Dis *17*, 426-430.

Provost, P.J., and Hilleman, M.R. (1979). Propagation of human hepatitis A virus in cell culture in vitro. Proc Soc Exp Biol Med *160*, 213-221.

Rabson, A.S., and Kirschstein, R.L. (1962). Induction of malignancy in vitro in newborn hamster kidney tissue infected with simian vacuolating virus (SV40). Proc Soc Exp Biol Med *111*, 323-328.

Randhawa, P., Shapiro, R., and Vats, A. (2005a). Quantitation of DNA of polyomaviruses BK and JC in human kidneys. J Infect Dis *192*, 504-509.

Randhawa, P., Vats, A., and Shapiro, R. (2005b). Monitoring for polyomavirus BK And JC in urine: comparison of quantitative polymerase chain reaction with urine cytology. Transplantation *79*, 984-986.

Randhawa, P.S. (2005). Anti-BK virus activity of ciprofloxacin and related antibiotics. Clin Infect Dis *41*, 1366-1367.

Rathi, A.V., Cantalupo, P.G., Sarkar, S.N., and Pipas, J.M. (2010). Induction of interferon-stimulated genes by Simian virus 40 T antigens. Virology *406*, 202-211.

Rathi, A.V., Saenz Robles, M.T., Cantalupo, P.G., Whitehead, R.H., and Pipas, J.M. (2009). Simian virus 40 T-antigen-mediated gene regulation in enterocytes is controlled primarily by the Rb-E2F pathway. J Virol *83*, 9521-9531.

Rathi, A.V., Saenz Robles, M.T., and Pipas, J.M. (2007). Enterocyte proliferation and intestinal hyperplasia induced by simian virus 40 T antigen require a functional J domain. J Virol *81*, 9481-9489.

Reddy, V.B., Thimmappaya, B., Dhar, R., Subramanian, K.N., Zain, B.S., Pan, J., Ghosh, P.K., Celma, M.L., and Weissman, S.M. (1978). The genome of simian virus 40. Science *200*, 494-502.

Richter, C.A., Birnbaum, L.S., Farabollini, F., Newbold, R.R., Rubin, B.S., Talsness, C.E., Vandenbergh, J.G., Walser-Kuntz, D.R., and vom Saal, F.S. (2007). In vivo effects of bisphenol A in laboratory rodent studies. Reprod Toxicol *24*, 199-224.

Rigby, P.W., and Berg, P. (1978). Does simian virus 40 DNA integrate into cellular DNA during productive infection? J Virol *28*, 475-489.

Ritchie, B.W., Latimer, K.S., Leonard, J., Pesti, D., Campagnoli, R., and Lukert, P.D. (1998a). Safety, immunogenicity, and efficacy of an inactivated avian polyomavirus vaccine. Am J Vet Res *59*, 143-148.

Ritchie, B.W., Vaughn, S.B., Leger, J.S., Rich, G.A., Rupiper, D.J., Forgey, G., Greenacre, C.B., Latimer, K.S., Pesti, D., Campagnoli, R., *et al.* (1998b). Use of an inactivated virus vaccine to control polyomavirus outbreaks in nine flocks of psittacine birds. J Am Vet Med Assoc *212*, 685-690.

Rohaly, G., Korf, K., Dehde, S., and Dornreiter, I. (2010). Simian virus 40 activates ATR-Delta p53 signaling to override cell cycle and DNA replication control. J Virol *84*, 10727-10747.

Roy, R., Trowbridge, P., Yang, Z., Champoux, J.J., and Simmons, D.T. (2003). The cap region of topoisomerase I binds to sites near both ends of simian virus 40 T antigen. J Virol *77*, 9809-9816.

Rubin, B.S. (2011). Bisphenol A: An endocrine disruptor with widespread exposure and multiple effects. J Steroid Biochem Mol Biol.

Rundell, K., Collins, J.K., Tegtmeyer, P., Ozer, H.L., Lai, C.J., and Nathans, D. (1977). Identification of simian virus 40 protein A. J Virol *21*, 636-646.

Russell, J.K., and Blalock, J.E. (1984). Vitamin A inhibition of polyoma virus replication. Biochem Biophys Res Commun *122*, 851-858.

Sablina, A.A., and Hahn, W.C. (2008). SV40 small T antigen and PP2A phosphatase in cell transformation. Cancer Metastasis Rev *27*, 137-146.

Saenz-Robles, M.T., Markovics, J.A., Chong, J.L., Opavsky, R., Whitehead, R.H., Leone, G., and Pipas, J.M. (2007). Intestinal hyperplasia induced by simian virus 40 large tumor antigen requires E2F2. J Virol *81*, 13191-13199.

Safak, M., and Khalili, K. (2003). An overview: Human polyomavirus JC virus and its associated disorders. J Neurovirol *9 Suppl 1*, 3-9.

Sawai, E.T., and Butel, J.S. (1989). Association of a cellular heat shock protein with simian virus 40 large T antigen in transformed cells. J Virol *63*, 3961-3973.

Sawai, E.T., Rasmussen, G., and Butel, J.S. (1994). Construction of SV40 deletion mutants and delimitation of the binding domain for heat shock protein to the amino terminus of large T-antigen. Virus Res *31*, 367-378.

Schaffhausen, B.S., and Roberts, T.M. (2009). Lessons from polyoma middle T antigen on signaling and transformation: A DNA tumor virus contribution to the war on cancer. Virology *384*, 304-316.

Scheidtmann, K.H., Buck, M., Schneider, J., Kalderon, D., Fanning, E., and Smith, A.E. (1991). Biochemical characterization of phosphorylation site mutants of simian virus 40 large T antigen: evidence for interaction between amino- and carboxy-terminal domains. J Virol *65*, 1479-1490.

Scheidtmann, K.H., Echle, B., and Walter, G. (1982). Simian virus 40 large T antigen is phosphorylated at multiple sites clustered in two separate regions. J Virol *44*, 116-133.

Schelhaas, M., Malstrom, J., Pelkmans, L., Haugstetter, J., Ellgaard, L., Grunewald, K., and Helenius, A. (2007). Simian Virus 40 Depends on ER Protein Folding and Quality Control Factors for Entry into Host Cells. Cell *131*, 516-529.

Schowalter, R.M., Pastrana, D.V., Pumphrey, K.A., Moyer, A.L., and Buck, C.B. (2010). Merkel cell polyomavirus and two previously unknown polyomaviruses are chronically shed from human skin. Cell Host Microbe *7*, 509-515.

Scott, W.A., Brockman, W.W., and Nathans, D. (1976). Biological activities of deletion mutants of simian virus 40. Virology *75*, 319-334.

Scuda, N., Hofmann, J., Calvignac-Spencer, S., Ruprecht, K., Liman, P., Kuhn, J., Hengel, H., and Ehlers, B. (2011). A novel human polyomavirus closely related to the African green monkey-derived lymphotropic polyomavirus (LPV). J Virol.

Seber, A., Shu, X.O., Defor, T., Sencer, S., and Ramsay, N. (1999). Risk factors for severe hemorrhagic cystitis following BMT. Bone Marrow Transplant *23*, 35-40.

Segel, I.H. (1976). Biochemical calculations : how to solve mathematical problems in general biochemistry, 2d edn (New York, Wiley).

Sencer, S.F., Haake, R.J., and Weisdorf, D.J. (1993). Hemorrhagic cystitis after bone marrow transplantation. Risk factors and complications. Transplantation *56*, 875-879.

Seo, B.S., Lee, S.H., Hong, S.T., Hong, S.J., Kim, C.Y., and Lee, H.Y. (1982). Studies On Intestinal Trematodes In Korea: V. A Human Case Infected By Fibricola Seoulensis (Trematoda: Diplostomatidae). Korean Journal of Parasitology *20*, 93-99.

Sever, J.L. (1962). Application of a microtechnique to viral serological investigations. J Immunol *88*, 320-329.

Shah, K.V. (1996). Polyomaviruses. In Fields Virology, B.N. Fields, D.M. Knipe, and P.M. Howley, eds. (Philadelphia, Lippincott - Raven Publishers).

Sharma, P.M., Gupta, G., Vats, A., Shapiro, R., and Randhawa, P.S. (2007). Polyomavirus BK non-coding control region rearrangements in health and disease. J Med Virol *79*, 1199-1207.

Sharp, C.P., Norja, P., Anthony, I., Bell, J.E., and Simmonds, P. (2009). Reactivation and Mutation of Newly Discovered WU, KI, and Merkel Cell Carcinoma Polyomaviruses in Immunosuppressed Individuals. J Infect Dis *199*, 398-404.

Sharpe, R.M. (2010). Is it time to end concerns over the estrogenic effects of bisphenol A? Toxicol Sci *114*, 1-4.

Shein, H.M., and Enders, J.F. (1962). Transformation induced by simian virus 40 in human renal cell cultures. I. Morphology and growth characteristics. Proc Natl Acad Sci U S A *48*, 1164-1172.

Shein, H.M., Enders, J.F., and Levinthal, J.D. (1962). Transformation induced by simian virus 40 in human renal cell cultures. II. Cell-virus relationships. Proc Natl Acad Sci U S A *48*, 1350-1357.

Shein, H.M., Enders, J.F., Levinthal, J.D., and Burket, A.E. (1963). Transformation induced by simian virus 40 in newborn Syrian hamster renal cell cultures. Proc Natl Acad Sci U S A *49*, 28-34.

Shi, Y., Dodson, G.E., Shaikh, S., Rundell, K., and Tibbetts, R.S. (2005). Ataxia-telangiectasia-mutated (ATM) is a T-antigen kinase that controls SV40 viral replication in vivo. J Biol Chem *280*, 40195-40200.

Shimazu, T., Komatsu, Y., Nakayama, K.I., Fukazawa, H., Horinouchi, S., and Yoshida, M. (2006). Regulation of SV40 large T-antigen stability by reversible acetylation. Oncogene *25*, 7391-7400.

Shivapurkar, N., Wiethege, T., Wistuba, II, Milchgrub, S., Muller, K.M., and Gazdar, A.F. (2000). Presence of simian virus 40 sequences in malignant pleural, peritoneal and noninvasive mesotheliomas. Int J Cancer *85*, 743-745.

Shivapurkar, N., Wiethege, T., Wistuba, II, Salomon, E., Milchgrub, S., Muller, K.M., Churg, A., Pass, H., and Gazdar, A.F. (1999). Presence of simian virus 40 sequences in malignant mesotheliomas and mesothelial cell proliferations. J Cell Biochem *76*, 181-188.

Shortle, D., and Nathans, D. (1978). Local mutagenesis: a method for generating viral mutants with base substitutions in preselected regions of the viral genome. Proc Natl Acad Sci U S A *75*, 2170-2174.

Shortle, D., and Nathans, D. (1979). Regulatory mutants of simian virus 40: constructed mutants with base substitutions at the origin of DNA replication. J Mol Biol *131*, 801-817.

Shuda, M., Arora, R., Kwun, H.J., Feng, H., Sarid, R., Fernandez-Figueras, M.T., Tolstov, Y., Gjoerup, O., Mansukhani, M.M., Swerdlow, S.H., *et al.* (2009). Human Merkel cell polyomavirus infection I. MCV T antigen expression in Merkel cell carcinoma, lymphoid tissues and lymphoid tumors. Int J Cancer *125*, 1243-1249.

Shuda, M., Feng, H., Kwun, H.J., Rosen, S.T., Gjoerup, O., Moore, P.S., and Chang, Y. (2008). T antigen mutations are a human tumor-specific signature for Merkel cell polyomavirus. Proc Natl Acad Sci U S A *105*, 16272-16277.

Simmons, D.T. (2000). SV40 large T antigen functions in DNA replication and transformation. Adv Virus Res *55*, 75-134.

Simmons, D.T., Chang, C., and Martin, M.A. (1979). Multiple forms of polyoma virus tumor antigens from infected and transformed cells. J Virol *29*, 881-887.

Smith, A.E., Kalderon, D., Roberts, B.L., Colledge, W.H., Edge, M., Gillett, P., Markham, A., Paucha, E., and Richardson, W.D. (1985). The nuclear location signal. Proc R Soc Lond B Biol Sci *226*, 43-58.

Smith, H.S., Scher, C.D., and Todaro, G.J. (1971). Induction of cell division in medium lacking serum growth factor by SV40. Virology *44*, 359-370.

Snider, J., Thibault, G., and Houry, W.A. (2008). The AAA+ superfamily of functionally diverse proteins. Genome Biol *9*, 216.

So, A.G., and Downey, K.M. (1988). Mammalian DNA polymerases alpha and delta: current status in DNA replication. Biochemistry *27*, 4591-4595.

Sontag, E., Fedorov, S., Kamibayashi, C., Robbins, D., Cobb, M., and Mumby, M. (1993). The interaction of SV40 small tumor antigen with protein phosphatase 2A stimulates the map kinase pathway and induces cell proliferation. Cell *75*, 887-897.

Soussi, T. (1986). DNA-binding properties of the major structural protein of simian virus 40. J Virol *59*, 740-742.

Spence, S.L., and Pipas, J.M. (1994). Simian virus 40 large T antigen host range domain functions in virion assembly. J Virol *68*, 4227-4240.

Srinivasan, A., McClellan, A.J., Vartikar, J., Marks, I., Cantalupo, P., Li, Y., Whyte, P., Rundell, K., Brodsky, J.L., and Pipas, J.M. (1997). The amino-terminal transforming

region of simian virus 40 large T and small t antigens functions as a J domain. Mol Cell Biol *17*, 4761-4773.

Stahl, H., Droge, P., and Knippers, R. (1986). DNA helicase activity of SV40 large tumor antigen. EMBO J *5*, 1939-1944.

Stahl, H., Droge, P., Zentgraf, H., and Knippers, R. (1985). A large-tumor-antigen-specific monoclonal antibody inhibits DNA replication of simian virus 40 minichromosomes in an in vitro elongation system. J Virol *54*, 473-482.

Stahl, H., and Knippers, R. (1983). Simian virus 40 large tumor antigen on replicating viral chromatin: tight binding and localization on the viral genome. J Virol *47*, 65-76.

Stehle, T., Gamblin, S.J., Yan, Y., and Harrison, S.C. (1996). The structure of simian virus 40 refined at 3.1 A resolution. Structure *4*, 165-182.

Stehle, T., Yan, Y., Benjamin, T.L., and Harrison, S.C. (1994). Structure of murine polyomavirus complexed with an oligosaccharide receptor fragment. Nature *369*, 160-163.

Stewart, S.E., Eddy, B.E., and Borgese, N. (1958). Neoplasms in mice inoculated with a tumor agent carried in tissue culture. J Natl Cancer Inst *20*, 1223-1243.

Stoner, G.L., Alappan, R., Jobes, D.V., Ryschkewitsch, C.F., and Landry, M.L. (2002). BK virus regulatory region rearrangements in brain and cerebrospinal fluid from a leukemia patient with tubulointerstitial nephritis and meningoencephalitis. Am J Kidney Dis *39*, 1102-1112.

Stratton, K., Almario, D.A., and McCormick, M.C. (2003). Immunization Safety Review: SV40 Contamination of Polio Vaccine and Cancer (Washington D.C., The National Academies Press).

Subramanian, K.N. (1982). Effect of in vitro methylation at CpG sites on gene expression in a genome functioning autonomously in a vertebrate host. Nucleic Acids Res *10*, 3475-3486.

Sullivan, C.S., Baker, A.E., and Pipas, J.M. (2004). Simian virus 40 infection disrupts p130-E2F and p107-E2F complexes but does not perturb pRb-E2F complexes. Virology *320*, 218-228.

Sullivan, C.S., Cantalupo, P., and Pipas, J.M. (2000). The molecular chaperone activity of simian virus 40 large T antigen is required to disrupt Rb-E2F family complexes by an ATP-dependent mechanism. Mol Cell Biol *20*, 6233-6243.

Sullivan, C.S., Grundhoff, A.T., Tevethia, S., Pipas, J.M., and Ganem, D. (2005). SV40-encoded microRNAs regulate viral gene expression and reduce susceptibility to cytotoxic T cells. Nature *435*, 682-686.

Sweet, B.H., and Hilleman, M.R. (1960). The vacuolating virus, S.V. 40. Proc Soc Exp Biol Med *105*, 420-427.

Takemoto, K.K., and Segawa, K. (1983). A new monkey lymphotropic papovavirus: characterization of the virus and evidence of a related virus in humans. Prog Clin Biol Res *105*, 87-96.

Takeuchi, T., Kobayashi, S., Tanabe, M., and Fujiwara, T. (1985). In vitro inhibition of Giardia lamblia and Trichomonas vaginalis growth by bithionol, dichlorophene, and hexachlorophene. Antimicrob Agents Chemother *27*, 65-70.

Talos, F., and Moll, U.M. (2010). Role of the p53 family in stabilizing the genome and preventing polyploidization. Adv Exp Med Biol *676*, 73-91.

Tan, C.S., and Koralnik, I.J. (2010). Progressive multifocal leukoencephalopathy and other disorders caused by JC virus: clinical features and pathogenesis. Lancet Neurol *9*, 425-437.

Tan, Y., Sangfelt, O., and Spruck, C. (2008). The Fbxw7/hCdc4 tumor suppressor in human cancer. Cancer Lett *271*, 1-12.

Tanaka, Y., Yoshihara, K., Tohno, Y., Kojima, K., Kameoka, M., and Kamiya, T. (1995). Inhibition and down-regulation of poly(ADP-ribose) polymerase results in a marked resistance of HL-60 cells to various apoptosis-inducers. Cell Mol Biol (Noisy-le-grand) *41*, 771-781.

Tegtmeyer, P. (1972). Simian virus 40 deoxyribonucleic acid synthesis: the viral replicon. J Virol *10*, 591-598.

Tegtmeyer, P., Lewton, B.A., DeLucia, A.L., Wilson, V.G., and Ryder, K. (1983). Topography of simian virus 40 A protein-DNA complexes: arrangement of protein bound to the origin of replication. J Virol *46*, 151-161.

Tei, S., Saitoh, N., Funahara, T., Iida, S., Nakatsu, Y., Kinoshita, K., Kinoshita, Y., Saya, H., and Nakao, M. (2009). Simian virus 40 large T antigen targets the microtubule-stabilizing protein TACC2. J Cell Sci *122*, 3190-3198.

Templeton, D., and Eckhart, W. (1984). Characterization of viable mutants of polyomavirus cold sensitive for maintenance of cell transformation. J Virol *49*, 799-805.

Testa, J.R., and Giordano, A. (2001). SV40 and cell cycle perturbations in malignant mesothelioma. Semin Cancer Biol *11*, 31-38.

Todaro, G.J., and Green, H. (1964). An assay for cellular transformation by SV40. Virology *23*, 117-119.

Todaro, G.J., and Green, H. (1966). High frequency of SV40 transformation of mouse cell line 3T3. Virology *28*, 756-759.

Todaro, G.J., Green, H., and Swift, M.R. (1966). Susceptibility of human diploid fibroblast strains to transformation by SV40 virus. Science *153*, 1252-1254.

Tonegawa, S. (1987). Susumu Tonegawa - Autobiography. In The Nobel Prizes 1987, W. Odelberg, ed. (Stockholm, The Nobel Foundation).

Tornow, J., and Cole, C.N. (1983a). Intracistronic complementation in the simian virus 40 A gene. Proc Natl Acad Sci U S A *80*, 6312-6316.

Tornow, J., and Cole, C.N. (1983b). Nonviable mutants of simian virus 40 with deletions near the 3' end of gene A define a function for large T antigen required after onset of viral DNA replication. J Virol *47*, 487-494.

Trowbridge, P.W., and Frisque, R.J. (1995). Identification of three new JC virus proteins generated by alternative splicing of the early viral mRNA. J Neurovirol *1*, 195-206.

Tsai, B., Gilbert, J.M., Stehle, T., Lencer, W., Benjamin, T.L., and Rapoport, T.A. (2003). Gangliosides are receptors for murine polyoma virus and SV40. EMBO J *22*, 4346-4355.

Tsukamoto, H., Kawano, M.A., Inoue, T., Enomoto, T., Takahashi, R.U., Yokoyama, N., Yamamoto, N., Imai, T., Kataoka, K., Yamaguchi, Y., *et al.* (2007). Evidence that SV40 VP1-DNA interactions contribute to the assembly of 40-nm spherical viral particles. Genes Cells *12*, 1267-1279.

Tsurimoto, T., Fairman, M.P., and Stillman, B. (1989). Simian virus 40 DNA replication in vitro: identification of multiple stages of initiation. Mol Cell Biol *9*, 3839-3849.

Tsurimoto, T., Melendy, T., and Stillman, B. (1990). Sequential initiation of lagging and leading strand synthesis by two different polymerase complexes at the SV40 DNA replication origin. Nature *346*, 534-539.

Tsurimoto, T., and Stillman, B. (1989). Multiple replication factors augment DNA synthesis by the two eukaryotic DNA polymerases, alpha and delta. EMBO J *8*, 3883-3889.

Udall, V. (1972). Drug-induced blindness in some experimental animals and its relevance to toxicology. Proc R Soc Med *65*, 197-200.

Unterholzner, L., and Bowie, A.G. (2008). The interplay between viruses and innate immune signaling: recent insights and therapeutic opportunities. Biochem Pharmacol *75*, 589-602.

van der Meijden, E., Janssens, R.W., Lauber, C., Bouwes Bavinck, J.N., Gorbalenya, A.E., and Feltkamp, M.C. (2010). Discovery of a new human polyomavirus associated with trichodysplasia spinulosa in an immunocompromized patient. PLoS Pathog *6*, e1001024.

van Roy, F., Fransen, L., and Fiers, W. (1983). Improved localization of phosphorylation sites in simian virus 40 large T antigen. J Virol *45*, 315-331.

Vats, A., Randhawa, P.S., and Shapiro, R. (2006). Diagnosis and treatment of BK virus-associated transplant nephropathy. Adv Exp Med Biol *577*, 213-227.

Vogt, M., and Dulbecco, R. (1960). Virus-Cell Interaction with a Tumor-Producing Virus. Proc Natl Acad Sci U S A *46*, 365-370.

vom Saal, F.S., Akingbemi, B.T., Belcher, S.M., Birnbaum, L.S., Crain, D.A., Eriksen, M., Farabollini, F., Guillette, L.J., Jr., Hauser, R., Heindel, J.J., *et al.* (2007). Chapel Hill bisphenol A expert panel consensus statement: integration of mechanisms, effects in animals and potential to impact human health at current levels of exposure. Reprod Toxicol *24*, 131-138.

Waga, S., Bauer, G., and Stillman, B. (1994). Reconstitution of complete SV40 DNA replication with purified replication factors. J Biol Chem *269*, 10923-10934.

Waga, S., and Stillman, B. (1994). Anatomy of a DNA replication fork revealed by reconstitution of SV40 DNA replication in vitro. Nature *369*, 207-212.

Walczak, C.P., and Tsai, B. (2011). A PDI family network acts distinctly and coordinately with ERp29 to facilitate polyomavirus infection. J Virol *85*, 2386-2396.

Walsh, P., Bursac, D., Law, Y.C., Cyr, D., and Lithgow, T. (2004). The J-protein family: modulating protein assembly, disassembly and translocation. EMBO Rep *5*, 567-571.

Waterhouse, A.M., Procter, J.B., Martin, D.M., Clamp, M., and Barton, G.J. (2009). Jalview Version 2--a multiple sequence alignment editor and analysis workbench. Bioinformatics *25*, 1189-1191.

Wattier, R.L., Vazquez, M., Weibel, C., Shapiro, E.D., Ferguson, D., Landry, M.L., and Kahn, J.S. (2008). Role of human polyomaviruses in respiratory tract disease in young children. Emerg Infect Dis *14*, 1766-1768.

Weinberg, D.H., and Kelly, T.J. (1989). Requirement for two DNA polymerases in the replication of simian virus 40 DNA in vitro. Proc Natl Acad Sci U S A *86*, 9742-9746.

Weinberg, G.A., and Mian, A.N. (2010). BK virus nephropathy and other polyoma virus infections. Pediatr Infect Dis J *29*, 257-260.

Weisshart, K., Bradley, M.K., Weiner, B.M., Schneider, C., Moarefi, I., Fanning, E., and Arthur, A.K. (1996). An N-terminal deletion mutant of simian virus 40 (SV40) large T antigen oligomerizes incorrectly on SV40 DNA but retains the ability to bind to DNA polymerase alpha and replicate SV40 DNA in vitro. J Virol *70*, 3509-3516.

Weisshart, K., Friedl, S., Taneja, P., Nasheuer, H.P., Schlott, B., Grosse, F., and Fanning, E. (2004). Partial proteolysis of simian virus 40 T antigen reveals intramolecular contacts between domains and conformation changes upon hexamer assembly. J Biol Chem *279*, 38943-38951.

Weisshart, K., Taneja, P., and Fanning, E. (1998). The replication protein A binding site in simian virus 40 (SV40) T antigen and its role in the initial steps of SV40 DNA replication. J Virol *72*, 9771-9781.

Welcker, M., and Clurman, B.E. (2005). The SV40 large T antigen contains a decoy phosphodegron that mediates its interactions with Fbw7/hCdc4. J Biol Chem *280*, 7654-7658.

Westphal, H., and Dulbecco, R. (1968). Viral DNA in polyoma- and SV40-transformed cell lines. Proc Natl Acad Sci U S A *59*, 1158-1165.

Wheeler, D.L., Barrett, T., Benson, D.A., Bryant, S.H., Canese, K., Chetvernin, V., Church, D.M., DiCuccio, M., Edgar, R., Federhen, S., *et al.* (2007). Database resources of the National Center for Biotechnology Information. Nucleic Acids Res *35*, D5-12.

White, M.K., and Khalili, K. (2006). Interaction of retinoblastoma protein family members with large T-antigen of primate polyomaviruses. Oncogene *25*, 5286-5293.

WHO (2008). Annex 1: HIV and AIDS estimates and data, 2007 and 2001. In 2008 Report on the Global AIDS epidemic (Geneva, Switzerland, World Health Organization).

Wickramasinghe, S.R., Inglis, K.A., Urch, J.E., Muller, S., van Aalten, D.M., and Fairlamb, A.H. (2006). Kinetic, inhibition and structural studies on 3-oxoacyl-ACP reductase from Plasmodium falciparum, a key enzyme in fatty acid biosynthesis. Biochem J *393*, 447-457.

Williams, G.L., Roberts, T.M., and Gjoerup, O.V. (2007). Bub1: escapades in a cellular world. Cell Cycle *6*, 1699-1704.

Wisen, S., Androsavich, J., Evans, C.G., Chang, L., and Gestwicki, J.E. (2008). Chemical modulators of heat shock protein 70 (Hsp70) by sequential, microwave-accelerated reactions on solid phase. Bioorg Med Chem Lett *18*, 60-65.

Wisen, S., Bertelsen, E.B., Thompson, A.D., Patury, S., Ung, P., Chang, L., Evans, C.G., Walter, G.M., Wipf, P., Carlson, H.A., *et al.* (2010). Binding of a small molecule at a protein-protein interface regulates the chaperone activity of hsp70-hsp40. ACS Chem Biol *5*, 611-622.

Wisen, S., and Gestwicki, J.E. (2008). Identification of small molecules that modify the protein folding activity of heat shock protein 70. Anal Biochem *374*, 371-377.

Wobbe, C.R., Weissbach, L., Borowiec, J.A., Dean, F.B., Murakami, Y., Bullock, P., and Hurwitz, J. (1987). Replication of simian virus 40 origin-containing DNA in vitro with purified proteins. Proc Natl Acad Sci U S A *84*, 1834-1838.

Wold, M.S., and Kelly, T. (1988). Purification and characterization of replication protein A, a cellular protein required for in vitro replication of simian virus 40 DNA. Proc Natl Acad Sci U S A *85*, 2523-2527.

Wold, M.S., Li, J.J., and Kelly, T.J. (1987). Initiation of simian virus 40 DNA replication in vitro: large-tumor-antigen- and origin-dependent unwinding of the template. Proc Natl Acad Sci U S A *84*, 3643-3647.

Wold, M.S., Weinberg, D.H., Virshup, D.M., Li, J.J., and Kelly, T.J. (1989). Identification of cellular proteins required for simian virus 40 DNA replication. J Biol Chem *264*, 2801-2809.

Wright, C.M., Chovatiya, R.J., Jameson, N.E., Turner, D.M., Zhu, G., Werner, S., Huryn, D.M., Pipas, J.M., Day, B.W., Wipf, P., *et al.* (2008). Pyrimidinone-peptoid hybrid molecules with distinct effects on molecular chaperone function and cell proliferation. Bioorg Med Chem *16*, 3291-3301.

Wright, C.M., Seguin, S.P., Fewell, S.W., Zhang, H., Ishwad, C., Vats, A., Lingwood, C.A., Wipf, P., Fanning, E., Pipas, J.M., *et al.* (2009). Inhibition of Simian Virus 40 replication by targeting the molecular chaperone function and ATPase activity of T antigen. Virus Res *141*, 71-80.

Wu, J.K., and Harris, M.T. (2008). Use of leflunomide in the treatment of polyomavirus BK-associated nephropathy. Ann Pharmacother *42*, 1679-1685.

Wu, X., Avni, D., Chiba, T., Yan, F., Zhao, Q., Lin, Y., Heng, H., and Livingston, D. (2004). SV40 T antigen interacts with Nbs1 to disrupt DNA replication control. Genes Dev *18*, 1305-1316.

Wu, X., and Levine, A.J. (1994). p53 and E2F-1 cooperate to mediate apoptosis. Proc Natl Acad Sci U S A *91*, 3602-3606.

Wun-Kim, K., and Simmons, D.T. (1990). Mapping of helicase and helicase substrate-binding domains on simian virus 40 large T antigen. J Virol *64*, 2014-2020.

Wyatt, A.J., Sachs, D.L., Shia, J., Delgado, R., and Busam, K.J. (2005). Virus-associated trichodysplasia spinulosa. Am J Surg Pathol *29*, 241-246.

Xiao, C.Y., Hubner, S., and Jans, D.A. (1997). SV40 large tumor antigen nuclear import is regulated by the double-stranded DNA-dependent protein kinase site (serine 120) flanking the nuclear localization sequence. J Biol Chem *272*, 22191-22198.

Yang, L., Wold, M.S., Li, J.J., Kelly, T.J., and Liu, L.F. (1987). Roles of DNA topoisomerases in simian virus 40 DNA replication in vitro. Proc Natl Acad Sci U S A *84*, 950-954.

Ye, Y., Shibata, Y., Kikkert, M., van Voorden, S., Wiertz, E., and Rapoport, T.A. (2005). Recruitment of the p97 ATPase and ubiquitin ligases to the site of retrotranslocation at the endoplasmic reticulum membrane. Proc Natl Acad Sci U S A *102*, 14132-14138.

Yeh, E., Cunningham, M., Arnold, H., Chasse, D., Monteith, T., Ivaldi, G., Hahn, W.C., Stukenberg, P.T., Shenolikar, S., Uchida, T., *et al.* (2004). A signalling pathway

controlling c-Myc degradation that impacts oncogenic transformation of human cells. Nat Cell Biol *6*, 308-318.

Yoneda, Y., Arioka, T., Imamoto-Sonobe, N., Sugawa, H., Shimonishi, Y., and Uchida, T. (1987). Synthetic peptides containing a region of SV 40 large T-antigen involved in nuclear localization direct the transport of proteins into the nucleus. Exp Cell Res *170*, 439-452.

Yu, J., Boyapati, A., and Rundell, K. (2001). Critical role for SV40 small-t antigen in human cell transformation. Virology *290*, 192-198.

Yu, Y., and Alwine, J.C. (2008). Interaction between simian virus 40 large T antigen and insulin receptor substrate 1 is disrupted by the K1 mutation, resulting in the loss of large T antigen-mediated phosphorylation of Akt. J Virol *82*, 4521-4526.

Zhai, W., Tuan, J.A., and Comai, L. (1997). SV40 large T antigen binds to the TBP-TAF(I) complex SL1 and coactivates ribosomal RNA transcription. Genes Dev *11*, 1605-1617.

Zhang, J.H., Chung, T.D., and Oldenburg, K.R. (1999). A Simple Statistical Parameter for Use in Evaluation and Validation of High Throughput Screening Assays. J Biomol Screen *4*, 67-73.

Zhao, L., Qian, Y., Zhu, R., Deng, J., Wang, F., Sun, Y., and Ding, Y. (2010). Identification of WU polyomavirus from pediatric patients with acute respiratory infections in Beijing, China. Arch Virol *155*, 181-186.

Zhao, R., Gish, K., Murphy, M., Yin, Y., Notterman, D., Hoffman, W.H., Tom, E., Mack, D.H., and Levine, A.J. (2000). The transcriptional program following p53 activation. Cold Spring Harb Symp Quant Biol *65*, 475-482.

Zheng, H.Y., Kitamura, T., Takasaka, T., Chen, Q., and Yogo, Y. (2004). Unambiguous identification of JC polyomavirus strains transmitted from parents to children. Arch Virol *149*, 261-273.

zur Hausen, H. (2008). Harald zur Hausen - Autobiography. In Nobel Lectures, K. Grandin, ed. (Stockholm, The Nobel Foundation).

zur Hausen, H., and Gissmann, L. (1979). Lymphotropic papovaviruses isolated from African green monkey and human cells. Med Microbiol Immunol *167*, 137-153.